NORTHWESTERN UNIVERSITY

Stability of Graphene Oxide Membranes in Water:

The Mystery, the Answer, and the Implications.

A DISSERTATION

SUBMITTED TO THE GRADUATE SCHOOL
IN PARTIAL FULFILLMENT OF THE REQUIREMENTS

for the degree

DOCTOR OF PHILOSOPHY

Field of Materials Science and Engineering

By

Che-Ning Yeh

EVANSTON, ILLINOIS

September 2018

ABSTRACT

Stability of Graphene Oxide Membranes in Water:

The Mystery, the Answer, and the Implications.

Che-Ning Yeh

Graphene oxide (GO), a product of oxidative exfoliation of graphite powders, has received significant attention due to its excellent solution dispersibility, rich functionality, and ease of conversion to chemically modified graphene (also known as “reduced graphene oxide” or “r-GO”). These properties make GO an attractive building block for constructing various forms of bulk graphene-based materials. Layer-to-layer stacking, either between sheets or in the form of folds, are the fundamental structural feature in all graphene-based bulk materials. Research in this dissertation clarifies a misunderstanding of the inter-layer interactions in stacked GO sheets and demonstrates the implications of the new insights in better understanding of GO properties and new ways to use this material.

First, a mystery about the stability of GO membranes in water is presented - GO membranes are known to be highly stable in water, but they should disintegrate since individual GO sheets dissolve in water very well. We discovered a long-overlooked factor behind this puzzling contradiction. Our findings show that pristine GO membranes indeed disintegrate in water; however, ionic contaminants unintentionally introduced during synthesis and processing of GO cross-link the sheets and make the film stable in water. One of the overlooked sources of contamination is the porous anodized aluminum oxide (AAO) filter membrane, which can readily corrode during filtration of GO dispersions to release Al^{3+}.

This new insight is crucial to understanding the intrinsic properties of GO-like lamellar membranes. First, it explains why some earlier reports could use GO papers as separation membranes in water. And it reminds researchers that it is the multivalent ionic contaminants that hold the GO membranes together in water; the presence of which should be considered when interpreting the ionic transport results. Second, it resets the baseline understanding of the mechanical properties of GO papers. In many previous studies, the Young's modulus values of GO papers were actually measured with Al^{3+} cross-linked GO papers. Therefore, the stiffness of neat GO papers should be significantly smaller.

The insight also leads to the development of a "cut-and-paste" approach to turn GO papers into complex and even dynamic three-dimensional structures. Since the layer-to-layer interactions can be weakened by introducing water, it suggests that all pristine GO structures are reversible (*i.e.*, they can be re-dispersed in water). Indeed, water was found to be able to heal damaged GO papers, reconnect separated GO pieces, and release internal stress in strained GO papers to fix their shapes. Such approach is complementary to origami and pop-up-based fabrication techniques for creating functional 3D structures from paper-like precursors.

Lastly, a GO-water continuum with continuous transitions between states of a dilute dispersion, a thick gel, a malleable dough, and a dense solid is demonstrated, as the water content decreases. The GO dough is found to be highly processable and exhibit super extensibility. Dense solids with isotropically packed sheets, lamellar films, and porous foams can be readily fabricated from the dough state. Overall, the GO dough shows its potential as a versatile starting material to construct bulk GO, and potentially graphene materials with tunable shapes and microstructures.

ACKNOWLEDGEMENT

First and foremost, I would like to thank my advisor, Jiaxing Huang, for his great support and guidance throughout the years. I am always impressed by his unrelenting passion to science and engineering, especially by how he aims to do research that connects to people and provide solutions (and sometimes surprising) that can potentially make our ordinary lives better. I am also grateful to him for spending so much time and effort teaching us how to communicate research, through writing, speaking, and presentation, and the importance of taking care of your readers/audiences. I will always remember his favorite term “Keep it crispy!”. There are ups and downs in my graduate student life, and I am especially thankful for his encouragement during the not so good times. I would also like to thank my thesis committee members, Prof. Michael Bedzyk, Prof. Ken Shull, and Prof. SonBinh Nguyen for their time and valuable discussions. I am especially grateful for Prof. SonBinh Nguyen’s concern about the progress of the GO dough project, which truly expedited the manuscript preparation and made the work stronger and more complete.

This work would not be possible without the help and support from all the fantastic mentors, colleagues, and friends I am fortunate to have gained at Northwestern. In particular, I’d like to thank Dr. Kalyan Raidongia, the beginning of my Ph.D. journey would not have been that smooth without his helpful guidance and discussions. I’d also like to thank Alane Lim for her help with all the editing and for always being so cheerful. I am grateful for having a wonderful REU student Jesus Baltazar, his hard working and great motivation initiated the cut and paste project and provided it a great start. I would also thank Chong Luo for taking over the cut and paste project and elevating the scope of this work. Without him the work wouldn’t have been completed. Huang

group members past and present are just great: Jaemyung Kim, Jiayan Luo, Andrew Koltonow, Alex Smith, Deepti Krishnan, Xuan Dou, Kevin Chiou, Luke Prestowitz, Haiyue Huang, Sarah Schlossberg, Jiaojing Shao, Chenlong Cui, Jun Gao, Ying Tao, Limei Liu, and all others, I am lucky to have them as friends and coworkers. And to all my friends in graduate school, thank you for sharing happiness and sadness with me and for your willingness to try the food I made from all my experiments in the kitchen. You guys make my time here full of great memories, and I enjoyed each and every moment we've had together.

I would also like to thank my advisor at National Tsing Hua University, Prof. Tri-Rung Yew. I wouldn't have made it this far without her continuous support and encouragement from undergrad till now. I must thank my friends from home, high school, and college, the love and warmth they have given me is invaluable. Though we are far apart, I know they are always there for me, for that I will be forever grateful. In particular, I'd like to thank Yen-Lin for giving me so much encouragement. We started Ph.D. about the same time, and it is great to have him sharing all my feelings (good or bad) and discussing research with me. I am especially grateful for Po-Yung Huang's continued love, patience, and support. I am so blessed to have his accompany and to have someone who understands me so well. I could not imagine the life without him for the past ten years.

Last but definitely not the least, I'd like to thank my family for their endless love and support. My grandparents are the cutest, and it feels so warm when they say how much they are proud of me. And to my grandparents on my father's side, it is unfortunate that you don't get to see me getting my Ph.D., I will always remember your kindness and love, and I miss you so very much. To my dearest parents Shih-Chen Yeh and Hui-Chen Hsieh, my appreciation for you is

beyond words. Thank you for always being there for me and cheering me up all the time. Dad, you always call me your baby daughter, and whenever I feel frustrated, you just simply say “that’s alright, come home!”. You provide so much comfort, and I know I will always have your back. Mom, you are such an inspiration to me. Till this day, I am still amazed by how you are always so positive and cheerful, and how you are capable of handling everything with ease and grace. I appreciate you telling me to take care of others since I was a kid, and I am deeply influenced by your philanthropic spirit. Thank you both for filling me with love and joy, and for always supporting me and believing in me. I am the luckiest person in the world to have you as my parents. Okay, I’m tearing up so let’s stop here.

Table of Contents

List of Figures

List of Tables

Chapter 1

Introduction

Graphene is a two-dimensional (2D) and single-atom-thick sp^2-hybridized carbon network (**Figure 1.1**a). In 2004, Geim and Novoselov successfully isolated graphene monolayer from graphite crystal by mechanical exfoliation. Since then, graphene has attracted significant attention due to its intriguing structure and exceptional electrical, mechanical, and thermal properties[1]. Promising potentials of graphene have been demonstrated in applications ranging from electronics[1-3], polymer composites[4], energy storage materials[5-7], and so on. In 2010, Geim and Novoselov were recognized with the Nobel Prize in Physics for their groundbreaking experiments regarding the two-dimensional material graphene[8].

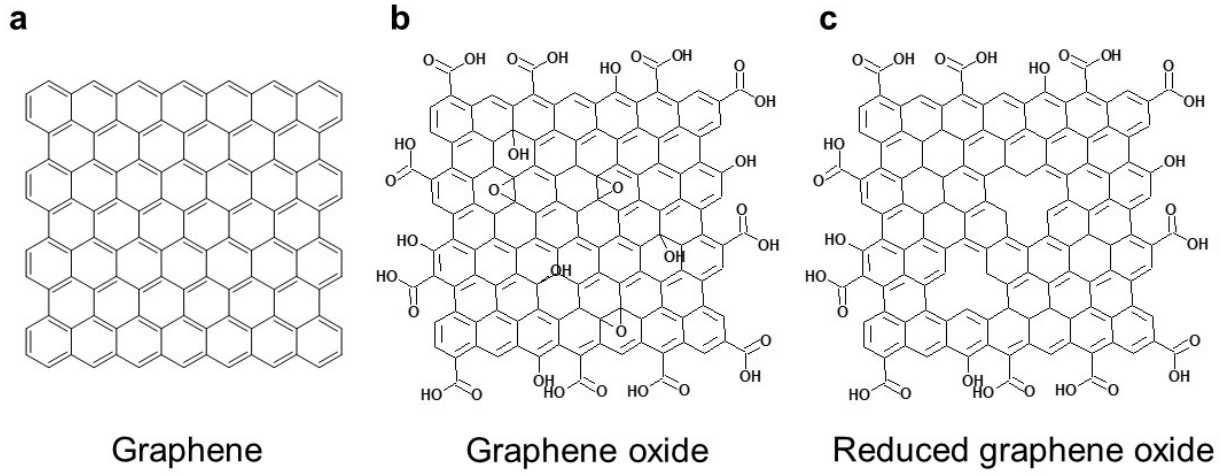

Figure 1.1. Representative chemical structures of graphene, GO, and r-GO. (a) Graphene consists of carbon atoms connected in a hexagonal pattern to form a single-atom-thick sheet. Oxidation and exfoliation of graphite yields graphene oxide (b). GO is derivatized by oxygen functional groups, which break the sheet-wide delocalization and render the sheet insulating. Reduction of graphene oxide produces reduced graphene oxide (c). r-GO has a partially restored π-conjugated network, making the sheet conductive once again.

Graphene was first prepared by mechanical exfoliation, so called scotch-tape method[1], where a bulk graphite crystal is repeatedly peeled off using a cellophane tape until graphene monolayers are isolated. Although the quality of graphene produced by this method is the highest, the production yield is extremely low. Therefore, various synthetic methods have been developed to scale up the production, including chemical vapor deposition (CVD) growth of graphene on catalytic metal surfaces[9] and epitaxial growth from SiC substrates[10]. However, specific substrates are required for the growth of graphene in these methods, limiting their potential for large-scale production. In order to obtain large quantities of single-layer graphene, researchers have turned to the derivatives of graphene, in particular, graphene oxide (GO).

Although first synthesized by Brodie through a reaction of graphite powders with fuming nitric acid and potassium chlorate almost 160 years ago[11], GO has only recently raised extensive interest in the scientific community due to the discovery of graphene. Nowadays, GO is commonly synthesized using a variant of Hummer's method[12]. GO is an oxidative exfoliation product of graphite, which can be prepared by reacting graphite powders with strong oxidizing agents such as potassium permanganate in concentrated sulfuric acid (**Figure 1.2**a). After oxidation, the graphene sheets are exfoliated and derivatized with carboxylic acid at the edges, and phenol hydroxyl and epoxide groups mainly on the basal plane (**Figure 1.1**b)[13-15]. These oxygen functional groups enable GO to be readily dispersed in water to form a stable and single-layer suspension[16]. While GO is insulating, its conductivity can be partially restored by chemical, thermal, and photochemical reduction, producing chemically modified graphene (CMG) or reduced graphene oxide (r-GO) (**Figure 1.1**c)[16-22]. Although the resulting r-GO is more defective and thus less conductive than pristine graphene, the ease of GO synthesis and processing still

makes GO a very attractive precursor for graphene-based applications, especially in large-scale production[23-25]. In addition, the excellent solution processability and rich functionality of GO facilitates the design of graphene-based materials with a wide variety of chemical, macro-, and micro- structures.

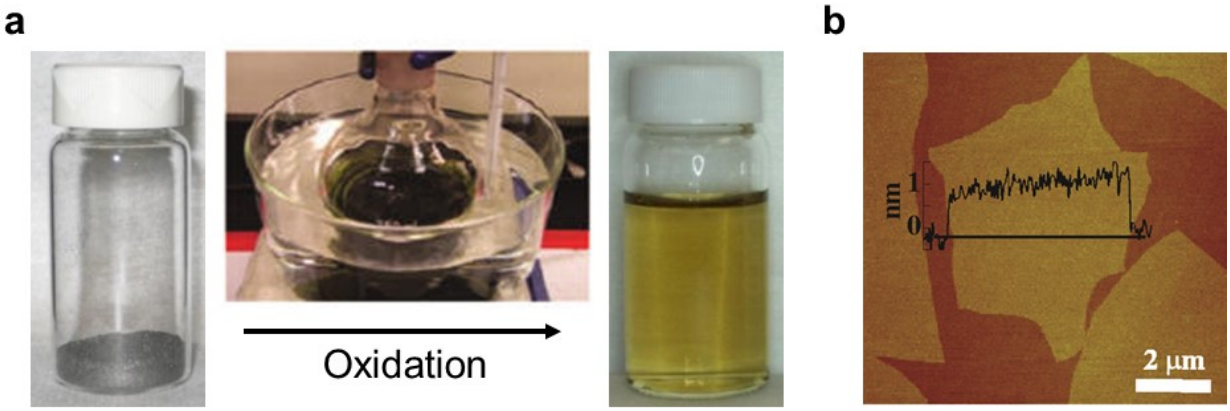

Figure 1.2. Synthesis of GO and its morphology. (a) GO can be synthesized by oxidizing and exfoliating graphite powders, which results in a highly stable colloidal dispersion in water. (b) AFM image of GO sheets shows two abruptly different length scales - the apparent thickness of the sheet is about 1 nm, while its lateral dimension ranges from nanometers to hundreds of micrometers.

Apart from being a precursor to graphene, GO is an intriguing material in its own right and can be considered an unconventional 2D soft material[26]. A GO sheet is characterized by two abruptly different length scales, with its thickness of molecular dimensions, measured to be around 1 nm by atomic force microscopy (AFM), and a lateral dimension of typical colloidal particles, ranging from nanometers up to hundreds of micrometers (**Figure 1.2**b). Therefore, GO sheets can be viewed as either molecules or particles, depending on the length scale of interest. Additionally, the flexible GO sheet with a mix of hydrophilic edges and hydrophobic, π-conjugated patches on

its basal plane can be considered an amphiphile, which can act as a surfactant or dispersing agent to help disperse insoluble solids in a liquid[27,28].

The extremely high aspect ratio of GO makes it a flexible and soft building block leading to many possible assembly structures. GO thin films and membranes can be prepared by Langmuir-Blodgett assembly[29], spin-coating[18], drop-casting[30], interfacial assembly[31], and filtration[32]. Other than membranes consisting layered GO sheets, different micro- and macro- morphologies can also be achieved by changing the shape or the alignment of the flat GO sheets, which leads to new properties without changing its surface chemistry. For example, GO sheets can be crumpled into a paper-ball-like shape, which can resist aggregation[33]; they can be rolled into nanoscrolls with open ends/edges[34]; they can be spun into fibers with strong mechanical strength due to the large overlapping area of aligned GO sheets and good flexibility due to locally crumpled structures of individual sheets[35]. The formation of these structures is determined by the interesting interactions between the sheets in the processing of the material, and their properties depend not only on the quality of individual sheets, but also on how they are assembled together. Therefore, it is of great importance to understand the layer-to-layer interactions between these sheets during the processing of the materials in order to better interpret the processing-structure-properties relationships for GO.

In this dissertation, I will first start with investigating inter-layer interactions between the GO sheets in GO membranes. The insight into water dispersibility of individual GO sheets triggers the study of the stability of GO membranes in water (Chapter 2). We discovered a long-overlooked factor which explained why, counter to our understanding, GO membranes remain stable in water. Our findings show that while neat GO membranes are indeed found to readily disintegrate in water, they become stable if they are cross-linked by multivalent cationic metal contaminants. Since

various forms of bulk GO-based structures such as papers, fibers, foams, or other geometries are made of stacked or folded sheets, the above discovery about the inter-layer interactions between GO sheets suggests that all pristine GO structures should disintegrate in water. We then demonstrated that water can be used to heal damaged GO, reconnect separate GO pieces, and release the stress in pre-strained GO structures, which leads us into designing a cut-and-paste approach to create three-dimensional GO architectures that are hard to obtain by other paper-handling techniques based on folding (*e.g.*, origami) and bending (*e.g.*, pop-up fabrications) (Chapter 3). With the better understanding of the layer-to-layer interactions between the GO sheets, we demonstrated a GO-water continuum with continuous transitions between states of a dilute dispersion, a thick gel, a malleable dough, and a dense solid, as the water content is reduced. A new state of GO, the dough state, with high GO mass loadings (up to 60 wt. %) can serve as a versatile starting material to prepare free-standing GO, and potentially graphene materials with arbitrary shapes and structures. This work sheds light on realizing direct manipulation of graphene-based materials on micro- and macroscopic scales in a controllable manner for practical applications (Chapter 4).

Chapter 2

Graphene Oxide Membranes in Water: To Disintegrate or Not to Disintegrate?

Material in this chapter is reproduced in part with permission from reference 36, "On the origin of the stability of graphene oxide membranes in water" by Che-Ning Yeh, Kalyan Raidongia, Jiaojing Shao, Quan-Hong Yang, and Jiaxing Huang; Nature Chemistry, 7, 166-170[36].

2.1 Introduction: Graphene-Based Membranes

Graphene and its derivatives such as GO and r-GO have attracted significant attention due to their exceptional electrical, mechanical, and thermal properties[1]. Among various methods for generating graphene-based materials, oxidation and exfoliation of graphite into GO is the most versatile and easily scalable method. Assemblies of GO sheets into macroscopic membranes and paper-like materials are of great interest because of their promising applications in catalysis[37], energy conversion[38], gas separation[39], molecular filtration[40], sensing[41], and so on.

Various methods, such as Langmuir-Blodgett assembly[29], filtration[32], molecular templates[42], and direct chemical vapor deposition[43] have been employed to obtain macroscopic graphene or graphene oxide films. Among these, the technique typically favored for fabricating GO papers is vacuum filtration. Here, GO solution is pulled through a frit-supported nanoporous filter membrane with pore size smaller than the size of GO sheets. During the filtering process, solvent and salts pass through the nanopores while the larger GO sheets pile up. When dried, the stack of GO sheets can be peeled off the filter membrane as a free-standing film (**Figure 2.1**).

Filtration is particularly appealing as this flow-directed fabrication provides a simple way to obtain free-standing films with controllable thickness.

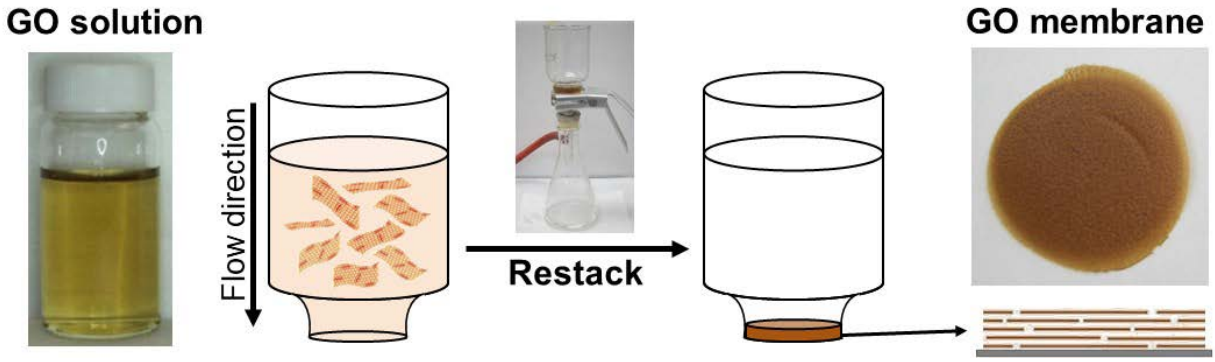

Figure 2.1. Vacuum filtration is commonly used to prepare GO membranes. GO solution of designed concentration and volume is pulled through a nanoporous filter membrane. During the filtering process, GO sheets pile up and restack into a free-standing GO film after dried.

2.2 Puzzle: Are GO Membranes Stable in Water?

GO sheets are the oxidative exfoliation product of graphite and readily disperse in water because of the ionized oxygen-containing functional groups attached to their basal plane[25,26,32,44-46]. On filtration, the sheets restack to form paper-like membranes with extraordinary mechanical properties that have attracted significant interests[32,39,40,47,48]. The extraordinary stability of GO films in water has been noted in previous work[32,47]. For instance, Nguyen group and Ruoff group prepared the first graphene oxide paper and specifically described the stability of GO membranes in the supplementary information – "*A piece of graphene oxide paper left in water for several hours does not disperse and maintains its shape (in contrast, graphite oxide powder samples disperse immediately).*[32]" Again, Geim group and Nair group utilized GO membranes for molecular sieving and also stated that GO membranes are highly stable in water in the

supplementary information – "*Although graphite oxide is known to be soluble in water, the vacuum-filtered GO laminates were found to be highly stable in water, and it was practically impossible to re-disperse them without extensive sonication.*[47]" While stability of GO membranes is a prerequisite for their membrane application in solution, this is counterintuitive because GO sheets become negatively charged on hydration[49,50] (**Figure 2.2**) and should overcome van der Waals attraction or hydrogen bonding to separate from each other. In fact, re-dispersion of GO films in water has also been reported occasionally[51,52], and the need to ensure their integrity in water-based membrane applications has been discussed[53-57].

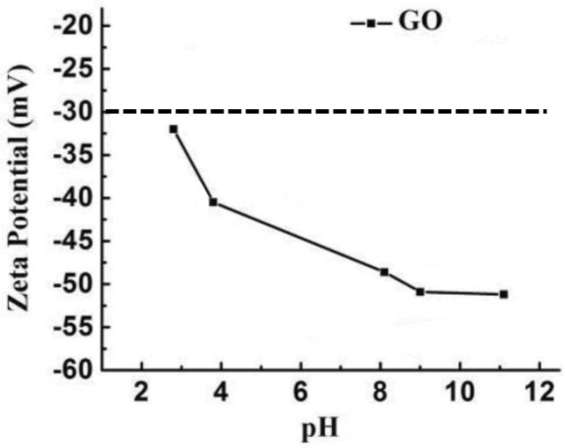

Figure 2.2. GO sheets are negatively charged in water. Zeta potential measurement shows the charge density (*i.e.*, hydrophilicity) of GO increases with higher pH[50].

Before GO membranes can be deployed in solution-based applications, there must be consensus about whether these films are stable in water, and why. In this chapter, a long-overlooked factor behind this contradiction has been discovered, and we have found that neat GO membranes indeed readily disintegrate in water. It is the multivalent cationic metal contaminants

introduced during synthesis and processing that are responsible for their stability. In particular, the most commonly used porous anodized aluminum oxide (AAO) filter discs can corrode to release significant amount of Al^{3+} during filtration of the acidic GO dispersion, which very effectively cross-links the GO sheets and significantly strengthens the resulting membranes.

2.3 Verification of Al Cross-Linking

AAO discs are the most commonly used filters for preparing membranes of many nanomaterials, especially two-dimensional materials. Presumably, this is due to their flat surface and rigidity, which are believed to promote a tighter packing of the sheets under vacuum filtration, leading to stronger membranes than those made with flexible and rough polymeric filter papers. However, **Figure 2.3** shows that GO membranes prepared by filtration using AAO and polymeric filter papers, such as Teflon, actually have very similar microstructures. Here, the two types of GO membranes are denoted as GO (AAO) and GO (Teflon), respectively. As the AAO discs have smoother surface than Teflon filter paper, the resulting GO (AAO) does appear smoother than GO (Teflon) (**Figure 2.3**a, b). However, neither cross-sectional scanning electron microscopy (SEM) images (**Figure 2.3**a, b, insets) nor X-ray diffraction (XRD) patterns (**Figure 2.3**c) show any apparent difference in their lamellar ordering. The inter-layer spacing of GO (AAO) and GO (Teflon) membranes are found to be 8.04 and 8.05 Å, respectively. The diffraction peak of GO (Teflon) is actually slightly sharper than that of GO (AAO). Therefore, contrary to common speculation, the lamellar structures of GO membranes obtained from rougher Teflon filter papers are actually as ordered as those obtained from smoother AAO discs. Although the two types of GO membranes have very similar microstructures, we discovered that they have drastically

different mechanical properties and stability in water. As shown in the typical stress-strain curves obtained from tensile tests (**Figure 2.3**d), GO (AAO) is much stronger and stiffer than GO (Teflon). The average tensile strength and Young's modulus of GO (AAO) were measured to be 100.5 ± 19.2 MPa and 26.2 ± 4.6 GPa, respectively, significantly higher than those of GO (Teflon), which has an average tensile strength of 86.9 ± 8.9 MPa and Young's modulus of 7.6 ± 1.1 GPa. Remarkably, switching filter discs from Teflon to AAO resulted in more than a 340 % enhancement of the stiffness of the resulting GO membranes. The most striking difference between the two types of GO is their stability in water. **Figure 2.3**e shows a GO (Teflon) film disintegrates immediately on hydration without any mechanical agitation and is completely re-dispersed after one day. In contrast, GO (AAO) film remains intact in water (**Figure 2.3**f) as found previously[32,47].

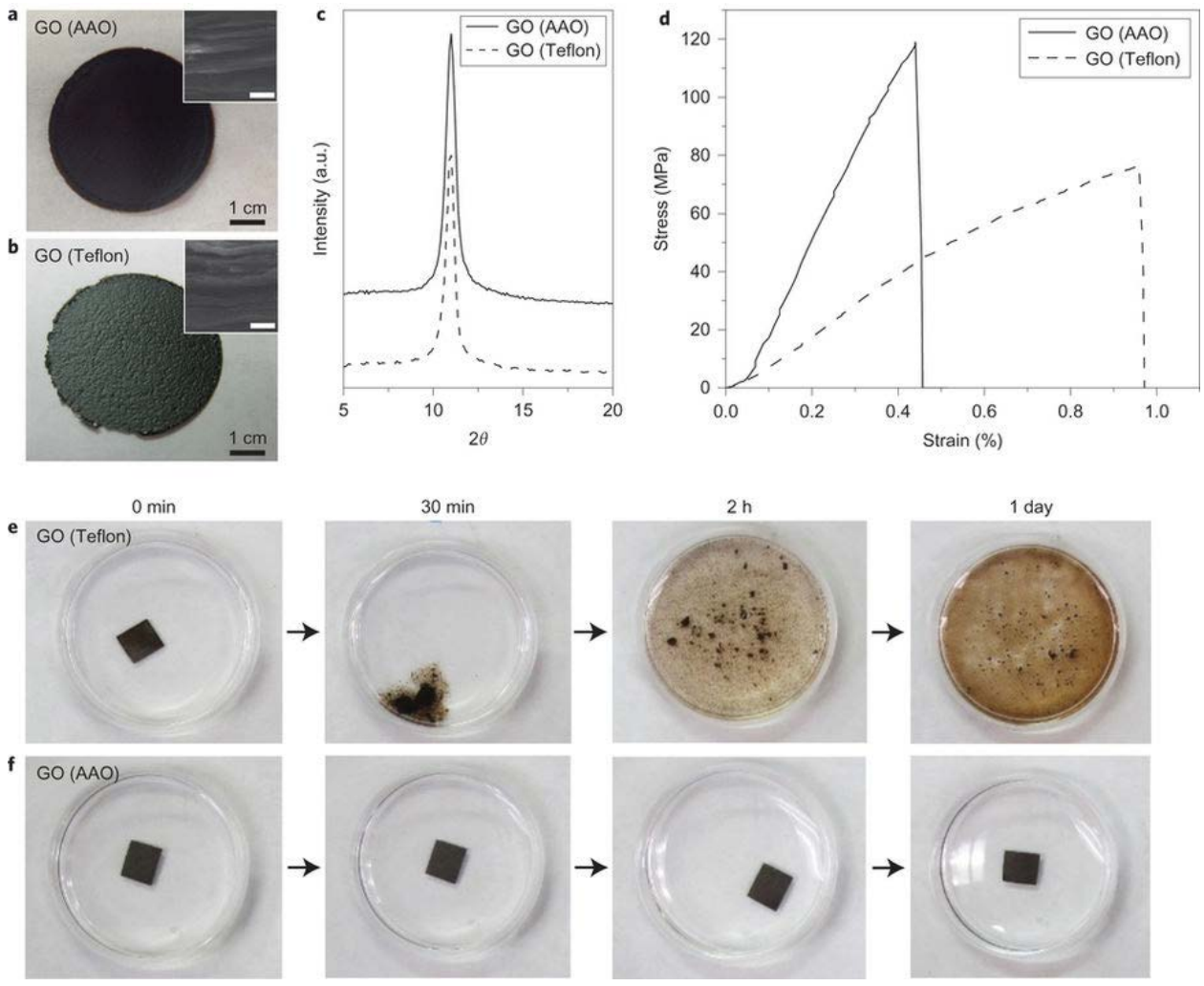

Figure 2.3. GO membranes obtained from AAO and Teflon filters have similar microstructures but drastically different mechanical properties and stability in water. Photos showing surface morphologies of GO (AAO) (a) and GO (Teflon) (b) paper. Inset: corresponding cross-sectional SEM images (scale bar, 2 μm). XRD patterns of the two GO papers show similar inter-layer spacing (c); however, tensile tests (d) reveal a significant difference in their mechanical properties. Additionally, GO (Teflon) readily disintegrates in water (e), whereas GO (AAO) remains intact (f). Thick GO membranes of 18 - 20 μm were used in these experiments to exemplify the rapid disintegration of GO films in water. The photos in e and f were taken after the solutions had been stirred with a lab spatula, except for the one showing GO (Teflon) in water for 30 minutes.

The two types of GO have nearly identical lamellar ordering, and therefore the significantly higher stiffness and water stability of GO (AAO) suggest an additional strengthening mechanism other than van der Waals attraction or hydrogen bonding that holds the sheets together. As the synthesis of GO relies on the use of concentrated mineral acid[12], and GO is hard to wash because of its ease of gelation[58], GO dispersion is often acidic. We hypothesized that the AAO discs might be etched by acid to release Al^{3+}, which can very effectively cross-link the sheets and strengthen the final membrane, as is common with divalent metal ions[59]. X-ray photoelectron spectroscopy was employed to see if the GO (AAO) membrane was contaminated by Al (**Figure 2.4**a). The Al 2*p* spectra were collected during depth profiling up to 100 nm of a nominal etching depth into the film from both sides (**Figure 2.4**b, c), and clearly revealed the presence of Al. The calculated Al/C atomic ratio started from around 4.5 % on the AAO-contacting bottom side, and gradually decreased through this 18-μm-thick film to around 1 % on the top side. It is remarkable that the GO (AAO) membrane was contaminated with Al throughout its tens of thousands of layers. This indicates that Al^{3+} was released to the entire dispersion during vacuum filtration, and contamination was not caused by contact transfer from AAO. Filtration of GO sheets, as well as that of other 2D materials with high aspect ratios, tends to be self-limiting and extremely slow, and therefore GO sheets at the bottom side of the film (that is, the filter cake) would have had a longer exposure to Al^{3+}, which leads to a higher Al content. In contrast, XPS depth profiling of GO obtained from Teflon filter paper did not detect any Al (**Figure 2.4**e).

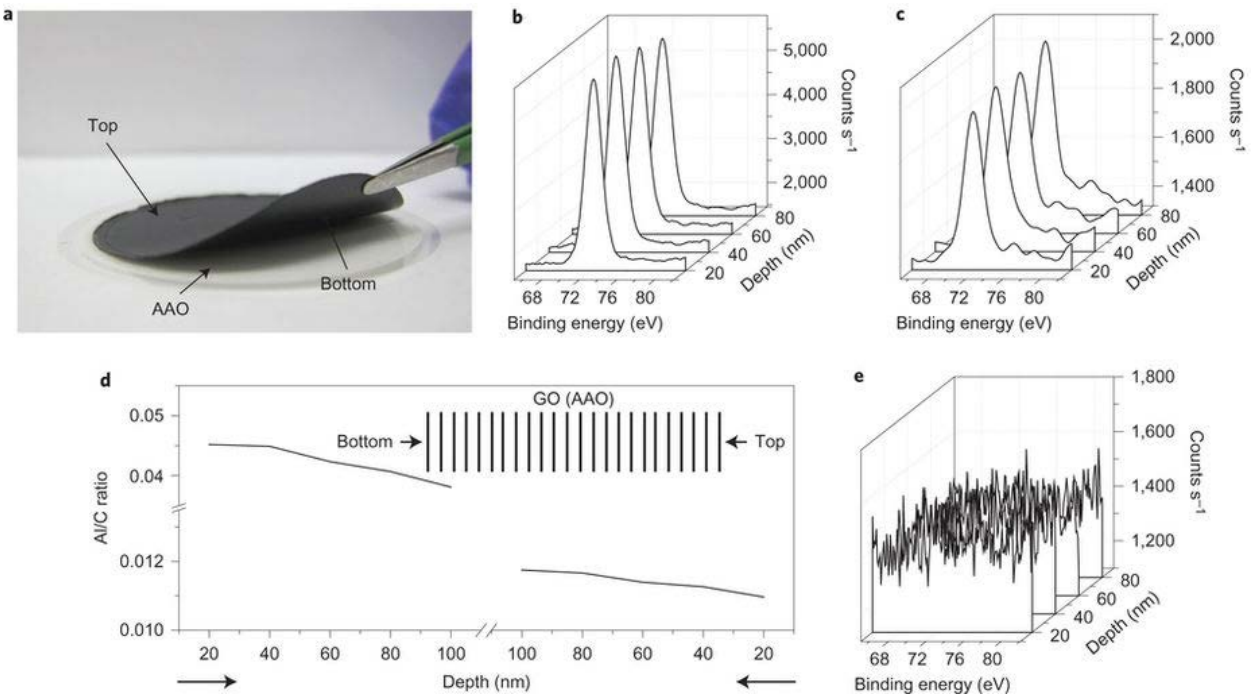

Figure 2.4. GO membrane obtained from the AAO filter is contaminated with Al. (a) Photo showing an 18-μm-thick GO membrane detached from an AAO filter disc. Sets of Al 2*p* spectra measured during XPS depth profiling of GO (AAO) from the bottom side (b) and from the top side (c). (d) Al/C ratio as a function of the etching depth from both sides of the GO (AAO). (e) Depth profiling of GO (Teflon) from the bottom side suggests that no Al is present.

We also prepared Al-free GO films using cellulose nitrate filter paper (GO (CN)). The resulting films have similarly weak mechanical properties as those of GO (Teflon) and also disintegrate in water (**Figure 2.5**). **Figure 2.6** includes a complementary set of side-view photos to contrast the stability of neat GO and GO (AAO) membranes in water. GO films made by other methods, such as air-water interfacial assembly[31], also disintegrate in water. It is worth noting that in previous studies that reported the extraordinary stability of GO membranes in water, the samples were obtained by filtration using AAO[32,47]. While in studies that reported the dissolution of GO films in water, the samples were made with polymeric filters[51,52]. Section 2.5 will discuss these

prior observations in more details, which collectively support our findings that the stability of GO papers in water can be attributed to the unexpected contaminants acting as cross-linkers.

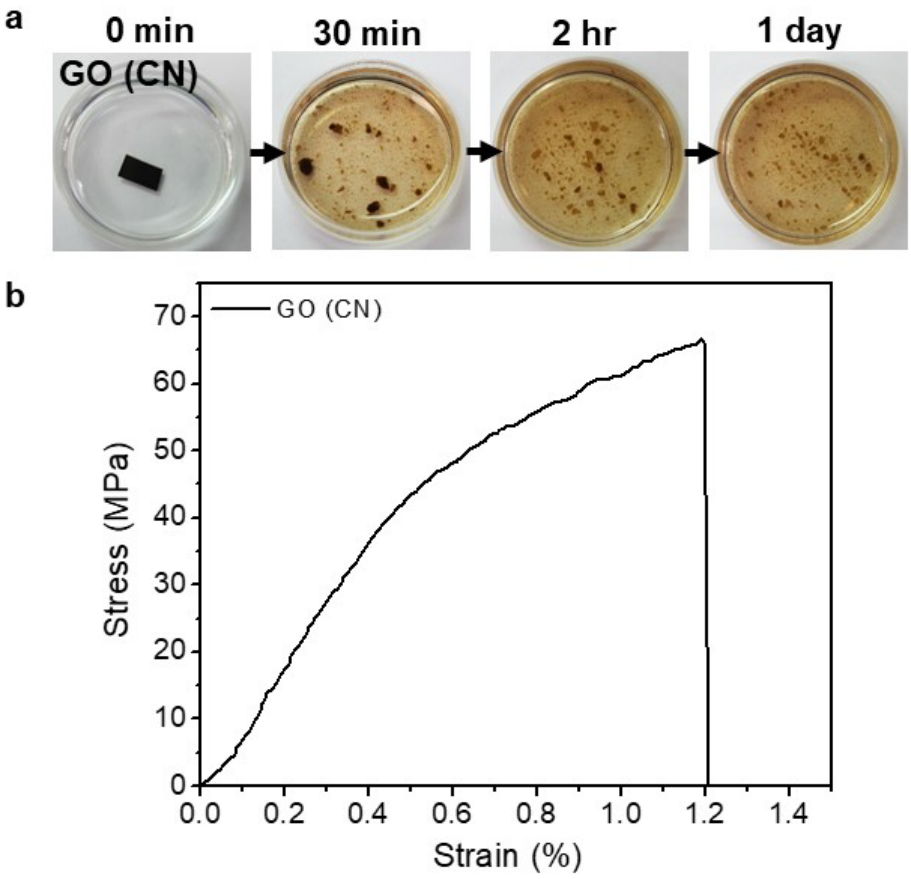

Figure 2.5. GO membranes obtained from a cellulose nitrate filter membrane (denoted as GO (CN)) also readily disintegrate in water. (a) Similar to GO membranes obtained from Teflon filter, GO membranes obtained from cellulose nitrate filter paper also dissolve in water. (b) The average tensile strength and Young's modulus of GO(CN) papers were measured to be 70.0 ± 4.9 MPa and 9.4 ± 0.8 GPa, respectively, which are also much weaker than those of Al^{3+} contaminated GO (AAO) papers. Note: photos in (a) were taken after the solutions were gently stirred with a lab spatula.

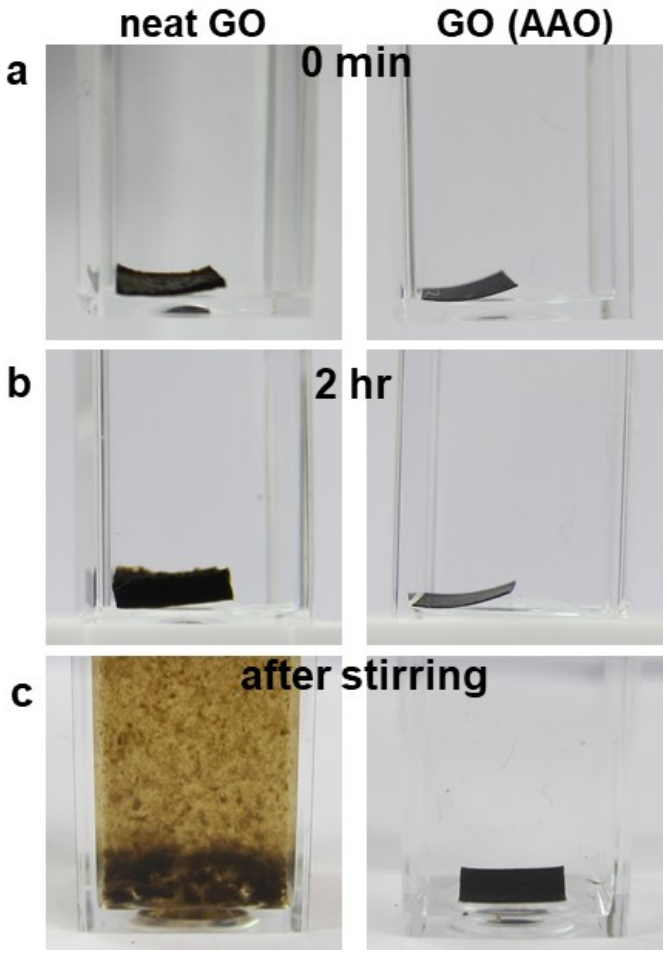

Figure 2.6. A set of side-view photos complementary to those shown in Figure 2.3e, f and Figure 2.5 contrasting the stability of neat GO film and Al^{3+} contaminated GO film in water. Left column: (a) The neat GO film (obtained with Teflon or cellulose nitrate filter paper) readily swells upon being soaked in water. (b) After 2 hours of soaking, disintegration can already be observed without any agitation. (c) After gentle stirring with a lab spatula for a few seconds, it completely disintegrates and starts to re-disperse in water. Right column: In contrast, the Al^{3+} cross-linked GO (AAO) film remains stable in water after days of soaking. The behaviors of the two films under stirring clearly show that GO (AAO) is stable and neat GO readily disintegrates.

2.4 Effect of pH on Corrosion of AAO and the Stability of Corresponding Membranes in Water

Al_2O_3 is amphoteric[60,61], so an AAO disc can be corroded in water at all pH values. **Figure 2.7**a shows the effect of pH values (pH = 1 - 11) on AAO corrosion. AAO discs were soaked in solutions for one day, and the concentration of released Al in the supernatant was measured by inductively coupled plasma mass spectrometry (ICP-MS). Three zones of corrosion behaviors can be identified in the highly acidic (pH < 4), near neutral (4 < pH < 8), and highly basic (pH > 8) solutions, which released Al^{3+}, $Al(OH)_3$, and $Al(OH)_4^-$, respectively[61,62]. The corrosion of AAO is faster in the acidic and basic zones, releasing 10 - 90 ppm of Al after one day. In the near neutral zone, the released Al is less than 3 ppm. As filtration of GO typically takes days, the range of Al concentrations displayed in **Figure 2.7**a should be representative of the level of Al released during filtration. There is a strong dependence of the property of the final thin film on the pH values of the dispersion. GO (AAO) obtained from acidic dispersion (pH = 3) is highly stable in water because of Al^{3+} cross-linking (**Figure 2.7**b). Although films obtained from near neutral (pH = 5.5, **Figure 2.7**c) and basic solutions (pH = 8.5, **Figure 2.7**d) are contaminated with Al, they can still disintegrate in water, probably because of the inability of neutral $Al(OH)_3$ and the anionic $Al(OH)_4^-$ to cross-link the negatively charged sheets. All the GO films can be ultrasonically re-dispersed in water. Using a tabletop sonicator, the GO film obtained at pH = 8.5 can be re-dispersed after less than ten minutes to yield single-layer dispersions (**Figure 2.8**a). In contrast, the film obtained at pH = 3 was barely dispersed. A large fraction of heavily aggregated and stacked flakes was found in its supernatant (**Figure 2.8**b).

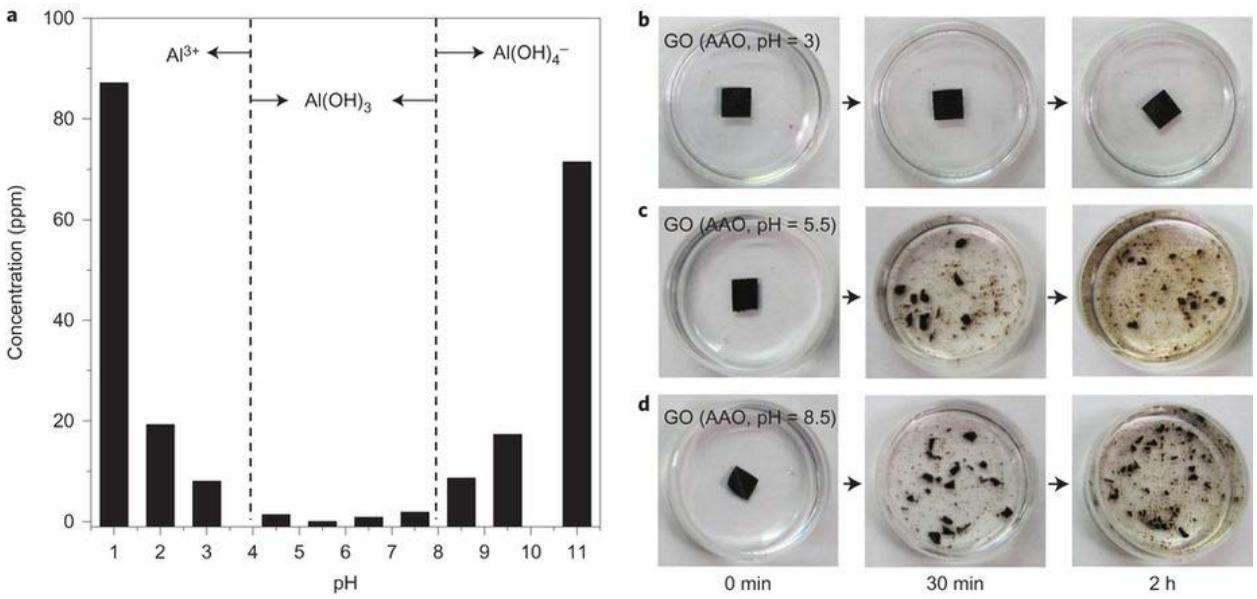

Figure 2.7. Effect of pH on the corrosion of AAO and the stability of the corresponding GO membranes in water. (a) Concentration of released Al as a function of pH after one day. (b - d) Photos of GO (AAO) prepared from GO solutions at pH = 3, pH = 5.5, and pH = 8.5 before and after being soaked in water for 30 minutes and two hours, respectively. Photos in b - d were taken after the solutions had been stirred with a lab spatula.

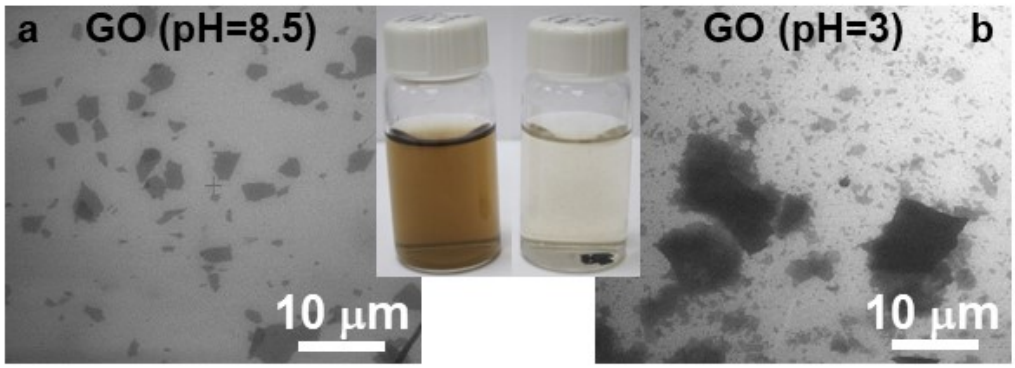

Figure 2.8. Effect of Al contaminant on dispersity of GO sheets in water. Inset: Photo showing vials containing GO (AAO) membranes after being sonicated in water for 30 minutes. (a) The GO (AAO) film obtained from a basic solution (pH = 8.5) was completely re-dispersed. (b) The film obtained from an acidic solution (pH = 3) was only partially re-dispersed due to Al^{3+} cross-linking. The corresponding SEM images of drop cast samples reveal that the suspension in (a) is made of largely single layers, while the suspension in (b) is still made of heavily stacked and aggregated sheets.

2.5 Impact of Unintentional Al Cross-Linking

2.5.1 Variation in Mechanical Properties of GO Membranes

Immense interest in GO paper-like materials was initiated in 2007, when Nguyen group and Ruoff group fabricated GO papers *via* flow-directed assembly of aqueous GO dispersion (*e.g.*, filtration), and their results suggested that GO papers exhibit much higher stiffness and strength than those of carbon-based papers including bucky papers and flexible graphite foils[32]. Since then, a tremendous amount of work has been devoted to the preparation and characterization of graphene oxide papers. While the GO paper prepared by Nguyen group and Ruoff group showed superior mechanical properties, with the maximum Young's modulus of 42 GPa, the collective reported moduli lay in a relatively wide range of 5 - 42 GPa (**Table 2.1**). Therefore, we would like to re-visit the mechanical properties of the GO papers reported in previous work and provide a possible reason behind this variation.

Preparation method	Young's modulus (GPa)
Filtration - polyester[63]	~ 5
Filtration - PTFE[64]	3.4 - 7.6
Filtration - cellulose[65]	9.1 - 13
Filtration - polycarbonate[51]	11
Self-assembly at liquid/air interface[31]	10.3 - 14.5
Filtration - AAO[66]	13.25
Filtration - AAO[67]	5.3 - 15.3
Filtration - AAO[59]	25.6 ± 1.1
Filtration - AAO[32]	32 (Max. 42)

Table 2.1. Young's modulus of "pristine" GO papers and their corresponding preparation method, along with the type of filter for GO papers obtained by filtration.

Table 2.1 shows the Young's modulus of as-prepared GO papers reported in previous work. Most of the GO papers were fabricated *via* filtration for the reasons discussed in Section 2.1, and some commonly used filter membranes include anodic aluminum oxide (AAO), cellulose, polycarbonate, polyester, polytetrafluoroethylene (PTFE, Teflon), and polyvinylidene fluoride (PVDF). Various efforts have been made to understand the factors influencing mechanical properties of GO papers and to improve those properties. For example, M. Cano *et al.* modified GO with poly(vinyl alcohol) (PVA) and studied the relationship of mechanical properties of modified papers with the molecular weight of grafted PVA. Their results showed that the Young's modulus increased from ~ 5 GPa for the unmodified GO paper to ~ 8 GPa for the paper modified with PVA of 50 kg/mol molecular weight[63]. Alternatively, Y. Gao *et al.* tailored the inter-layer adhesions of the GO papers by introducing small molecules, such as glutaraldehyde (GA) and water, to their inter-layer spacings, and investigated the effect of inter-layer adhesions on the mechanical properties of GO papers. While the water-treated GO paper had a lower Young's modulus (~ 6.5 GPa), the GA-treated GO paper showed a much higher modulus (~ 30.4 GPa) than that of the unmodified GO paper (~ 10.5 GPa), which was attributed to the improved load-bearing capabilities of the GO sheets as a result of better inter-layer adhesions[65]. X. Wang *et al.* prepared GO papers *via* filtration of GO sheets with large and small lateral dimensions. Their results showed that the tensile modulus of GO papers consisting of only large sheets was measured to be about twice that of the paper consisting of only smaller sheets ($E_{\text{large sheet}}$ ~ 7.6 GPa, $E_{\text{small sheet}}$ ~ 3.4 GPa) due to the more compact structure and fewer defects in the stack of large sheets[64]. Nguyen group and Ruoff group modified GO papers with divalent metal ions (Mg^{2+} and Ca^{2+}) and demonstrated that excessive amount of intercalated metal ions would lead to reduced mechanical properties

because of the increased d-spacing and the cross-sectional area of the as-prepared modified GO papers. Alternatively, introducing a small amount (less than 1 wt. %) of divalent metal ions resulted in an around 10 % enhancement in the maximum Young's modulus of GO papers owing to the chemical cross-linking of the functional groups on the GO sheets and the divalent metal ions[59]. Apart from fabricating GO papers *via* filtration, they can also be prepared by a self-assembly method. C. Chen *et al.* heated a GO aqueous suspension to 353 K and collected a GO thin film at the liquid/air interface. After drying, they obtained a flexible and free-standing GO membrane with an average Young's modulus of ~ 12.7 GPa[31].

Looking at the Young's modulus of "unmodified" GO papers and their corresponding preparation methods (**Table 2.1**), it is interesting to note that for all the GO papers with higher Young's modulus, they were obtained by filtration using AAO as a filter. On the other hand, for the GO papers with relatively low Young's modulus, they were fabricated by filtration using polymeric membranes as filters or by other assembly methods. These variations can now be explained by the discovery in our work.

2.5.2 Possible Reason behind the Variated Mechanical Properties of GO Membranes

The new insights about the released Al^{3+} have wide implications since AAO discs are the most commonly used filter for preparing membranes of many nanomaterials, especially 2D materials. The amphoteric nature of Al_2O_3 is well known[60,61] and corrosion of AAO in aqueous solution has also been found[68], yet surprisingly there has been insufficient awareness of its impact on the final thin film properties. Corrosion of AAO is most relevant to 2D materials because they tend to block the pores, which drastically slows down the filtration and increases the exposure time

to released Al, leading to nontrivial level of contamination. Being a trivalent cation, Al^{3+}, or its hydrated form, is highly effective at flocculating negatively charged colloids[69] and subsequently cross-links the sheets in dried state. As GO dispersion is usually acidic, it is very likely that GO films filtered with AAO are already partially cross-linked by the Al^{3+}, which could cause misinterpretation of the measured modulus and strength of GO films, especially for those intentionally modified with other cross-linking agents. For example, in the aforementioned work about the strengthening of GO papers by cross-linking with divalent metal ions, only a modest, around 10 %, increase in overall stiffness was observed after cross-linking[59]. In contrast, in our work even partial Al^{3+} contamination resulted in a more than 340 % enhancement of the membrane stiffness (see **Figure 2.3**d as an example). This conflict can now be explained well by the current findings because the GO membranes used in the earlier work were obtained with an AAO filter. Therefore, the "unmodified" GO papers were probably already cross-linked by Al^{3+}, which led to only a modest stiffness difference between unmodified and "cross-linked" GO papers. In fact, the moduli measured from GO (AAO) and GO (Teflon) films (**Figure 2.3**d) are actually close to the upper and lower boundaries of reported values for GO films obtained with different filtrating papers or with thin film processing techniques[31,32,51,59,63-67,70] (**Table 2.1**), respectively. This implies that the variation in reported moduli values of GO films obtained with different filter papers could be, at least partially, attributed to different degrees of cross-linking by unintentionally introduced contaminants. In another area, AAO released Al^{3+} is probably responsible for the formation of continuous, ultrathin, few-layer GO membranes on AAO, which have been used for gas transport studies in recent reports[39,40,48]. This brings up a new perspective as to whether Al^{3+} can contribute to regulate molecular transport through the inter-layer spacing in GO membranes.

2.6 Manipulation of the Cross-Linking Effect

The inter-layer Al^{3+} ions can be removed from GO films by ionic exchange with hydrochloric acid (H^+) or other monovalent cations such as Na^+ and Li^+, after which the film readily disintegrates in water (**Figure 2.9**a, c, d). XPS detected no Al after the exchange (**Figure 2.9**b). The removal of Al^{3+} can also be accelerated by soaking the contaminated GO films in a solution of metal chelating agent, such as ethylenediaminetetraacetic acid (EDTA). However, one can take advantage of this cross-linking effect and intentionally treat a clean GO film with Al^{3+} to make it water stable (**Figure 2.10**a). The Al^{3+} strengthened film can swell to expand its inter-layer spacing. The results of XRD studies (**Figure 2.10**b) confirmed that a neat GO film obtained with a Teflon paper loses its lamellar ordering on hydration. After Al^{3+} treatment, it maintained the lamellar ordering, which is reflected by a new broad XRD peak. The inter-layer spacing expanded from 7.76 to 17.63 Å. Drying this Al^{3+} cross-linked film shrank the inter-layer spacing to around 8.5 Å, which was reversed to 15.44 Å on rehydration. The final swollen film had a more defined, narrower XRD peak, which indicates an improved alignment of the GO sheets, probably because of the capillary pressure exerted during the drying step.

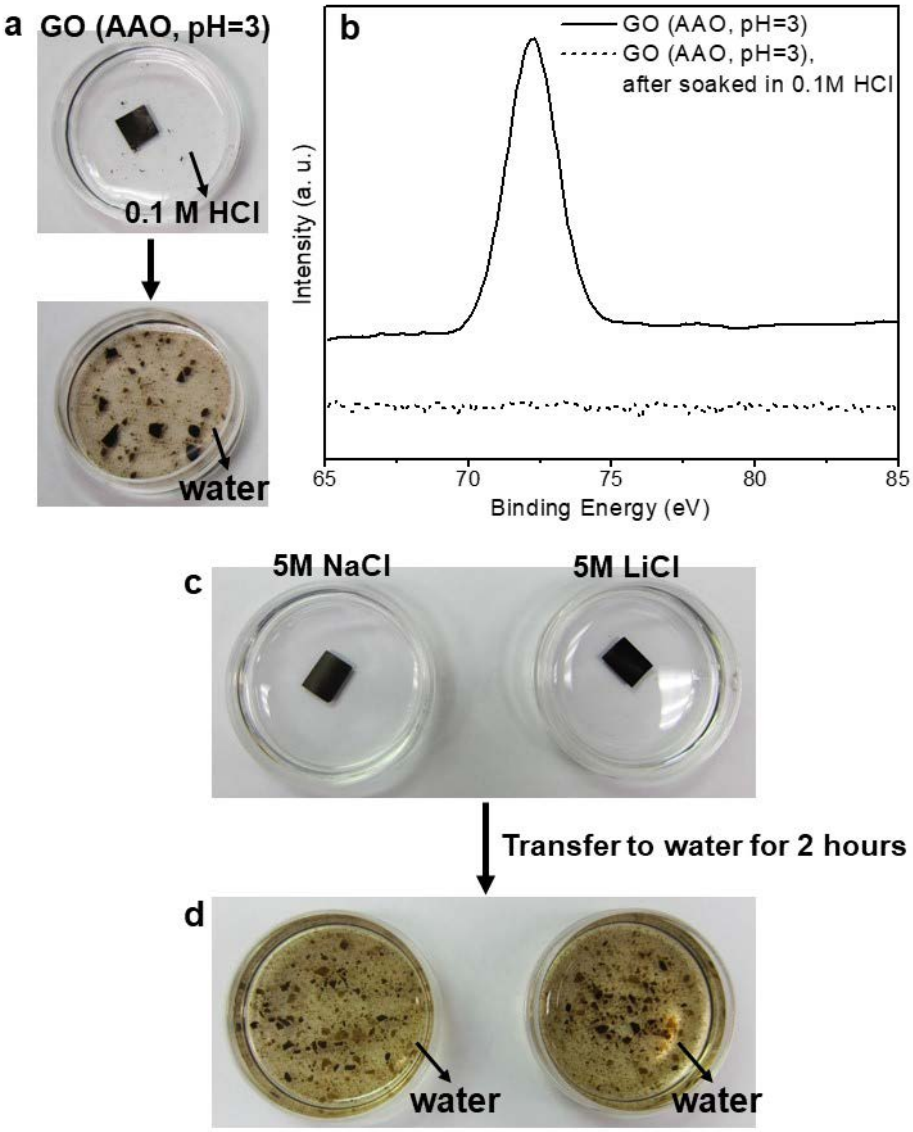

Figure 2.9. Removal of Al^{3+} by ionic exchange. (a) Photos of GO (AAO) paper soaked in 0.1 M HCl for 3 days (top) and then in water for 30 minutes (bottom). (b) XPS Al 2*p* spectra of GO (AAO) paper before and after HCl treatment, suggesting removal of Al^{3+}. (c - d) Ionic exchange with monovalent cations such as Na^{+} and Li^{+} can also lead to the removal of Al^{3+} and disintegration of GO membranes in water. Note: All the photos were taken after the solutions were stirred with a lab spatula.

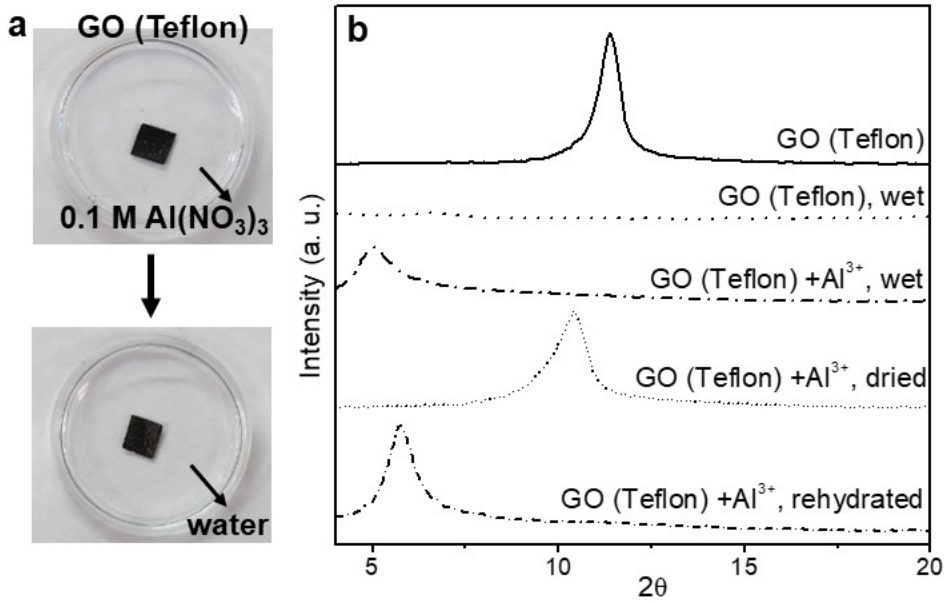

Figure 2.10. Strengthening of GO (Teflon) by Al^{3+} cross-linking. (a) Photos of GO (Teflon) paper soaked in 0.1 M $Al(NO_3)_3$ for one day (top) and then in water for five days (bottom). (b) As shown in the XRD patterns, GO (Teflon) disintegrates in water and loses inter-layer ordering. While in $Al(NO_3)_3$, it swells and maintains the lamellar structure. On drying, the presence of inter-layer Al^{3+} results in slightly larger spacing than that of neat GO. On rehydration, the Al^{3+} cross-linked GO swells to yield a lamellar structure with better stacking. Note: photos in (a) were taken after the samples were stirred with a lab spatula.

2.7 Template-Assisted Synthesis of Inorganic Materials

Two-dimensional nanomaterials have attracted significant research interest since the discovery of graphene. The anisotropy and nanosized effect differing from their bulk counterparts render the 2D materials interesting properties. For bulk materials with layered structures, such as graphite, clay, MoS_2, WS_2, and h-BN[71-75], the most popular method to obtain their corresponding 2D nanomaterials is based on the exfoliation of their layered compounds, including mechanical, chemical, electrochemical, and intercalation methods. However, such strategy is not applicable to materials which do not have layered crystal structure such as metal oxides (ZnO, TiO_2, SnO_2, and perovskite ABO_3 ($BiFeO_3$, $BaTiO_3$))[76]. Therefore, it is desirable to develop a general strategy to fabricate 2D nanomaterials with controllable structure and morphology.

Because of the unique properties of graphene-based sheets, they are attractive as potential building blocks for fabricating new materials. Among which, GO and r-GO sheets have been widely used as support materials to stabilize metal and semiconductor nanoparticles[37,38,77,78]. For example, G. Goncalves *et al.* have shown that the presence of oxygen functionalities at GO surface can act as reactive sites for the nucleation and growth of gold nanoparticles[78]. Alternatively, N. Li *et al.* have demonstrated a direct growth of TiO_2 nanospheres on graphene as the existence of hydroxyl and epoxy functional groups on GO acted as heterogeneous nucleation sites to anchor the nanoparticles, thereby forming well-dispersed nanosized mesoporous TiO_2[77]. Therefore, the large surface area and tunable surface functional groups of graphene-based materials provide promising potential of controllable synthesis of new materials using known carbon surface chemistry.

Our work has shown that cross-linked GO membranes remained stable in water and swelled to expand their inter-layer spacing. Such water swollen films provide a new opportunity to fabricate lamellar membranes of other materials through templated synthesis in aqueous reactions. The use of GO sheets as templates to synthesize inorganic free-standing membranes has been reported by C. Xu *et al*[79]. In their study, GO sheets were initially used as carriers to anchor particles, followed by assembling the composite sheets into films. After subsequent calcinations, they were able to get free-standing Fe_2O_3 particle films. However, the GO sheets used in that study were only sacrificial templates and the resulting products were sub-micrometer-thick, single-layered films, which did not inherit the lamellar structure of the GO template. As the cross-linked GO membrane remains its lamellar structure upon hydration, it provides a continuous two-dimensional area with confined inter-layer spacing. This provides a novel and exciting direction of utilizing the spatial confinement of GO papers to synthesize unconventional two-dimensional materials.

As a proof-of-concept, a hydrated GO film was first immersed in 0.1 M $Zn(NO_3)_2$ solution (**Figure 2.11**a), and then subjected to a two-step annealing treatment in air at 150 °C and 500 °C to form ZnO and decompose GO sheets, respectively. The final product was a macroscopically sized, continuous, free-standing, white ZnO membrane, which resembled the original shape of the GO film (**Figure 2.11**b). SEM images of edge and cross-sectional views reveal that the ZnO membrane also has a lamellar structure with a layer thickness around tens of nanometers. The XRD pattern of the ZnO product is consistent with that of the wurtzite hexagonal structure (JCPDS 36-1451). This experiment demonstrates the potential of swollen GO films for templated synthesis of new 2D materials and lamellar structures with macroscopic dimensions.

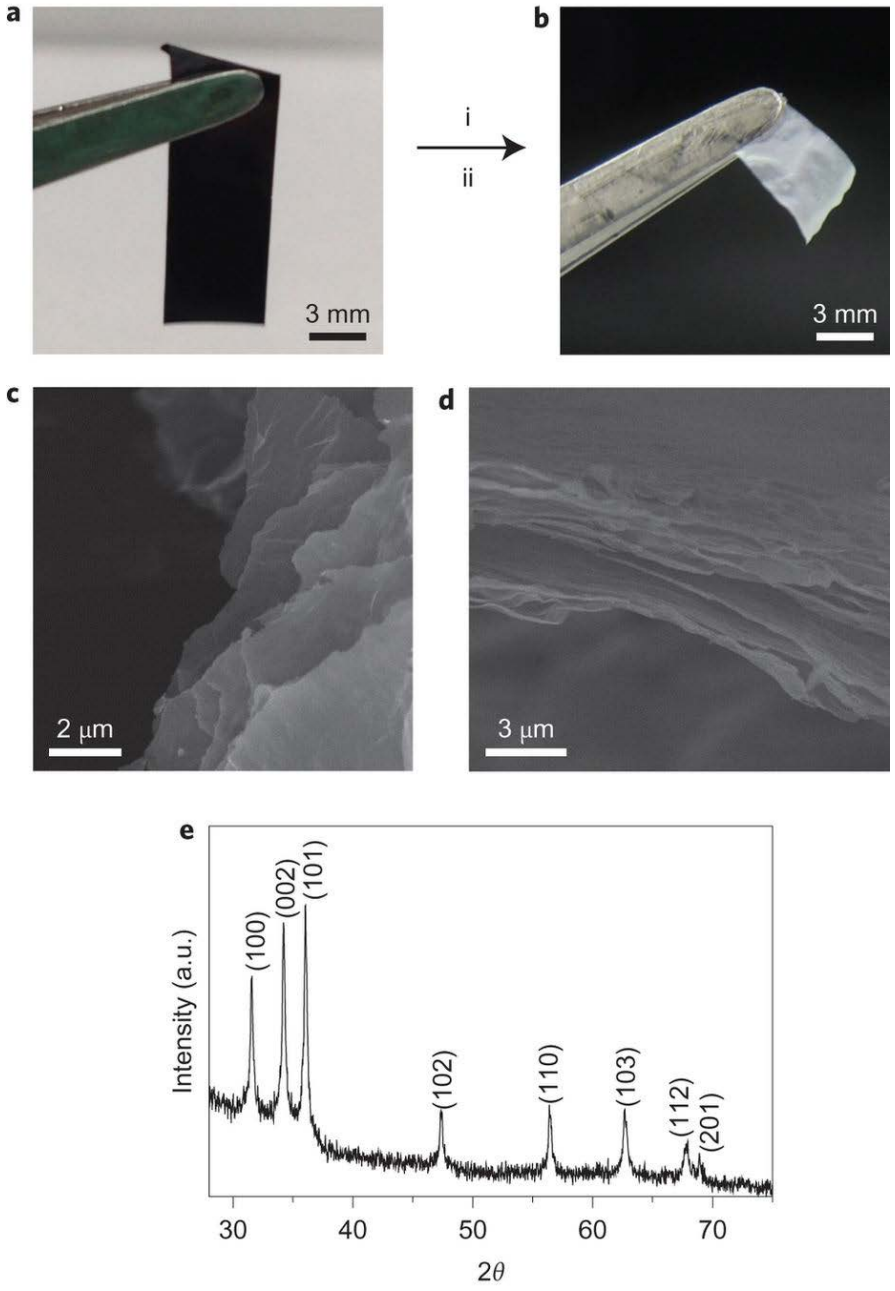

Figure 2.11. Cation-stabilized GO films can swell in water and function as a structural template for chemical reactions. The chemical reactions are confined between the layers and, therefore, a topochemical transform from GO to inorganic membranes can be achieved after carbon removal. The photos show a GO (AAO) paper loaded with $Zn(NO_3)_2$ (a) and the resulting ZnO membrane after annealing in air (b). Annealing was done in two steps: (i), at 150 °C for two hours to produce ZnO; (ii), at 500 °C for another four hours to decompose GO. SEM images that show the edge (c) and cross-section (d) of the resulting ZnO membrane. (e) XRD pattern of the ZnO product.

2.8 Conclusions and Implications

Our work has identified the long-overlooked reason for the stability of GO membranes in water. In addition to Al^{3+} released from an AAO filter disc, other multivalent metal cations, such as Mn^{2+}, a by-product from GO synthesis[12], can also strengthen the membrane (**Figure 2.12**). This work is yet another reminder that GO membranes are highly susceptible to contamination by these cross-linking cations, which can be unintentionally introduced during synthesis and processing (*e.g.*, filtration). The new insight is crucial to understanding the intrinsic mechanical properties of GO-like lamellar films, as well as for their membrane applications, especially those carried out in solution.

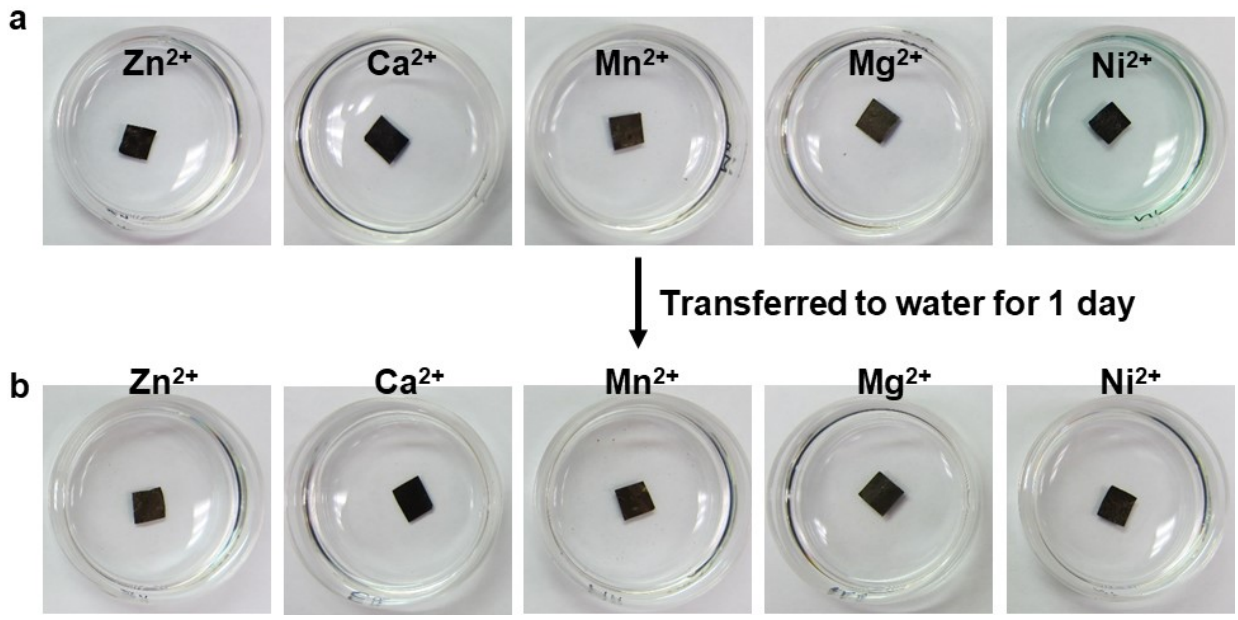

Figure 2.12. Neat GO membranes can also be cross-linked by a variety of divalent metal ions to become stable in water. In contrast, treatment in monovalent cations such as Na^+, K^+, and Li^+ does not result in improved stability in water. Note that Mn^{2+} is a common by-product from GO synthesis. Therefore, Mn^{2+} contaminated GO as a result of insufficient purification could also appear stable in water. All the photos were taken after the solutions were stirred with a lab spatula.

One can also utilize this effect to create water-stable, heavily swollen lamellar structures made of GO or other 2D materials, such as clay sheets (**Figure 2.13**). This opens up new opportunities to study wet-chemical reactions confined in the few nanometers of space between layers, and to rationally design 2D nanofluidic channels[80] for selective molecular and ionic transport.

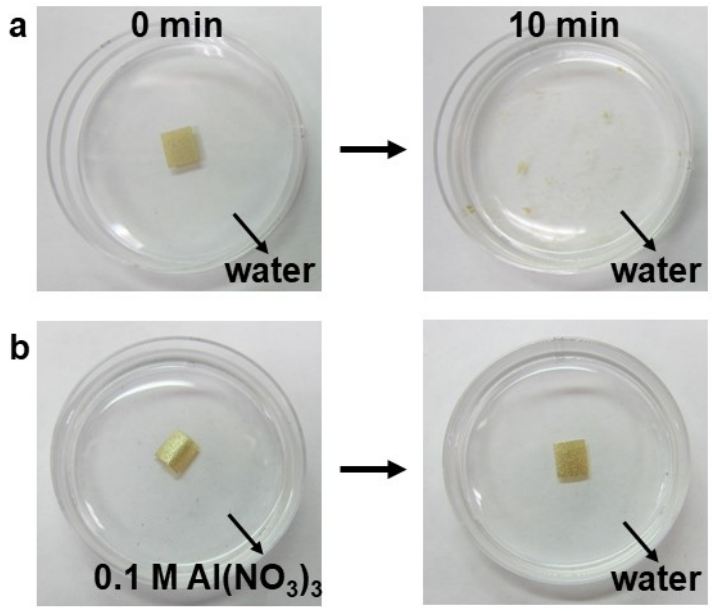

Figure 2.13. Stabilizing of clay membrane in water by Al^{3+} cross-linking. (a) Similar to GO, a lamellar membrane of negatively charged clay sheets readily dissociates in water within ten minutes. (b) A clay membrane treated in 0.1 M $Al(NO_3)_3$ for one day (left) becomes stable in water even after being soaked for three days (right). All the photos were taken after the solutions were stirred with a lab spatula.

2.9 Experimental Details

Preparation of GO membranes

Graphene oxide (GO) was synthesized using the modified Hummers method[12] with a two-step purification process as reported earlier[56,58] to remove by-product salt and excess acid. Aqueous dispersions of GO at the concentration of 1 mg/mL were prepared in 50 mL batches for making free-standing membranes. GO membranes were prepared by vacuum filtration of the as-prepared dispersions (pH value 3 to 5) through a porous anodized aluminum oxide (AAO) filter (Anodisc, 47 mm in diameter, 0.2 μm pore size, Whatman), a cellulose nitrate, or a Teflon membrane. Since GO sheets block the pores, it typically took 3 - 5 days to filter 50 mL of GO dispersion (1 mg/mL). Free-standing GO membrane can be peeled off the filter paper after drying in air for one day. The thicknesses of GO membranes were around 18 - 20 μm. GO membranes obtained using AAO, Teflon, and cellulose nitrate filter papers are denoted as GO (AAO), GO (Teflon), and GO (CN), respectively.

Corrosion of AAO discs

Aqueous solutions with pH values of 1 - 11 were prepared by modifying deionized water with HCl or NaOH. AAO filters were immersed in these solutions with initial solid concentration of l mg/mL. The supernatant of each solution was collected intermittently initially after soaking for 2, 4, 8, 12, and 24 hours, and then daily up to 8 days, to measure Al concentration by inductively coupled plasma mass spectrometry (ICP-MS, ThermoFisher X Series II). Al concentration was found to increase with soaking time and reach steady values after one day. Three GO membranes

were prepared from dispersions with pH values of 3, 5.5, and 8.5, respectively, to study the effect of pH values on the final membrane properties (**Figure 2.7**).

Synthesis of ZnO membranes

ZnO membranes were synthesized by first soaking GO (AAO) films (around 4 - 5 μm) in 0.1 M $Zn(NO_3)_3$ solution for 1 day, followed by two-step annealing. First, the membranes were heated in air at 150 °C for 2 hours to produce ZnO, and then at 500 °C for another 4 hours to anneal ZnO and decompose GO. Thicker GO film (18 - 20 μm) were used to produce thicker ZnO with sufficient amount of material to obtain XRD pattern.

Characterization

SEM images were obtained on a FEI NOVA 600 SEM microscope. The XRD patterns were collected by a Rigaku Dmax powder diffractometer with Cu Kα radiation (λ = 1.5418 Å) at 40 kV. Stress-strain curves of GO strips (5 mm × 40 mm) were obtained through static uniaxial in-plane tensile tests with a dynamic mechanical analyzer (2980 DMA, TA Instruments). X-ray photoelectron spectroscopy (XPS) measurements were carried out on an Omicron ESCA Probe XPS spectrometer (Thermo Scientific ESCALAB 250Xi). Depth profiling was performed by Ar ion etching of GO membranes to expose fresh surface for collecting spectra. The nominal etching depth was increased stepwise from 20, 40, 60, 80, to 100 nm.

Chapter 3

A Cut-and-Paste Approach to 3D GO-Based Architectures

Material in this chapter is reproduced in part with permission from reference 81, "A cut-and-paste approach to 3D graphene-oxide-based architectures" by Chong Luo, Che-Ning Yeh, Jesus M. Lopez Baltazar, Chao-Lin Tsai, and Jiaxing Huang; Advanced Materials, 30, 1706229[81].

3.1 Introduction: Fabrication of 3D Architectures

Techniques for forming 3D architectures from flat sheets have attracted significant interest for creating new forms of electronics, biomedical, and energy devices[82,83]. Taking inspiration from paper-crafting, one can identify three basic operations needed for creating 3D structures from properly cut sheets, which are folding, bending, and pasting. Folding tends to introduce local plastic deformation of the sheet, and the finished structure can maintain its shape freely. Both stochastic (*e.g.*, crumpling)[33,84] and deterministic folding (*e.g.*, origami and kirigami)[85-88] have been used to create functional material architectures from 2D precursors. J. Luo *et al.* prepared crumpled graphene balls by a novel aerosol method, where an aqueous dispersion of GO sheets was aerosolized to form aerosol droplets. When the droplets passed through a tube furnace preheated at high temperatures, crumpled graphene balls were formed by capillary compression in the rapidly evaporating aerosol droplets. The randomly wrinkled surfaces of crumpled graphene balls make it resistant to aggregation, which can be useful for energy storage applications[33]. Inspired by origami, an ancient art of paper folding, J. Mu *et al.* fabricated an all-graphene self-folding paper where function-designed graphene oxide was used as a nanoscale building block.

They created bilayer macroscopic graphene material papers (MGM papers) with GO-polydopamine (PDA) on one side and r-GO on the other side. Since GO-PDA readily absorbed/desorbed water molecules in response to environmental humidity while r-GO was inert to water molecules, these different water absorption/desorption abilities induced the bending/unbending of the MGM paper upon NIR/laser irradiation. As a result, they fabricated a self-folding box, a wormlike walking device that can walk and turn, and an artificial hand that can hold an object, all driven by light irradiation, which may find usefulness in sensors and robotics[86]. On the other hand, M. K. Blees *et al.* took inspiration from kirigami, an ancient art of paper cutting, and created various graphene microstructures with tunable mechanical properties. For example, kirigami springs were created using photolithography, and their elasticity is determined by the pattern of cuts and the bending stiffness of the graphene. They then prepared highly stretchable graphene transistors based on kirigami springs and showed that the device can be stretched by 240 % and that similar conductance was measured between unstretched and stretched states. Furthermore, they also fabricated graphene kirigami pyramid that can be actuated using an infrared laser, a long strip of kirigami graphene that can be twisted and untwisted by rotating static magnetic field, and a monolayer graphene hinge that can be closed and opened by a graphene arm. Their demonstrations showed that graphene kirigami may have promising potential for applications including remote actuation and environmental-responsive metamaterials[88].

Different from local plastic deformation created by folding, bending introduces local elastic deformation, and the resulting 3D structures are maintained under strain, which is reflected in recent development of pop-up fabrication[83,89]. S. Xu *et al.* presented a method to create 3D architectures based on residual stress-induced bending. They started with planar

micro/nanofabricated silicon ribbons as precursor structures which were bonded to a stretched silicone elastomer at selected points. Upon relaxing the strain in the elastomer, the induced compressive forces led to buckling, twisting, and translational motions in the silicon, transforming these planar silicon ribbons into well-defined 3D architectures with wide geometric diversity. Their method can be potentially realized in many different classes of materials and provided possibilities of using existing fabrication methods and processing techniques to create 3D electronic devices[89].

Lastly, pasting joins separated pieces or different parts of the same sheet together, which is often a necessary step for making even very simple structures such as a box. Complementary to folding and bending, pasting is capable of creating new free-standing geometries that are fundamentally unattainable by folding and bending alone. However, pasting has been much less explored for 3D fabrication, presumably due to limited choice of readily weldable thin film materials or residue-free glues for maintaining the native material properties at the junction.

In this chapter, we demonstrated that graphene oxide paper is one such suitable material platform for cut-and-paste fabrication of 3D structures. GO sheets are made by chemical exfoliation of graphite powders and can stack to form a free-standing paper-like thin film by casting or filtration. GO papers have become a material of great interest due to their intriguing mechanical[32], ionic and molecular transport properties[40,47,80,90], and the ease of converting them to chemically modified graphene (also known as "reduced graphene oxide" or "r-GO")[91-93]. It has long been reported that, once formed (*e.g.*, by filtration), GO papers become insoluble in water[32,47]. However, the work presented in Chapter 2 reveals that processing methods leading to insoluble GO paper often inadvertently introduce multivalent metal cations that electrostatically

cross-link the negatively charged GO sheets[36]. And clean GO papers, as expected, do readily re-disperse to individual single layers in water. Since all GO-based bulk materials such as papers, fibers, or other geometries are made of stacked or folded sheets, the above discovery about the layer-to-layer interactions between GO sheets suggests that pristine GO architectures should always disintegrate in water and can be restructured after water evaporation. Indeed, H. Cheng *et al.* recently noted that broken GO films can be reconnected with assistance of moisture, which they generally attributed to hydrogen-bonding interaction[94]. The scope of this work went beyond connecting GO pieces and demonstrated that water can help to heal several types of damage in GO thin films, release the stress in strained GO structures to reshape GO architectures, and act as a glue to create a diverse array of 3D architectures and dynamic structures using a cut-and-paste approach.

3.2 Healing of Damaged GO Films

GO films were prepared by vacuum filtration of their aqueous dispersion using cellulose nitrate membranes. To avoid ionic contamination that cross-links the GO sheets, the dispersion should be sufficiently washed to remove metal ion by-products from the synthesis[56,58]. Commonly used anodized aluminum oxide filter disk should be avoided to prevent contamination by Al^{3+}[36]. **Figure 3.1** illustrates that water can help to heal damage in GO paper caused by folding and cutting. For example, a fold line in a GO paper becomes its stress concentrator and significantly lowers its strength due to extensive local damage (**Figure 3.1**a1 - a4). Applying a drop of water along the fold line triggers the reorganization of GO sheets in the damaged area, bridging the cracks and flattening the folded area within a minute, leading to largely recovered

strength of the paper (**Figure 3.1**a5, a6). Folded GO papers tend to break at the fold line (**Figure 3.1**a4), while the water healed ones do not (**Figure 3.1**a6), suggesting that the caused structural damage have been repaired. Row (b) in **Figure 3.1** shows a GO film with a more severe laceration type of damage. The cut is about 20-μm-wide and also becomes a stress concentrator, leading to over 50 % reduction in strength (**Figure 3.1**b1 - b3, b5). Applying a drop of water over the cut reconnects it with dissolved GO sheets from the surrounding area within a minute (**Figure 3.1**b4, b6 and cross-sectional scanning electron microscopy (SEM) image in **Figure 3.2**). Although the reconnected part is thinner than the original film, the strength of the healed GO paper was restored to around 90 % of its initial value. Cuts of other shapes, such as circular holes punched by a needle, can also be healed by water (**Figure 3.3**). The limit of the healing effect on the lacerations would be determined by the size of the cut, and the amount of available GO sheets around that area.

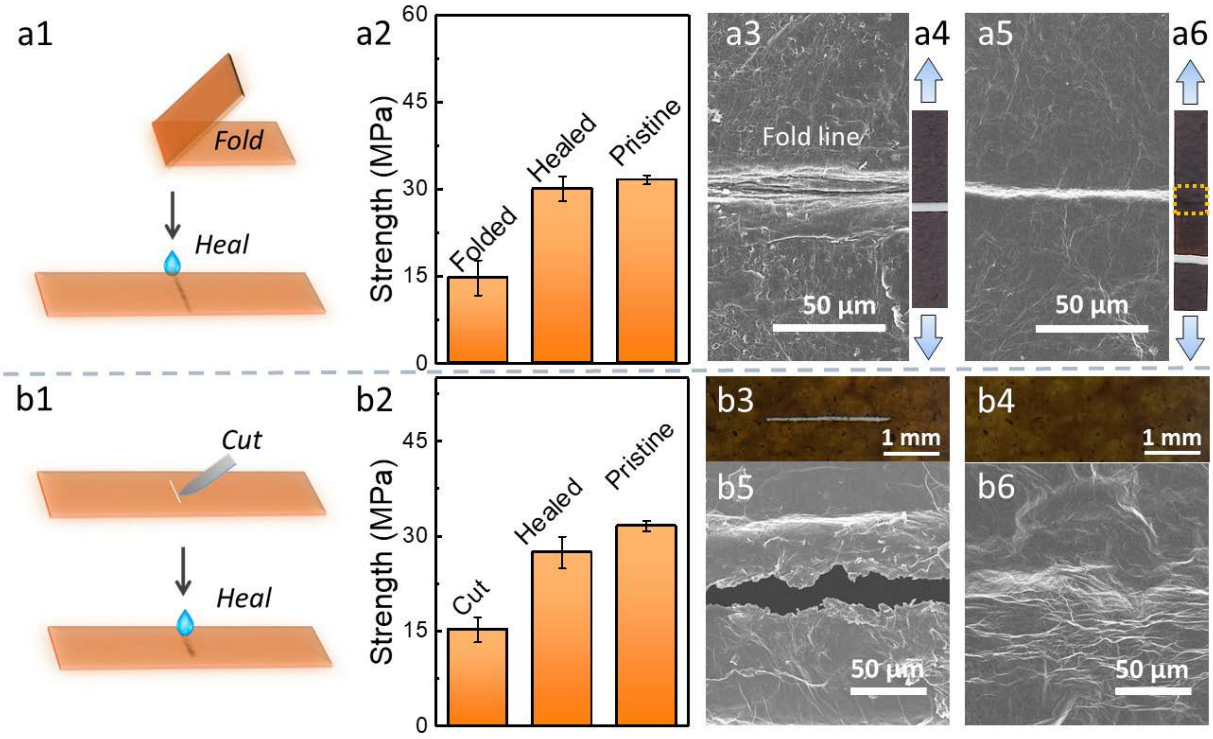

Figure 3.1. Water can heal GO films damaged by folding and cutting, as illustrated by the schematic drawings in the first column. Row (a) shows that a fold line significantly weakens the GO paper (a2), due to extensive local damage (SEM, a3), which eventually fractures along the fold line, located in the center of the strip (photo, a4). After applying water, the folded area was flattened and became crack-free (SEM, a5). The strength of the paper is largely recovered (a2). After tensile test, the healed paper did not break at the fold line (photo, a6, fold line highlighted by the yellow box). Row (b) shows that a "laceration" in GO paper (photo, b3 and SEM, b5) can be healed after applying water, which partially dissolves nearby GO sheets to fill the gap (photo, b4 and SEM, b6), leading to much restored strength (b2).

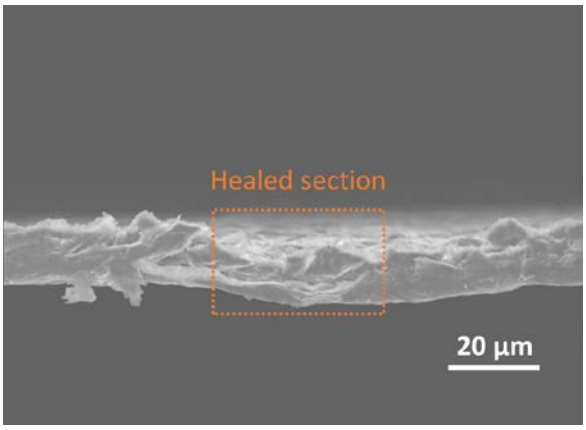

Figure 3.2. Water can heal the cut and reconnect it with dissolved GO sheets from the surrounding area, as evident by the cross-sectional SEM view of a healed cut in a GO film.

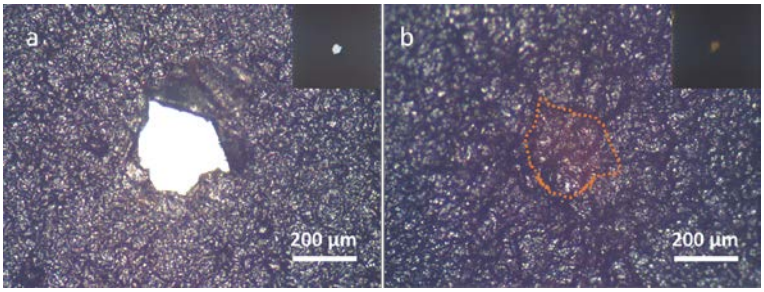

Figure 3.3. A circular hole punched by a needle can also be healed by water. Optical microscopy images showing a needle-punched hole in GO paper (a) before and (b) after healing. Corresponding photos are shown in the insets.

3.3 Reconnection of Separated GO Pieces

In row (a) of **Figure 3.4**, two separated GO pieces are shown to be pasted together with a drop of water as glue to form a long strip. The glued area was around 1 - 2 mm to ensure sufficient contact at the joint. The two strips were fused together within one minute (**Figure 3.5**) and further dried for about an hour before tensile test. The strength of the new long strip was found to be comparable to that of a pristine GO paper, and it does not break at the joint (**Figure 3.4**a1 - a3).

This is due to the formation of a continuous GO junction at the water treated area, which is confirmed by SEM (**Figure 3.4**a4). Similar healing effect has also been observed for thicker GO papers (**Figure 3.6**).

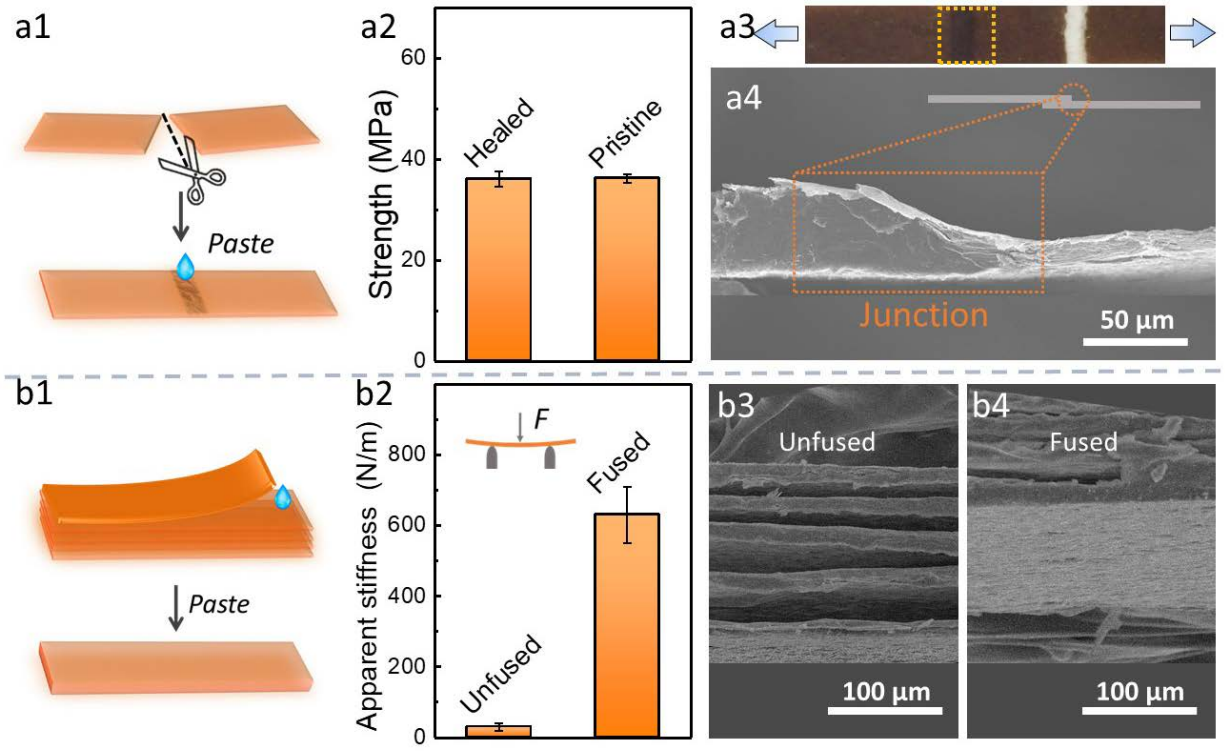

Figure 3.4. Water can paste separated GO pieces together, as illustrated by the schematic drawings in the first column. Row (a) shows that two scissor-cut GO pieces can be joined together by water to form a longer strip with comparable strength (a2), due to the formation of a continuous junction (a4). The glued strip did not break at the junction (highlighted by yellow box) after tensile test (photo, a3). Row (b) shows stacks of 5 GO strips can be glued to yield a thick film (b1). 3-point bending tests (b2) show that the final fused GO film is about 24 times stiffer than the unfused stacks, reflecting the high quality of the bonding between the five films, which is confirmed by the SEM observations (b3, b4).

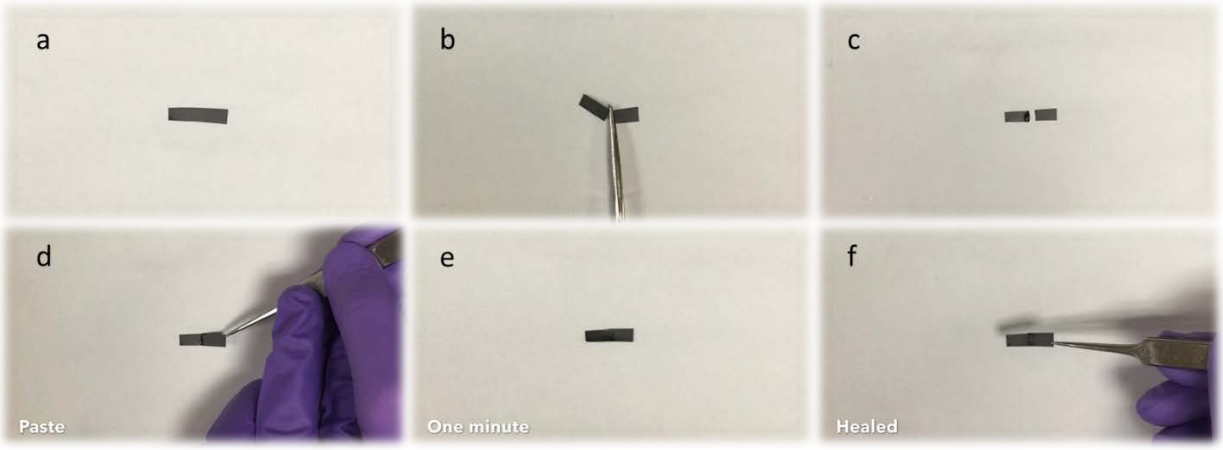

Figure 3.5. Two separated strips can be pasted together with a drop of water as the glue, and the two strips fused together within one minute.

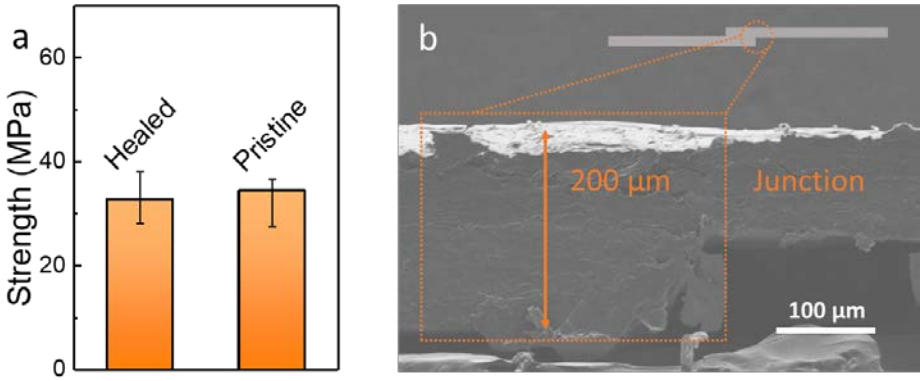

Figure 3.6. Pasting applies for thick GO papers as well. Thick GO papers (100 µm) can also be connected by water to form (b) fused junctions with (a) restored strength.

On the other hand, pasting is a very effective way to make thick GO films, which are very difficult to make by filtration. For example, in our previous experiments, making a 100-µm-thick GO films by filtration would likely take hundreds of hours. However, this can be readily achieved in minutes by gluing a few thinner ones together (**Figure 3.4**b1). An example is shown in row (b)

of **Figure 3.4**, where five stacked GO strips are glued together by water to yield a thick film. The high quality of bonding between the five strips is reflected in the drastically increased bending stiffness of the final film. Based on solid mechanics[95], the bending stiffness of stacked *n* layer films scales with *n*, if there is no inter-layer bonding or friction, but n^3 for perfect bonding between layers. Using 3-point bending tests, we compared the stiffness of five stacked GO films with and without being glued by water and found that the glued one is about 24 times stiffer (**Figure 3.4**b2). This is a strong evidence supporting the high quality of the junctions glued by water, which is also confirmed by SEM observation of their cross-sections (**Figure 3.4**b3, b4).

GO can be readily co-dispersed with other soluble materials, such as clay sheets in water. It can also be used as dispersing agents to process insoluble materials, such as carbon nanotubes (CNTs) in water[28]. These co-dispersions can readily yield GO-based hybrid thin films after filtration or casting. Hybrid thin films of GO/vermiculite (VMT) and GO/carbon nanotubes were also found to exhibit similar healing behaviors using water. They can be glued together by water to form a longer strip with comparable mechanical properties (**Figure 3.7**). Even strips of different material compositions can be connected by water (**Figure 3.8**).

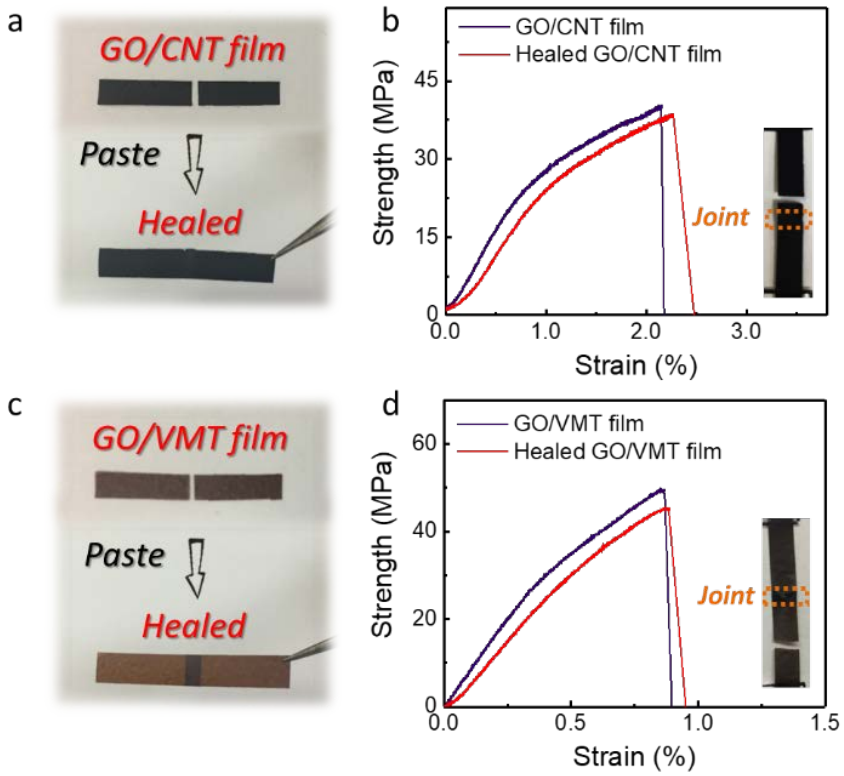

Figure 3.7. GO based hybrid papers can be glued together with restored mechanical properties. (a) Photos showing two GO/carbon nanotubes (CNT) strips glued together by water. (b) Stress-strain curves of a pristine and glued GO/CNT films, which are comparable to each other. The inset shows that the connected film did not break at the joint (highlighted by the orange box) after tensile test. (c) Photos showing two GO/vermiculite (VMT) composite films glued together by water. (d) Stress-strain curves of pristine and reconnected GO/VMT films, which are comparable to each other. The inset shows that the reconnected strip did not break at the joint (highlighted by the orange box) after tensile test.

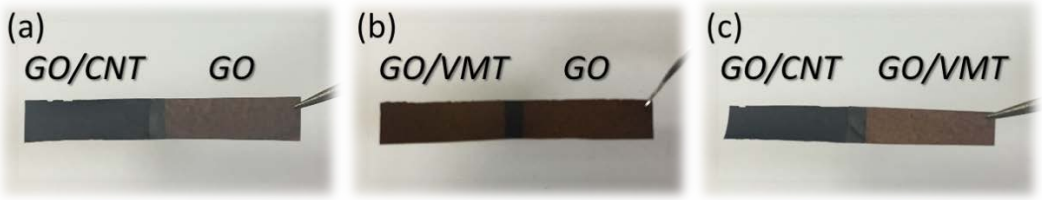

Figure 3.8. Strips of different material compositions can also be connected by water. (a - c) Photos showing strips of different compositions including GO/CNT, GO/VMT, and GO can be glued together by water.

3.4 Releasing the Stress in Pre-Strained GO Papers

Besides the healing effect, water also can be utilized to fix GO papers in various strained shapes by dissipating stress. As illustrated in **Figure 3.9**a - c, a flat GO strip under in-plane compression would buckle, and then return to flat state when the stress is removed. The buckled state is strained and needs to be maintained by stress. However, after the buckled GO strip is exposed to water mist, applied through a handheld ultrasonic nebulizer (**Figure 3.9**e), the shape can be retained even after removing the in-plane compression (**Figure 3.9**f). Upon hydration, GO sheets in the bent GO strip can slide against each other and reorganize in response to the stress, effectively dissipating it and fixing the buckled shape of GO.

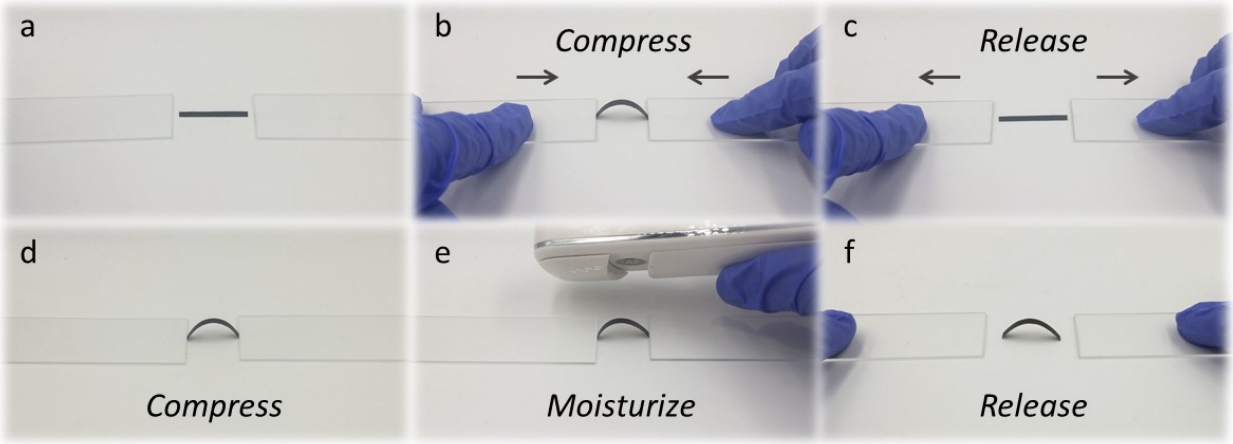

Figure 3.9. Water can dissipate the stress in strained GO shapes and make them free-standing. (a - c) Snapshots showing buckling/flattening of a GO strip upon applying/releasing in-plane compression. (d - f) After exposure to water mist for 30 seconds and dried for another 30 minutes, the compressed/buckled strip can maintain its shape without in-plane compression.

3.5 Cut-and-Paste Approach to Complex GO Architectures

Results in **Figure 3.1**, **Figure 3.4**, and **Figure 3.9** show that water can heal damage, make connections, and release stress in GO paper. Therefore, a cut-and-paste approach can be used to make complex GO architectures that cannot be easily made by other means such as origami or pop-up. **Figure 3.10**a, b shows that circular GO papers of 7.5 cm in diameter is sliced into many 0.5-cm-wide thin strips, which can then be reconnected to a continuous 1-meter-long ribbon. This exemplifies the capability of cut-and-paste approach to transform existing GO structures into new geometries with extreme dimensions. The GO ribbon can be rolled up and fixed in a loose coil shape by the mist treatment (**Figure 3.10**c). It can also be tightly rolled up to form a cylinder when its end is fixed by water (**Figure 3.10**d). Such GO cylinder has large cross-sectional area with GO sheets aligned along the vertical orientation, which could be useful for molecular separation[96] and energy storage applications[97].

Figure 3.10e - i shows a number of additional 3D shapes. A Möbius strip is a one-sided non-orientable surface (**Figure 3.10**e), which can be prepared by water-gluing the two ends of a twisted GO strip. An out-of-plane GO cross, resembling the shape of a crossroad sign, is shown in **Figure 3.10**f, which can be made by pasting two GO strips that are half cut in the center. The two GO strips intersect each other by a line, and the ion channels (*i.e.*, the inter-layer spacing)[80,90] in the four arms are found to be all interconnected (see ionic *I-V* curves in **Figure 3.11**). Such structure could be useful for studying how solvents or ions flowing along one direction affect the ionic or molecular transport in the orthogonal direction (*e.g.*, molecular/ionic gating)[98]. **Figure 3.11**g shows a helical GO coil that can be made by winding a long ribbon on a cylinder, followed by water mist treatment to fix the shape. The helical coil is stable, flexible, and elastic (**Figure**

3.12). **Figure 3.10**h shows a crisscross woven pattern made of GO strips. The overlapping areas of the strips are glued together by water to strengthen the structure. Such structure represents a new strategy to create multilayer GO- and graphene-based laminates with new mechanical properties. **Figure 3.10**i shows a GO loop in butterfly shape made by pasting a ribbon along the wetted periphery of a household cookie cutter, followed by drying. The butterfly shape is chosen to illustrate a complex shape with a number of sharp bending angles (highlighted by blue circles) that cannot be maintained by bending. A free-standing structure with this shape again highlights the stress-release capability of the fabrication approach, which broadens the scope of paper-based 3D fabrication techniques.

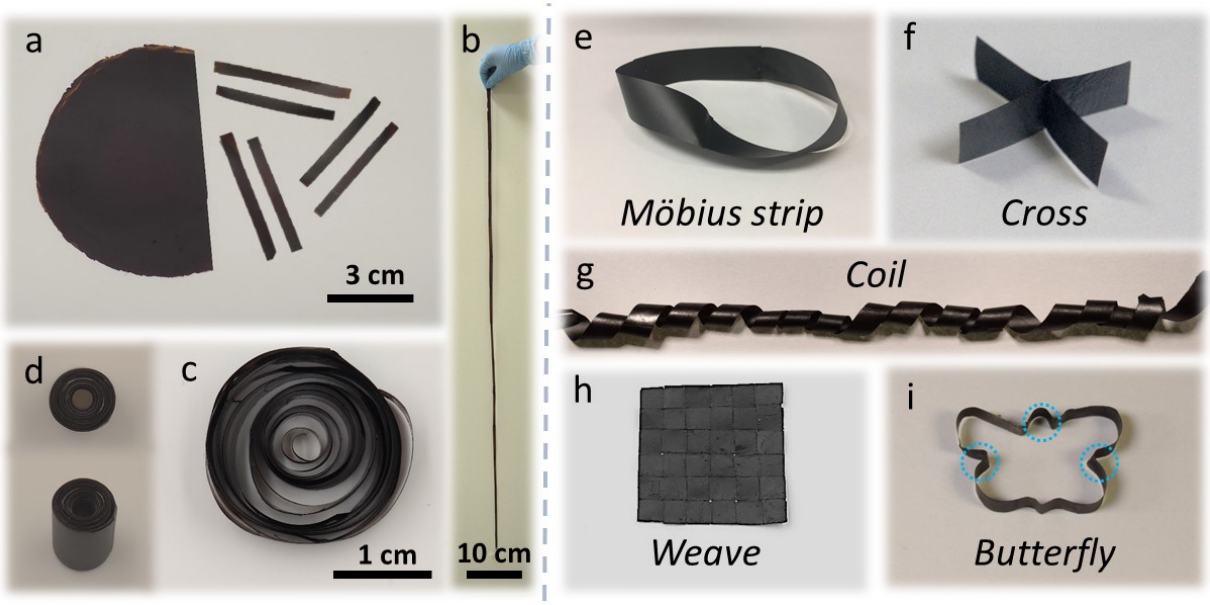

Figure 3.10. Cut-and-paste approach to GO architectures with extended dimensions and new geometries. Circular GO paper is cut into 0.5-cm-wide strips (a), and then glued together by water to form a 1-meter-long ribbon (b), which can be rolled up to form a free-standing loose (c) or tight (d) coil after treatment with water mist. The GO strips can also be glued together to yield complex 3D free-standing architectures such as: (e) a Möbius strip, (f) a “crossroad sign” made of two out-of-plane crossed strips, (g) a helical coil, (h) a crisscross woven mat, and (i) a butterfly shaped loop, in which sharp bending angles are highlighted with the blue circles.

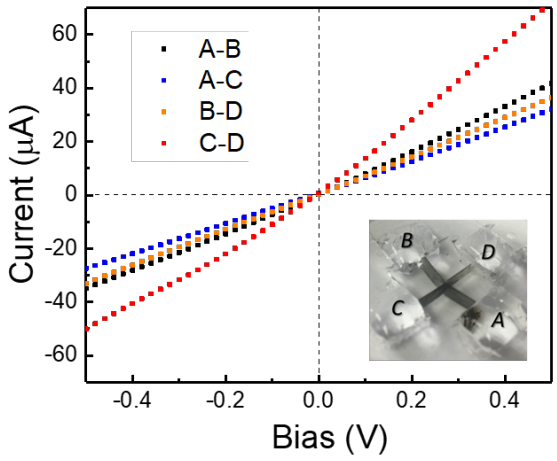

Figure 3.11. The ion channels in GO cross are all interconnected. The I-V curves measured through different combinations of the 4 arms of the cross structure of GO, suggesting that the ion channels are not blocked at the junction. The inset photo shows the geometry for measurement. The 4 reservoirs were filled with 1 mmol KCl solution.

Figure 3.12. A flexible and stretchable GO coil spring.

3.6 Fabrication of Functional 3D Structures

In the session below, precut GO pieces are pasted together to construct functional 3D structures that can dynamically change under IR. The basic strut of these structures is a r-GO/GO bilayer strip (**Figure 3.13**a), which is sliced from a large bilayer paper that can be made by brushing HI solution[93] on one side of the GO film to reduce it to r-GO. A flat r-GO/GO strip (30 mm × 4 mm × 22 μm) can bend upon the irradiation of IR light, curving to nearly 40° within 2

seconds (**Figure 3.14**), and rapidly unbend after the IR light is turned off. The mechanism of such responses is attributed to different degrees of water absorption/desorption in the two layers[86,99]. Upon IR heating, the hygroscopic GO layer can release water and shrink, and reabsorb water from the environment to expand upon cooling. However, the r-GO layer is non-hygroscopic and does not show such photothermal response. This asymmetric photothermal response makes the bilayer bend toward the GO side on exposure to IR. The bilayer struts are then assembled into predetermined structures. An example is shown in **Figure 3.13**a, b, where three bilayer strips were assembled into an H-shape. Next, the two legs in the H were bent into different angles and fixed by water mist (**Figure 3.13**c). This deforms the planar H into a partially standing "push-up" pose. Upon IR irradiation, it transforms into a "sitting puppy" pose (**Figure 3.13**d) in seconds. When IR is turned off, the "puppy" transformed from "sit-up" back to the "push-up" pose. The two poses can be reversibly transformed many times, as long as there is sufficient moisture around the structure to allow rehydration of the GO layer[100]. Besides the structure shown in **Figure 3.13**, a number of other IR transformable structures are also demonstrated, including a five-branch structure that can stand up and lay flat (**Figure 3.15**) and another five-branch standing structure that can rotate (**Figure 3.16**). All of these structures are assembled by cut-and-paste approach, and their motions can be adjusted by the length, bending angle, and relative orientations of the constituting strips.

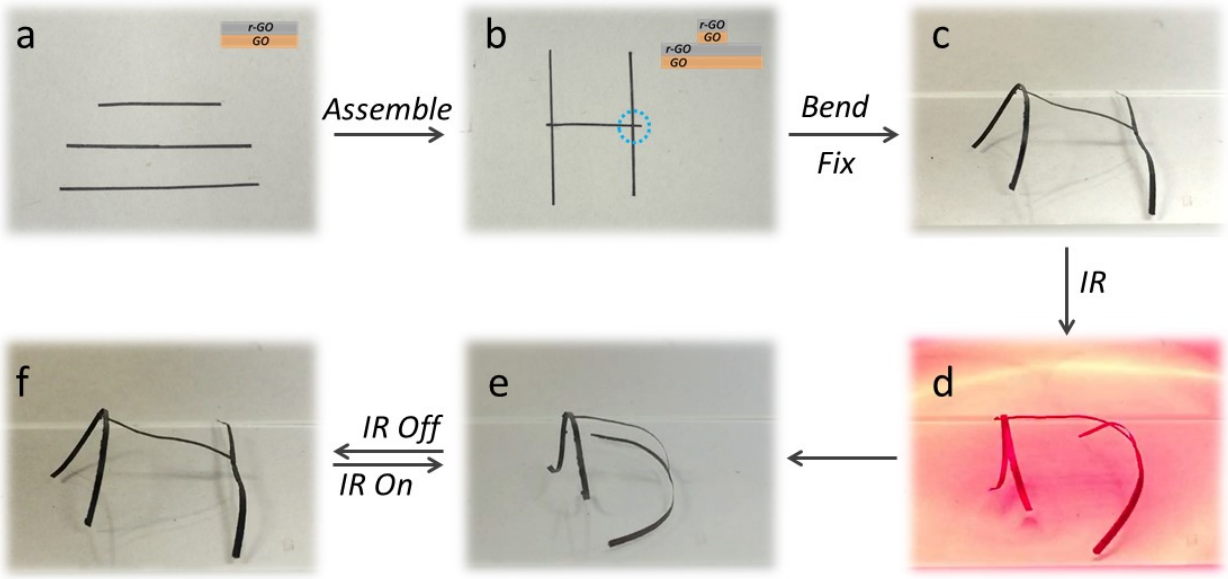

Figure 3.13. An IR-transformable architecture assembled from precut r-GO/GO strips. The starting components, three r-GO/GO bilayer strips (a), are assembled into an H shape using water as glue (b). The drawings in the insets illustrate the cross-sectional view of the junctions. (c) The two legs of the H are bent at different angles and fixed in the "push-up" pose by water mist. Upon IR irradiation (d), bending of the strips transforms the structure to a "sit up" pose (e), which can return to the push-up pose (f) after the IR irradiation is turned off.

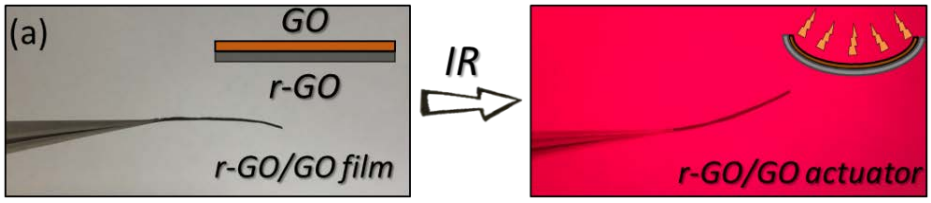

Figure 3.14. IR actuated bending of a r-GO/GO bilayer. A flat r-GO/GO strip can bend upon the irradiation of IR light, curving to nearly 40°.

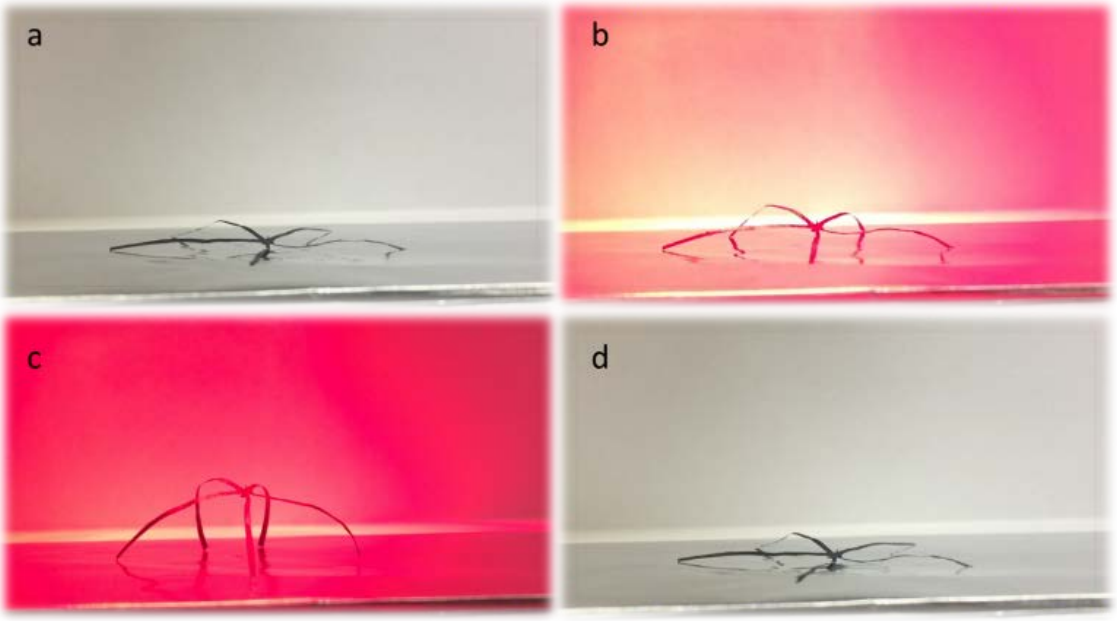

Figure 3.15. A standing up/lying flat starfish structure actuated by IR.

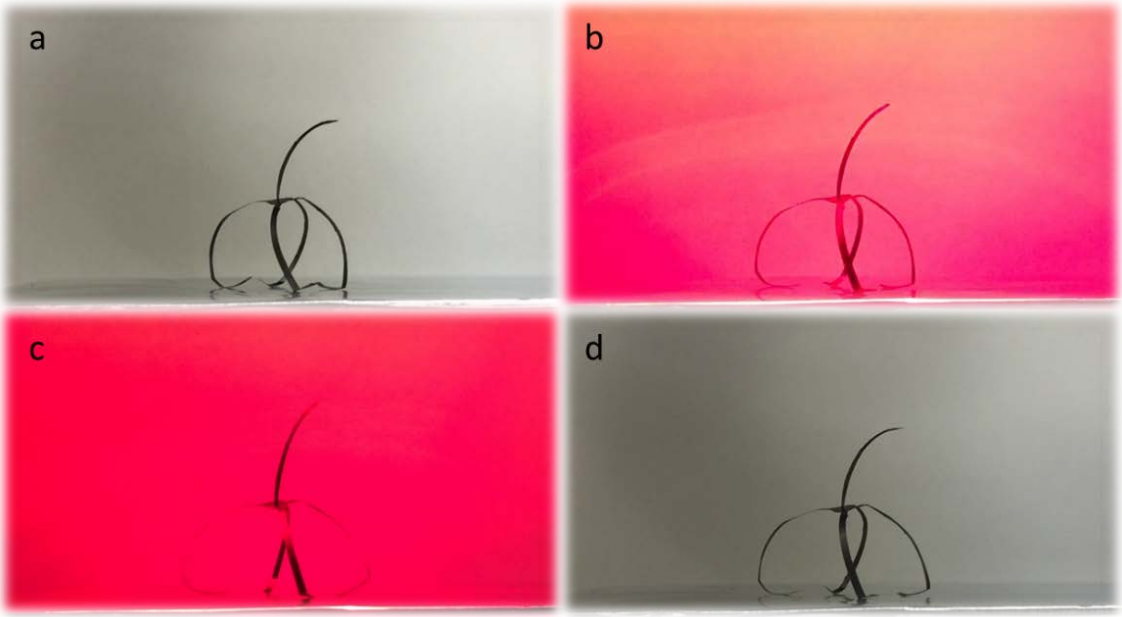

Figure 3.16. A five-branch standing GO structure that can rotate upon IR actuation, reassembling the pose of a ballet dancer.

3.7 Conclusions

In conclusion, water is found to be capable of healing damaged GO paper, connecting separated GO pieces, and releasing stress in strained GO structures and fixing their shape, which inspires a cut-and-paste approach for fabricating complex 3D GO architectures that are fundamentally unattainable by folding and bending. Upon further development, this approach is potentially complementary to origami and pop-up-based fabrication techniques for creating functional 3D structures from paper-like precursors.

3.8 Experimental Details

Preparation of GO films

GO was prepared using a modified Hummers' method and purified by two-step washing to remove ionic by-products[12,56,58]. Stock dispersions of GO (10 mg/mL) were used to make GO papers either by filtration through cellulose nitrate membranes or by casting on glass petri dishes and dried in air for 48 hours. The thickness of these GO films was about 20 - 30 μm based on SEM observation. During filtration, filter disks made of anodized aluminum oxide should not be used to avoid contamination by Al^{3+} ions[36].

Healing and pasting of damaged GO films (Figure 3.1 and Figure 3.4)

GO strips (20 mm × 4 mm) were used for all the experiments here. An unrecoverable fold line was generated by repeatedly folding the GO strip at the same position for five times. Another strip with 2-mm-long “laceration” was made by cutting the film with a surgical blade. Healing was done by spreading a small drop of water (~ 10 μL) on the damaged area and allowing it to dry in

air, which usually takes less than one minute. Similarly, two scissor-cut GO strips were glued together by water with about 2-mm overlap. The two strips were connected within one minute after drying (**Figure 3.5**), and the new long strip was left in air to dry for another hour before tensile test.

IR transformable architectures (Figure 3.13)

The r-GO/GO double-layer film was fabricated by brushing HI solution (57 wt %) on one side of the GO film. This resulted in an asymmetric r-GO/GO bilayer after drying. The bilayer film was sliced into thin strips, which were then used as the strut for building transformable architectures. IR irradiation was applied using a commercial infrared light source (Exo Terra, 100 W) from a distance of about 10 cm.

Characterization

SEM images were obtained on a Hitachi S-4800 SEM microscope. Tensile tests of GO films were performed using a dynamic mechanical analyzer (EltroForce 5500, BOSE). Ionic conductance measurements were done based on previously reported procedure[80], in a geometry shown in **Figure 3.11**, inset. The GO structure was embedded in poly(dimethylsiloxane) (PDMS). Reservoirs were carved in the PDMS to expose each of the four arms of GO paper to 1 mmol of KCl solution. The device was soaked in KCl for overnight before conductance measurements, using Ag/AgCl as the electrodes.

Chapter 4

Binder-Free Graphene Oxide Doughs

Material in this chapter is reproduced in part with permission from reference 101, "Binder-free Graphene Oxide Doughs" by Che-Ning Yeh, Haiyue Huang, Alane Tarianna O. Lim and Jiaxing Huang; *submitted* (2018)[101].

4.1 Introduction: Investigation of GO Dispersions

Graphene oxide (GO), an oxidative exfoliation product of graphite, has gained significant interest as a building block to create graphene-based (*a.k.a.*, reduced graphene oxide, r-GO) materials because of its excellent dispersibility in water and rich functionality[25,26,32,44-46]. GO dispersions are usually used as starting materials to construct various graphene-based architectures through solution-processing routes[18,29,32,35,102-104]. Therefore, it is of great scientific interest and technological importance to investigate the properties of GO dispersions so that 1) appropriate processing methods can be determined, and 2) structures and properties of the final products can be controlled by tuning the inter-layer interactions between the constituent GO sheets.

W. Tesfai *et al.* studied the rheology and microstructure of dilute GO suspension (0.05 mg/mL - 0.5 mg/mL) and investigated the effect of GO loading, shear rate, and temperature on the rheological properties of GO-water suspensions. Their findings showed that the suspensions exhibited shear thinning behavior for a wider range of shear rates and the behavior became more evident with the increase in GO loadings. They also probed the suspension status of the GO sheets *via* AFM and revealed the transformation of thin flakes of GO aggregates in dilute suspensions to

compact disk-like microstructure at higher concentrations[105]. S. Naficy *et al.* expended the investigation of GO dispersions to a higher range of concentrations (0.05 mg/mL - 13.3 mg/mL) and identified four distinct regions: 1) viscoelastic liquid, 2) a transition state consisting viscoelastic liquid and viscoelastic soft solid, 3) viscoelastic soft solid, and 4) viscoelastic gel. In addition, they provided processing techniques that are suitable for GO dispersions at different regions including electrospray, spray coating, inkjet printing, wet-spinning, extrusion printing, and dry-spinning[106]. Further, C. Valles *et al.* looked at the rheological behavior of concentrated dispersions of GO (0.03 vol. % - 8 vol. %) and categorized the behavior into three regimes depending on the GO concentration: 1) a fluid behavior for low concentrations (0.03 vol. %), 2) an intermediate response between fluid behavior and gel behavior at medium concentrations (0.03 - 1.2 vol. %), and 3) a strong-gel behavior at high concentrations (> 1.2 vol. %). They later showed that the results for aqueous GO dispersions can be adapted to more complex graphene-polymer systems and their rheological properties can be controlled by adjusting the degree of interaction between graphene and the polymer matrix[107].

While previous reports provide very useful information on the properties of GO dispersions, the materials studied in prior work are in dilute solution to gel regions, which cannot sustain their own shapes. Therefore, fabricating GO into three-dimensional and self-standing architectures with controlled shapes is challenging and generally requires either elaborate experimental setups or addition of binders and additives into GO dispersions. Thus, there has been strong demands for creating high-concentration and self-sustaining GO to develop scalable assembly methods and to realize practical applications of graphene-based materials.

4.2 Towards Gel-Like and Putty-Like GO

As mentioned in Section 4.1, to make fabrication of 3D GO network more efficiently, various attempts have been made to form gel-like and even putty-like GO materials. Shi group have made a series of study in preparation of GO hydrogels of various composition. They first prepared a nanocomposite hydrogel from GO and PVA solutions where GO sheets formed a network while PVA acted as a cross-linking agent. The GO/PVA composite hydrogel was found to be pH-sensitive – it formed a gel in acidic media and underwent gel-sol transition under alkaline conditions. Lastly, they provided the potential of using the hydrogel for loading and controlled releasing of drugs[108]. In another report, the Shi group introduced DNA into GO dispersions to bridge GO sheets *via* noncovalent interactions and formed a GO/DNA composite self-assembled hydrogel (GO/DNA SH). This GO/DNA SH was stable in various harsh conditions and maintained its form after being immersed in strong acidic, basic, and salty solutions. Further, such hydrogel possessed a self-healing property, which was attributed to the cross-linking of GO sheets by the excessive DNA remained in the hydrogel[109]. Later, the Shi group reported a systematical study to investigate the effects of different driving forces (*e.g.*, hydrogen bonding, π-stacking, electrostatic interaction, and coordination) on the gelation of GO. They demonstrated that 3D GO network was reinforced by increasing the bonding force or decreasing the repulsion force between the sheets. By carefully control the balance between GO sheets' electrostatic repulsion and bonding force, one can design "smart" hydrogels with functional properties such as materials that are responsive to environmental changes[110].

Although the various types of GO hydrogels demonstrate many opportunities to assemble GO sheets into 3D network, it remains challenging to directly manipulate GO materials in a more

straightforward way. To overcome this obstacle, researchers have turned to creating GO with higher mass loadings. A dough is a highly cohesive, malleable, and viscoelastic state of matter that can be readily reshaped without fracture, which is very useful for making free-standing three-dimensional (3D) structures[111,112]. As is with many other particulate materials, a semi-solid state of GO can be obtained by using additives with binder-like functions[113-115]. For example, Shi group created "pottery" of porous graphene materials (PPGM) with the inspiration from the processing of making pottery, including 1) mud-making, preparing a graphene oxide mud (GOM) from the wet cake of GO obtained during GO synthesis without the purification process, 2) formation, shaping GOM into desired structures, and 3) sintering, reducing pre-shaped GOM structures *via* a solvothermal process to fix their shapes and removing impurities by hydrothermal reaction. Using this method, they obtained the final PPGM with a much higher weight density (0.61 g/cm^3) than those of the graphene aerogels (0.16 - 24.4 mg/cm^3) previously reported[116-118]. The PPGM was utilized as the electrode material for supercapacitors, and the PPGM-based supercapacitor showed high gravimetric and volumetric capacitances owing to the high mass density of the PPGM[113]. Alternatively, Y. Jiang *et al.* prepared a GO putty-like material (GOP) by mixing GO aqueous solution with aniline. The GOP can be shaped into various shapes using molds and can also be processed using a household noodle machine. Because of its high viscosity, the GOP maintained the fabricated shape without deformation during processing, which made it a promising 3D printing material[115].

While advantages of direct manipulation of GO into arbitrary architectures have been demonstrated, the work on preparing self-sustaining GO is still limited. The existing methods rely on either the presence of impurities or the introduction of cross-linkers to create mud-like or putty-

like GO, and additional purification steps are required for additives removal. Therefore, it would be desirable to obtain ultrahigh concentration of GO (*e.g.*, > 10 wt. %) in water to see if a dough state is accessible without the need for binders or cross-linkers, which has been challenging. A. Akbari *et al.* used superabsorbent polymer hydrogel beads (in their case, cross-linked polyacrylate based copolymer) to absorb and retain water, which resulted in GO dispersions with concentrations up to 60 mg/mL. During the process, the dispersion had to be agitated by a magnetic stirrer to avoid possible concentration polarization around the beads[104]. This example manifests the difficulties of preparing uniform and concentrated GO dispersions, and concentrations of the dispersions are mostly below 100 mg/mL (about 10 wt. %).

One could in principle obtain ultrahigh concentration of GO in water by drying a dilute solution, or by rehydrating a dried GO solid. The work mentioned above is one of the examples to concentrate GO by drying dilute solutions. Alternatively, evaporation can also remove water from dilute GO solutions, but it is difficult to obtain very thick and uniform GO dispersions due to GO's tendency to go to the air-water surface, which hinders the evaporation process due to their barrier properties[28,31,119]. On the other hand, adding small amounts of water to dried GO solids has also been difficult, because small aliquot of water tends to be absorbed locally, leading to non-uniform hydration. In addition, there had been some misunderstanding concerning the solubility of GO solids in water. It was once believed that GO papers, a very common form of GO solid made by filtration, are insoluble and cannot be re-dispersed in water[32,47].

In Chapter 2, we found that the insoluble GO papers obtained by filtrations are unintentionally cross-linked by the multivalent cationic contaminants released from some filter disks, and neat GO papers are indeed readily re-dispersed in water[36] and can be glued together by

water droplets[81]. It further suggests that the inter-layer interactions between GO sheets can be weakened by water, and all neat GO structures should become dispersible in water. Based on this insight, in this chapter, we report a "continuum" of GO-water mixtures, showing continuous transitions between four states, starting from a dilute dispersion, a thick gel, a malleable dough, and eventually to a dense solid as the water content decreases. This continuum finally completes the scope of GO-water mixtures with the long missing dough state, which typically has a mass fraction of GO around tens of weight percent. GO doughs are found to be highly processable, can be shaped by common processing methods, and exhibit super extensibility[120]. This binder-free dough state of GO is a versatile material platform to fabricate bulk GO and graphene architectures with arbitrary shapes and tunable microstructures, including porosity and sheet alignment.

4.3 GO-Water Continuum

A system consisting of GO and water was prepared along a continuum of increasing concentration of GO, transitioning between four states starting with a dilute dispersion, a thick gel, a malleable dough, and a dense solid as shown in **Figure 4.1**a - d. GO was synthesized by a modified Hummer's method[12,56,58]. Powders of GO were obtained in the form of a filter cake after filtering a dispersion of purified sheets and drying in vacuum. Dilute dispersions (< 2 wt. %) were typically made by dispersing small pieces of dried GO filter cake in water. Direct preparation of higher-concentration dispersions from dried GO was difficult since the apparent volume of GO powders was already comparable or higher than the volume of water needed. Therefore, adding a small aliquot of water usually resulted in local, non-uniform hydration of GO powders. In order to obtain uniform GO-water mixtures with very high GO loadings, aerosolized water mists were

applied to GO foams obtained by freeze-drying, which collapsed upon water uptake. This process allows uniform hydration of GO by a minute amount of water throughout the entire volume of the material, which has been difficult by other means. Further kneading and rolling of the collapsed foam turned the material into a dough state (**Figure 4.2**). The dough state of GO can serve as a precursor to make high-concentration gels by dilution, or denser solids by drying.

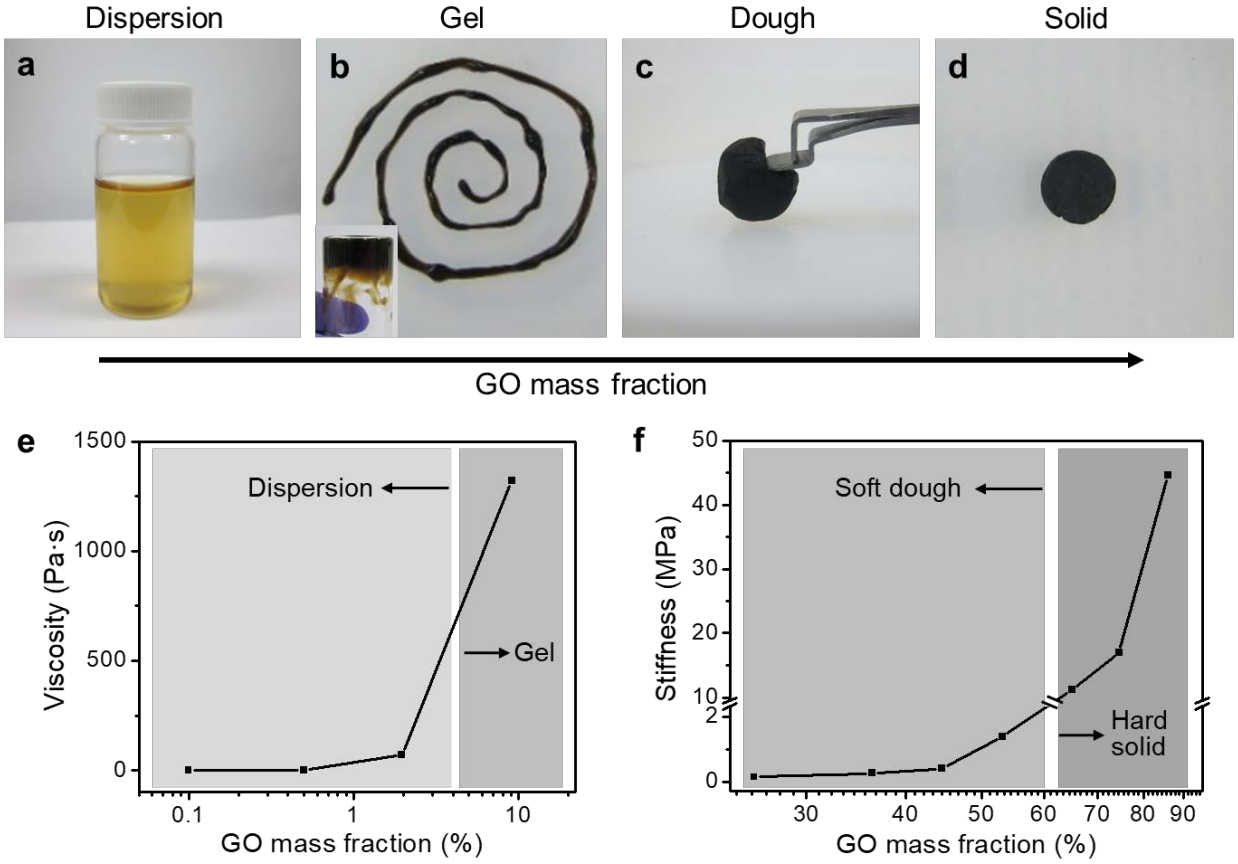

Figure 4.1. The GO-water continuum. Photos showing GO-water mixture transitioning from (a) a dilute dispersion, (b) a thick gel, (c) a malleable dough, to (d) a dense solid, as GO loading increases. (e) The transition from a dilute dispersion to a gel is characterized by a drastic increase in viscosity. (f) A dough-state GO is obtained when the mass fraction of GO exceeds 20 wt. %. GO dough is highly malleable until its mass fraction is increased to over 60 wt. %, after which the stiffness increases significantly.

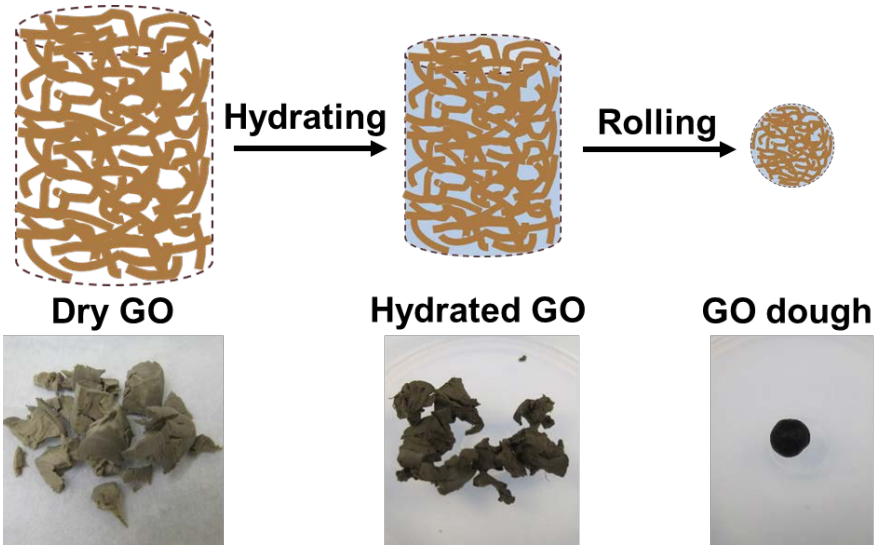

Figure 4.2. Preparation of GO doughs. Schematic diagrams and photos showing that GO doughs were obtained by hydrating dry GO foams with aerosolized water mist. After hydration, GO foams collapsed and turned into hydrated GO, which can then be kneaded and rolled into a GO dough.

Transitions between the four states were accompanied by significant changes in their rheological and mechanical properties. As the mass fraction of GO was increased, the dilute dispersion turned into a thick non-flowing gel as illustrated by the sample in an upside-down vial (**Figure 4.1**b inset). Accordingly, a significant increase in viscosity was observed when the GO mass fraction exceeded 2 wt. % (**Figure 4.1**e). Increasing the GO fraction to over 20 wt. % resulted in a new viscoelastic dough state. Unlike the thick gels, the dough state can be kneaded and rolled on a surface without leaving extensive stains. This dough state can be easily deformed without fracture, and dried to form a dense GO solid that retained the shape (**Figure 4.1**d). The dough state remained highly cohesive and processable until the mass fraction reached about 60 wt. %, after which the mixture became significantly stiffer, as characterized by a rapid increase of its

compression modulus (**Figure 4.1**f). As the loading of GO exceeded 60 wt. %, the solid became fragile and tended to fracture after compression.

Results of viscosity measurements of the GO-water mixtures including dispersions and gels are shown in **Figure 4.3**, showing shear thinning behaviors that can be attributed to shear alignment of sheets and reduced tangling at higher shear rates[121]. Making the gel from the dough state is a lot more straightforward than other methods, and the rheological properties of the gels can be tuned over a large range, by simply adjusting the volume of water added. This allows customization of GO gels for a broad array of materials-processing techniques[122], to create GO and graphene final products.

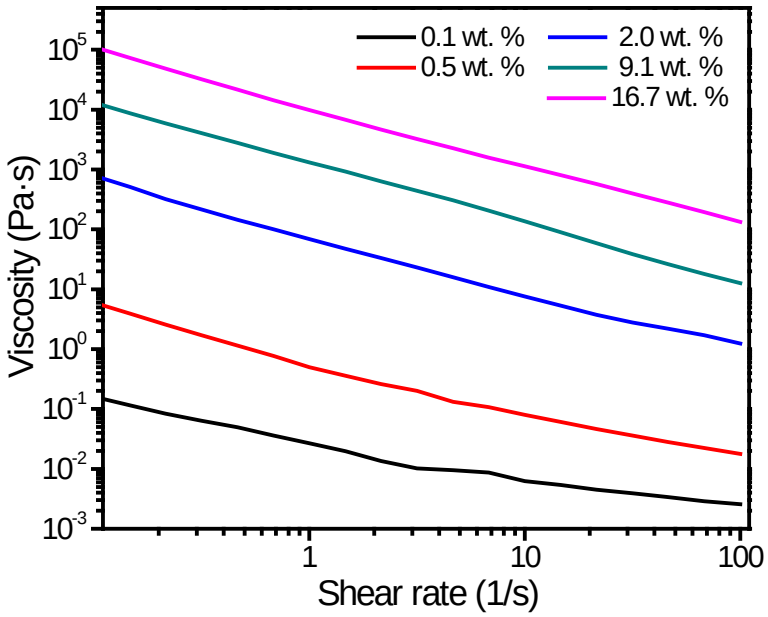

Figure 4.3. Rheological properties of the GO-water dispersions and gels. The evolution of viscosity against shear rate for the GO-water at various GO mass fractions, showing that they are shear thinning and that their viscosities can be tuned over a wide range of values.

4.4 Binder-Free GO Dough

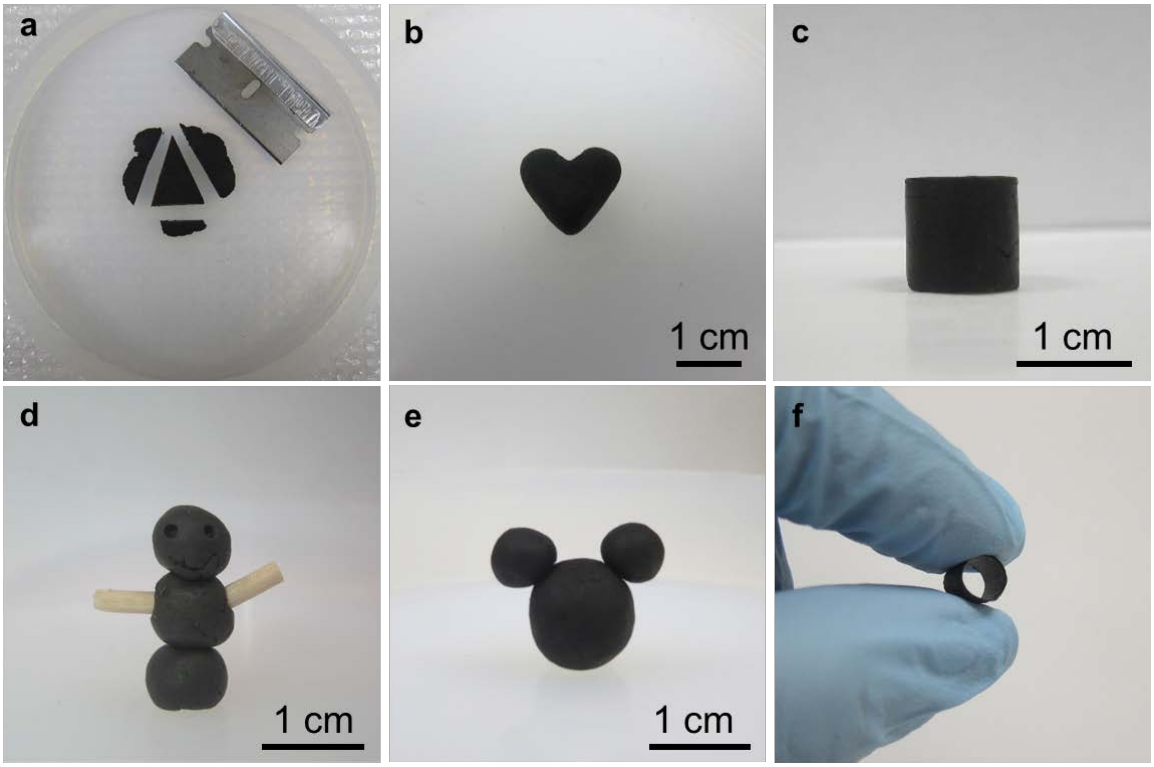

Figure 4.4. GO doughs are highly processable and versatile. GO doughs can be readily reshaped by (a) cutting, (b) pinching, (c) molding, and (d) carving. GO doughs can be easily connected together (d, e) or with other solid materials (d) using the wooden sticks as an example. (f) A tubular GO structure can be prepared by molding a GO dough around a rod, demonstrating the versatility of using GO doughs to make 3D architectures that are otherwise challenging to obtain.

The dough state of GO can be deformed into arbitrary form factors by common shaping methods, including cutting, shaping, molding, and carving (**Figure 4.4**a - d). Pieces of GO doughs can be connected together simply by bringing them into contact followed by gentle compression (**Figure 4.4**e). The versatility of GO dough allows unusual shapes to be made at ease, which has been hard by other means, as illustrated by the example of a tubular structure shown in **Figure 4.4**f. As made GO doughs isotropically shrinks upon air drying, yielding dense solids with

disorderly packed sheets that are heavily wrinkled and crumpled (**Figure 4.5**a - c). X-ray diffraction (XRD) pattern of the dried GO solid does not show an apparent peak around 11°, which is characteristic for lamellar GO structures with long-range stacking order of the sheets (**Figure 4.5**d).

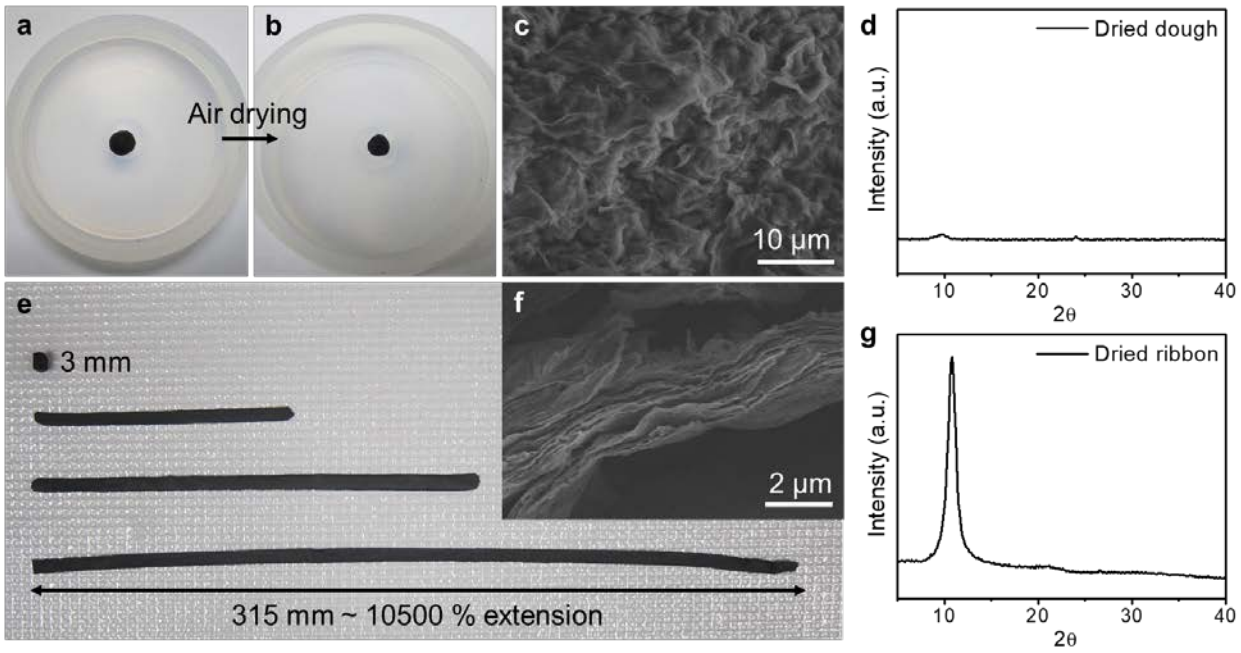

Figure 4.5. Super extensibility of GO doughs. Photos of a ball-shaped GO dough (a) before and (b) after drying in air, showing slight volume shrinkage. (c) Cross-sectional SEM image of the dried solid does not show lamellar microstructure, which is consistent with (d) the lack of a strong diffraction peak in the XRD pattern of the air-dried GO solid. (e) A short block of GO dough can be repeatedly cold rolled to a long GO ribbon with 10,500 % of extension. (f) Cross-sectional SEM image of the dried ribbon shows the development of lamellar microstructure, which is consistent with the strong diffraction peak around 11° in the XRD pattern.

The GO dough can sustain extreme deformation without fracture, exhibiting super extensibility. A proof-of-concept is shown in **Figure 4.5**e, where a 3-mm-long GO block was transformed into a long ribbon by cold rolling with lateral constraint. Two additional rolling steps

were performed to further increase the length to 315 mm, corresponding to an elongation of 10,500 %. The extraordinary extensibility of the GO dough is attributed to both unfolding of the sheets and their sliding under shear. Indeed, the final cold-rolled ribbon has a lamellar microstructure (**Figure 4.5**f). XRD pattern of the dried ribbon shows a strong diffraction peak, corresponding to an inter-layer spacing of 8.18 Å, which is consistent with what has been reported for vacuum-filtered GO membranes[36] (**Figure 4.5**g). Preparing thick GO films by vacuum filtration is quite tedious due to the barrier properties of the sheets that makes filtration process self-limiting. GO dough could thus serve as a more versatile starting material for creating large-area GO films by rolling with the thickness controllable by the gap between the rollers. Since GO doughs are free of binders or cross-linkers, GO solids obtained from GO doughs are all reversible, *i.e.*, they can be re-dispersed in water (**Figure 4.6**).

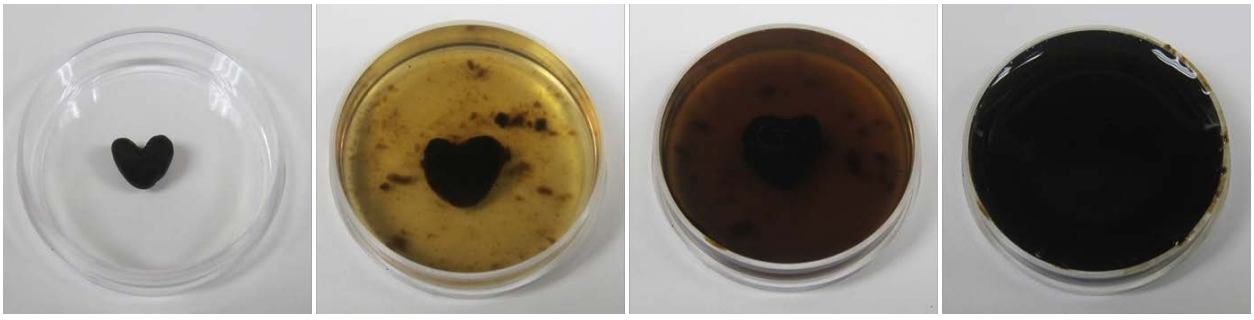

Figure 4.6. Water solubility of GO solids. A dried heart-shaped GO solid prepared from a similarly shaped GO dough can be readily re-dispersed in water and return to a concentrated GO dispersion.

The dough state of GO can be extended to a number of GO-based composites, leveraging GO's surfactant properties to incorporate other components[26,28]. For example, single-walled carbon nanotubes (SWCNTs) can be readily dispersed in water in the presence of GO, which can then be converted into a GO/SWCNT composite dough following the same procedure (**Figure 4.7**).

This GO/SWCNT composite dough is still highly cohesive and processable, which can also be cold rolled into a free-standing membrane, suggesting the potential of preparing composite doughs with various combinations of GO and functional materials based on the preparation method provided in this work.

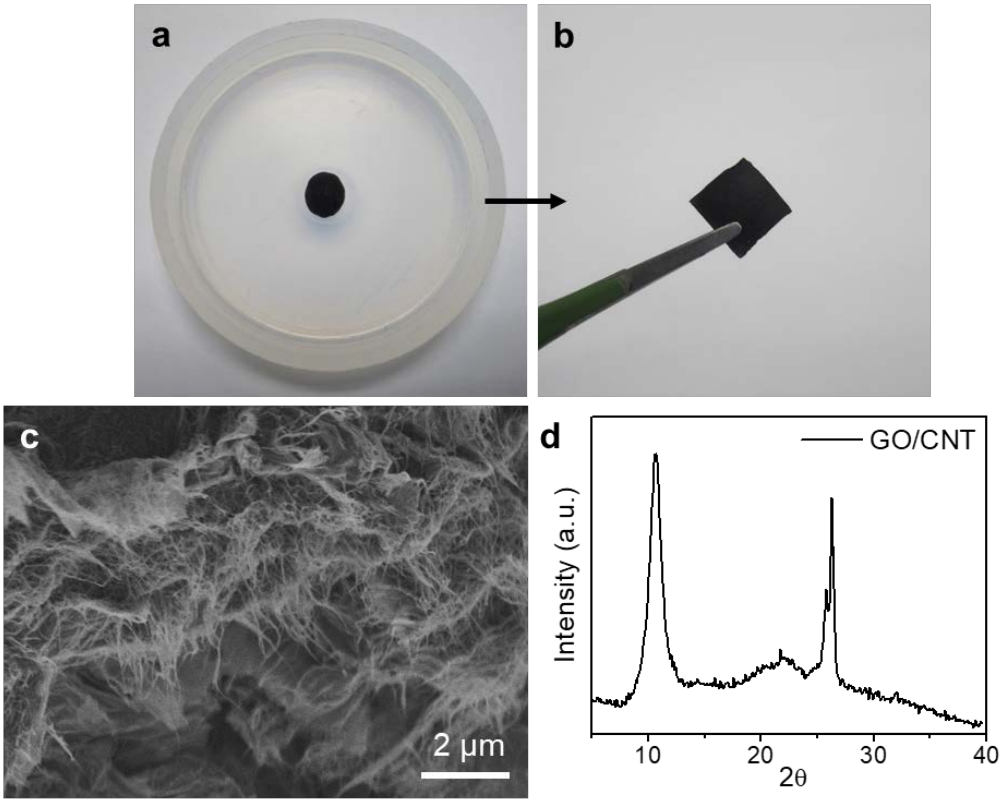

Figure 4.7. Preparation of GO/SWCNT composite dough and membrane. GO dough can serve as a versatile material platform to incorporate other components. For example, single-walled carbon nanotubes (SWCNTs) were added to an aqueous GO dispersion to form a uniform GO/SWCNT dispersion, which can then be converted into (a) a GO/SWCNT composite dough. Such dough was also highly processable and can be cold rolled into (b) a free-standing membrane. (c) Cross-sectional SEM image of the dried composite shows SWCNTs sandwiched between GO layers and (d) the XRD pattern shows characteristic peaks of GO (around 11º) and SWCNT (around 26º).

4.5 Glassy GO Solids

The GO dough is a precursor to prepare dense GO solid with unique isotropic microstructure and properties. Typically GO structures exhibit lamellar microstructures with long-range stacking order of GO sheets[123], which leads to orientation dependent properties. However, since the dough is obtained by a small degree of hydration of GO foam, followed by kneading, the sheets are not aligned. During drying, the dough experiences isotropic capillary compression and gradually densifies by squeezing and deforming the GO sheets. The final microstructure is made of densely packed, heavily deformed sheets without apparent long-range stacking order, which bears strong resemblance to that of pistachio shells[124]. To study the effect of sheet alignment in the properties of dense GO solids, two bulk pellets with similar size, shape, and density but with different types of microstructures were prepared. One pellet was made by compressing a freeze-dried GO foam at 200 MPa to induce alignment of the GO sheets (**Figure 4.8**a, b). Such uniaxial compression indeed rendered the resulting pellet a lamellar microstructure (**Figure 4.8**c) with a strong XRD peak corresponding to an inter-layer spacing of 8.74 Å (**Figure 4.8**g). The other pellet was made by gently molding a GO dough into the same shape, followed by drying in air (**Figure 4.8**d, e). Cross-sectional SEM image of the dried pellet did not show any obvious lamellar ordering (**Figure 4.8**f), which is consistent with the lack of a strong diffraction peak around 11° in the XRD pattern (**Figure 4.8**g). Both types of pellets have similar densities measured to be around 1.5 - 1.6 g/cm^3. The pellet with lamellar ordering is denoted as *l*-GO pellet, while the one with disordered sheets is denoted as glassy GO (*g*-GO) pellet.

Indentation tests were applied to study the mechanical properties of the two types of pellets at both their top and side surfaces. The corresponding force-displacement curves are shown in

Figure 4.8h. In the *l*-GO pellet, the sheets are aligned in parallel to the top surface. Indentation on the side should encounter smaller resistance, because the load can easily cause sliding, deformation, or even partial opening of the lamellar structure. Indentation along the top surface should encounter higher resistance since the force is normal to the sliding direction of sheets. Indeed, the *l*-GO pellet is significantly softer on the side with a measured hardness of 13.38 ± 3.02 MPa, in comparison to 25.29 ± 5.20 MPa measured on the top surface. Contrasting the anisotropic mechanical property of the *l*-GO pellet, the hardness of *g*-GO pellet does not exhibit significant orientation dependence, with a hardness of 133.37 ± 14.76 MPa measured on the top surface and 117.15 ± 12.66 MPa on the side. Similar displacement values were obtained when indenting the *g*-GO pellet from both its top surface and side. The hardness of *g*-GO pellet is drastically higher than those of *l*-GO. This is because the *g*-GO pellet is made of entangled and heavily crumpled sheets, which hinders sliding, making it much more resistant to deformation. Taken together, these results show that GO solids of similar size, shape, and density can exhibit significantly different properties due to different sheet alignment. The GO dough is thus very suitable for creating bulk GO materials with isotropic properties.

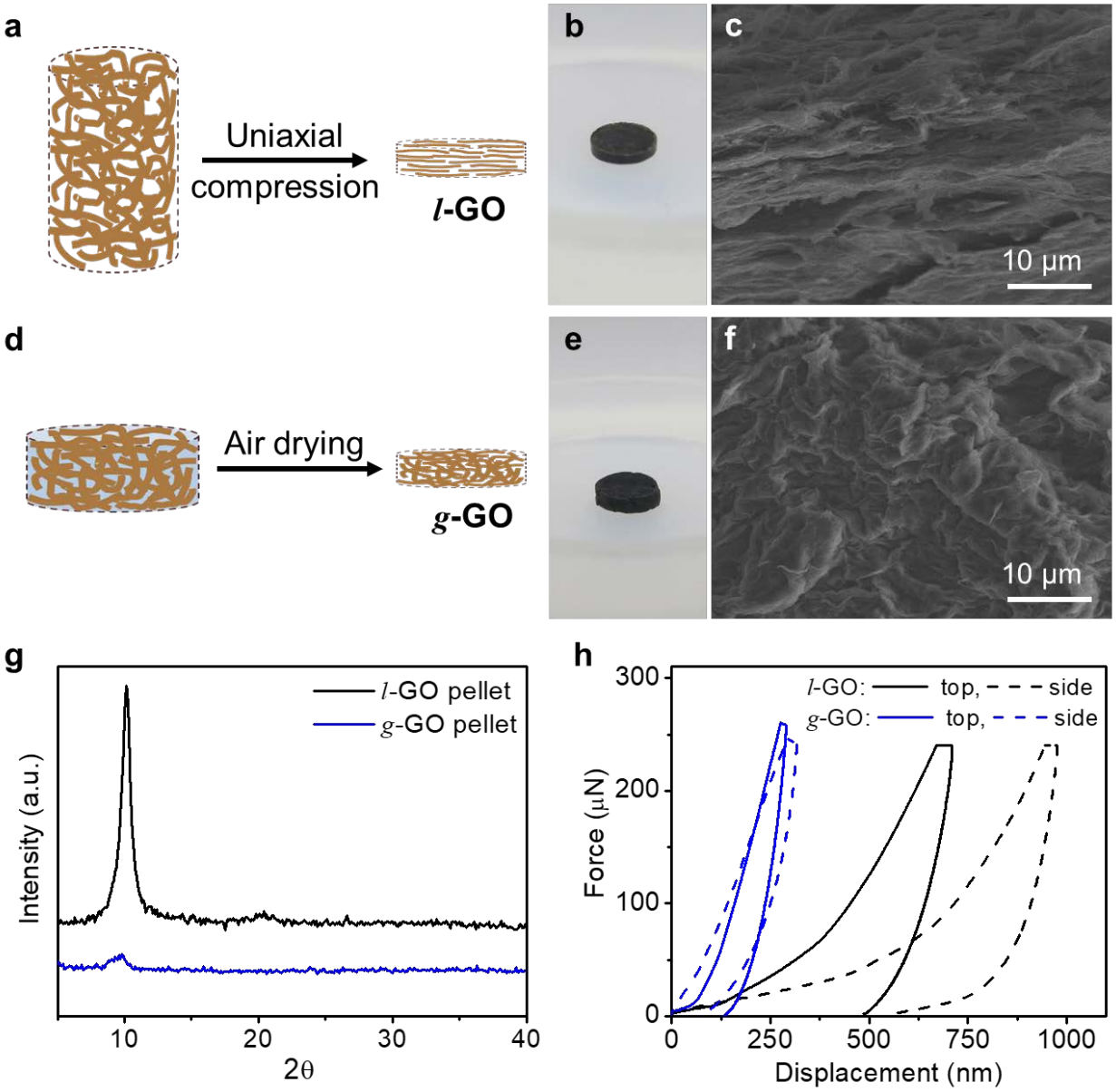

Figure 4.8. Glassy GO solid with enhanced and isotropic mechanical properties. (a - c) Uniaxial compression turns a freeze-dried GO foam to a GO pellet with lamellar microstructure, which is denoted as *l*-GO. (d - f) A glassy GO pellet made of disorderly packed sheets, denoted as *g*-GO, is made by first gently molding the dough into a pellet by hand, followed by drying in air. (g) XRD patterns and (h) nanoindentation curves of the two types of GO pellets. The *g*-GO pellet does not have a strong diffraction peak corresponding to lamellar ordering and exhibits largely isotropic properties and higher hardness.

Sample	Indentation direction	Hardness (MPa)
Lamellar GO pellet	Top	25.29 ± 5.20
	Side	13.38 ± 3.02
Glassy GO pellet	Top	133.37 ± 14.76
	Side	117.15 ± 12.66

Table 4.1. Hardness of lamellar and glassy GO pellets with the corresponding indentation directions.

4.6 Fabrication of GO Foams with Tunable Densities

In addition to making densely packed solids and lamellar membranes, porous GO and r-GO foams can also be fabricated using the same starting GO doughs. Freeze-drying a GO dough fixes its 3D network and results in a GO foam preserving the shape of the corresponding GO dough. Such GO foam can be further reduced by steam annealing to yield an r-GO foam with the same shape (**Figure 4.9**). Using this processing method, we can create GO and r-GO foams with arbitrary shapes and densities by tuning the shape and concentration of the starting GO doughs.

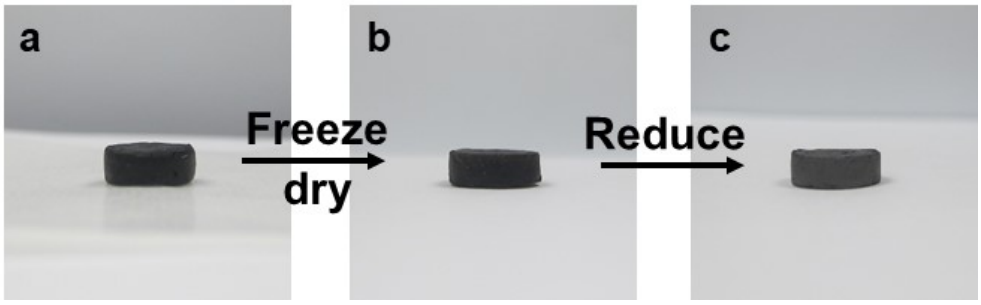

Figure 4.9. Fabrication processes of making a GO and r-GO foam. Freeze-drying a hydrated GO pellet followed by steam reduction removes water inside the dough while preserving its shape and structure.

Figure 4.10a - d show four molded GO doughs with the same amount of GO but are hydrated with different amounts of water to vary the GO concentrations. After using freeze-drying to remove water, GO foams with various densities can be obtained. All the GO foams exhibit porous structures, where large pores are clearly observed for GO foams with the lowest density and the pore size becomes smaller and smaller as the density increases (**Figure 4.10**e - h). A dense and compact microstructure can be seen for GO foam with density of ~ 480 mg/cm^3, and this seemingly compact foam is still porous. Such foams have the potential for solving the issue of low volumetric performance in electrochemical energy storage applications due to the low weight density of porous electrodes. **Figure 4.11** shows the Young's modulus as a function of density for the GO foams prepared in this work. The Young's modulus of porous materials typically scales with density as $E \alpha \rho^n$, where E is the Young's modulus, and ρ is the monolith density[125]. In this work, the Young's modulus is found to scale with density with n ~ 1.21, which is different from bulk CNT- or graphene-based monoliths (n ~ 2 - 3)[102,126-128]. With the Young's modulus scales almost linearly with the density, it indicates the deformation of the GO foams is stretching-dominated, as in a honeycomb-like structure[125]. The processable GO doughs can also be integrated with different materials such as wood sticks to form r-GO "swabs" that can absorb oils either floating on or sinking beneath water (**Figure 4.12**). This provides a potential of fabricating r-GO foams with controlled porosity and shape for oil absorption.

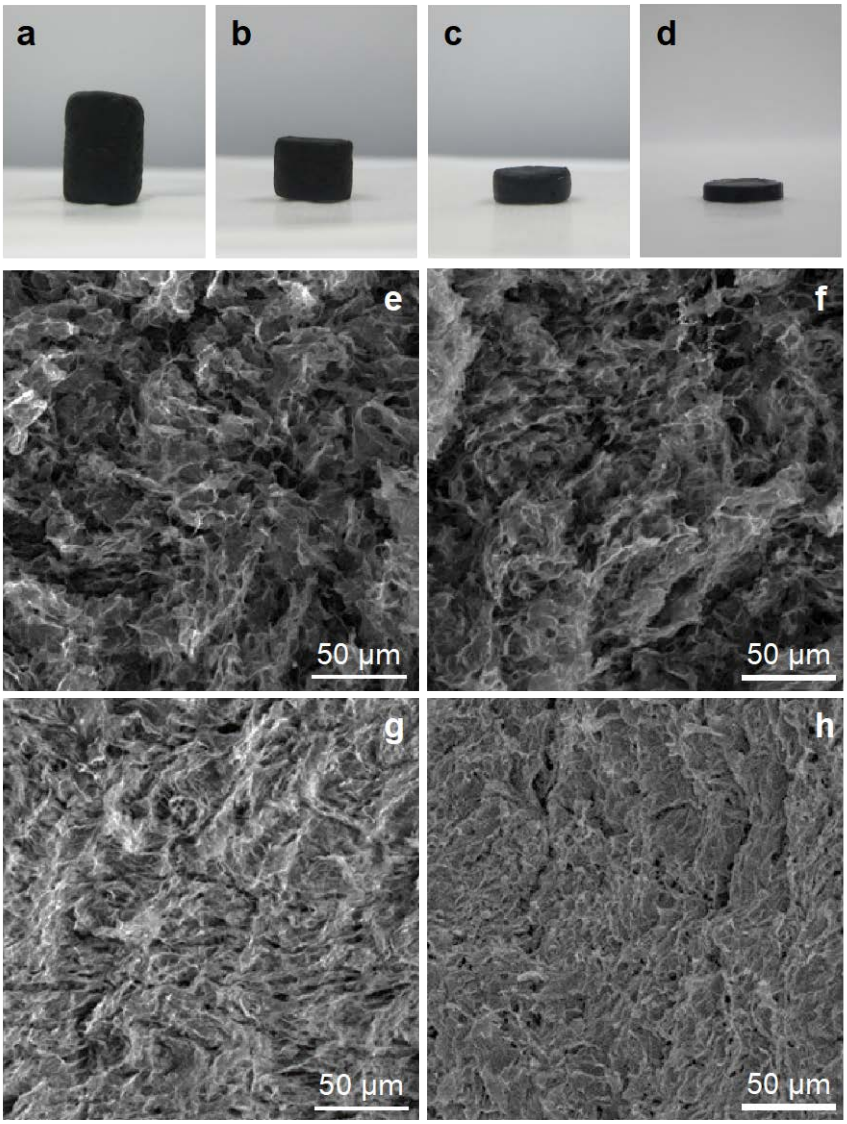

Figure 4.10. Fabrication of porous foams with tunable densities. By freeze-drying GO doughs of different concentrations, GO foams with densities of (a, e) 84.0 mg/cm^3, (b, f) 152.4 mg/cm^3, (c, g) 309.2 mg/cm^3, and (d, h) 478.5 mg/cm^3 can be obtained, with their pore size decreasing as the foam density increases.

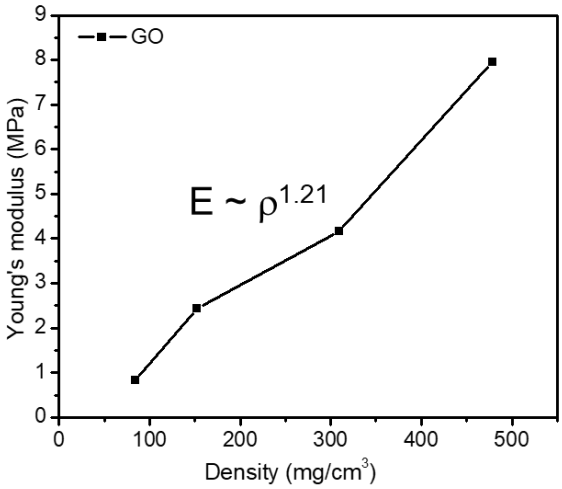

Figure 4.11. The Young's modulus of GO foams scales with their density as $E \sim \rho^{1.21}$, suggesting that the deformation is stretching-dominated.

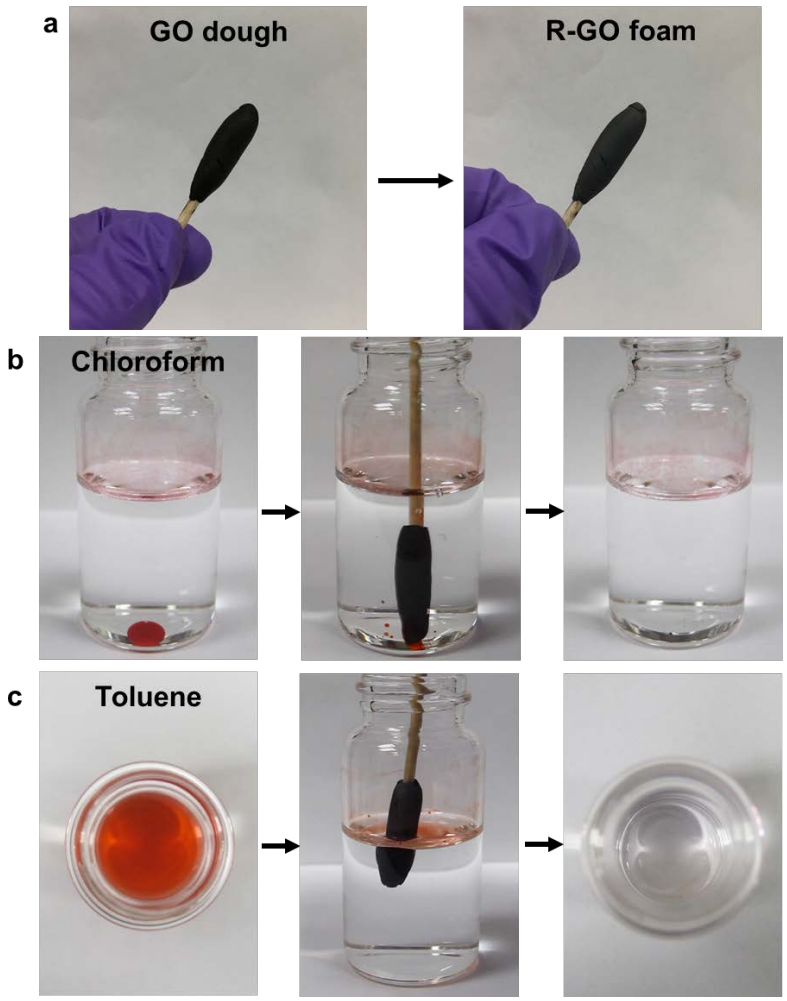

Figure 4.12. Oil absorption of r-GO foam "swabs." The processable GO doughs can be integrated with wood sticks and form r-GO foam "swabs." This design makes the r-GO foams capable of absorbing oils that are either on or under water.

4.7 Graphenic Glass

Since the dough state makes isotropic glassy GO solids readily accessible, it should also lead to glassy graphene solids after reducing GO. In such solids, the graphene sheets are densely but disorderly packed, exhibiting weak long-range stacking order. Therefore, they are named graphenic glass, taking inspirations from bulk metallic glass[129]. To prepare such glassy graphene solid, a GO dough (*c.a.*, 50 wt. %) was first molded into a cylindrical shape, and then reduced by HI vapor[93], followed by washing with ethanol. The dried solid was further hot pressed under 50 MPa at 800 °C to a final density of 1.71 g/cm^3 (**Figure 4.13**a, inset), which is comparable to the densities of compressed graphite materials[130]. XRD pattern of the resulting graphenic solid only shows a very weak diffraction peak around 26°, indicating the stacking of graphene sheets is rather disordered (**Figure 4.13**c).

As is with glassy GO, sheet sliding is also significantly hindered in graphenic glass, which should make them harder than their lamellar counterpart. For comparison, a commercially available high-strength graphite rod with a similar density of 1.78 g/cm^3 (**Figure 4.13**b, inset) was selected as a control sample. Typical processes for manufacturing such bulk graphite materials requires using binders such as petroleum pitch or synthetic resins to form mixed powders with carbon, followed by isostatic pressing to form isotropic blocks. Since binders are being used for making green compacts, an additional baking process is needed to decompose and carbonize the binder. Lastly, the semi-finished products have to undergo graphitization process where they are heated at extremely high temperatures (2500 - 3000 °C) to transform amorphous carbon precursors into graphite[131] (**Figure 4.14**). These processes yield isotropic graphite, which have widespread applications in areas including semiconductor industry and nuclear reactors[132]. Although the

graphite grains still have anisotropic properties, the bulk solid is considered isotropic due to the averaging effect of randomly oriented graphite grains.

The isotropic graphite cylinder sample used in this work has relatively fine grains around 5 μm and is known for its comparatively high strength and hardness, which makes them suitable for making die sets for hot-pressing applications. In contrast, the glassy graphene solid is made of much weaker and less graphitized r-GO sheets. Indeed, Raman spectra (**Figure 4.13**a, b) show that the r-GO sheets in the glassy graphene solid is a lot more defective (with an I_D/I_G ratio of 1.21) than those in the bulk graphite sample (with an I_D/I_G ratio of 0.61) (**Figure 4.13**a, b). Since the two samples have similar densities, and the isotropic graphite is much more graphitized and made of harder grains, one would expect the isotropic graphite should be harder than the graphenic glass. However, Vickers hardness tests show that the graphenic glass (with a hardness of 45.14 ± 1.84 HV_{300}) is actually harder than the isotropic graphite (with a hardness of 28.01 ± 1.29 HV_{300}) (**Figure 4.13**d). SEM images taken on their polished surfaces reveal drastically different microstructures. The graphenic glass has a relatively smooth texture, while the isotropic graphite shows a much rougher and more granular microstructure with visible voids (**Figure 4.13**e, f). Since the two samples have similar densities, they should have comparable level of free volume. Therefore, the smoother microstructure of the glassy graphene suggests that its free volume must be more finely divided and more uniformly distributed throughout the material. The higher hardness of the glassy graphene can be attributed to the finely distributed free volume and entangled network of the sheets within the solid, which renders it higher resistance to plastic deformation. In contrast, although the isotropic graphite has harder grains, it also has more segregated free volumes (*i.e.*, voids), which cannot hinder sliding of the graphite grains, leading

to lower hardness. The hardness of the graphenic glass is also higher than otherwise densified graphene materials including graphene-CNT hybrid solid made by pressure assisted welding[133], and is comparable to that of the bulk graphene nanoplatelets fabricated by spark plasma sintering[134]. Dense graphene monoliths can be obtained from hydrogels made from hydrothermal reactions, and their size and shape are limited by the volume and shape of the hydrothermal reactors[135-137]. Therefore, the GO dough is a more versatile precursor to make bulk graphitic materials with arbitrary form factors, which does not rely on the use of binders, extensive mechanical compression, or high-temperature treatment.

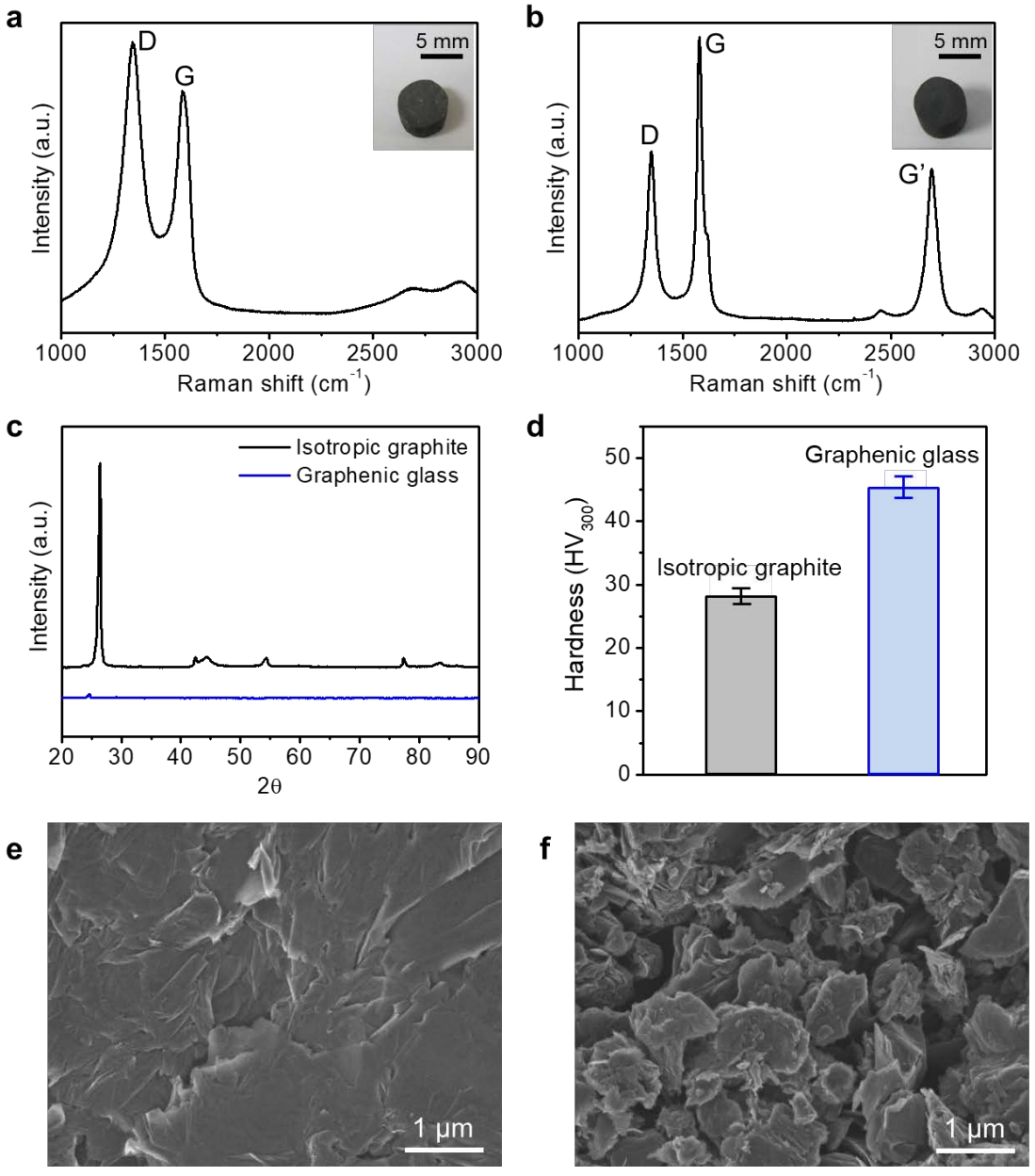

Figure 4.13. Glassy graphene solid. Raman spectra of (a) a graphenic glass and (b) an isotropic graphite, showing that the graphenic glass is composed of more defective graphene sheets (insets of a, b are photos of the two cylindrical samples). (c) XRD patterns show that the isotropic graphite is made of highly crystalline graphite grains while the graphenic glass, at similar density, does not have obvious long-range stacking order of the sheets. (d) Vickers hardness tests show that the graphenic glass is harder than the isotropic graphite, which can be attributed to (e) its smoother microstructure with finely distributed free volume (*i.e.*, voids). In contrast, (f) the isotropic graphite has a much rougher and more granular microstructure, with much larger voids.

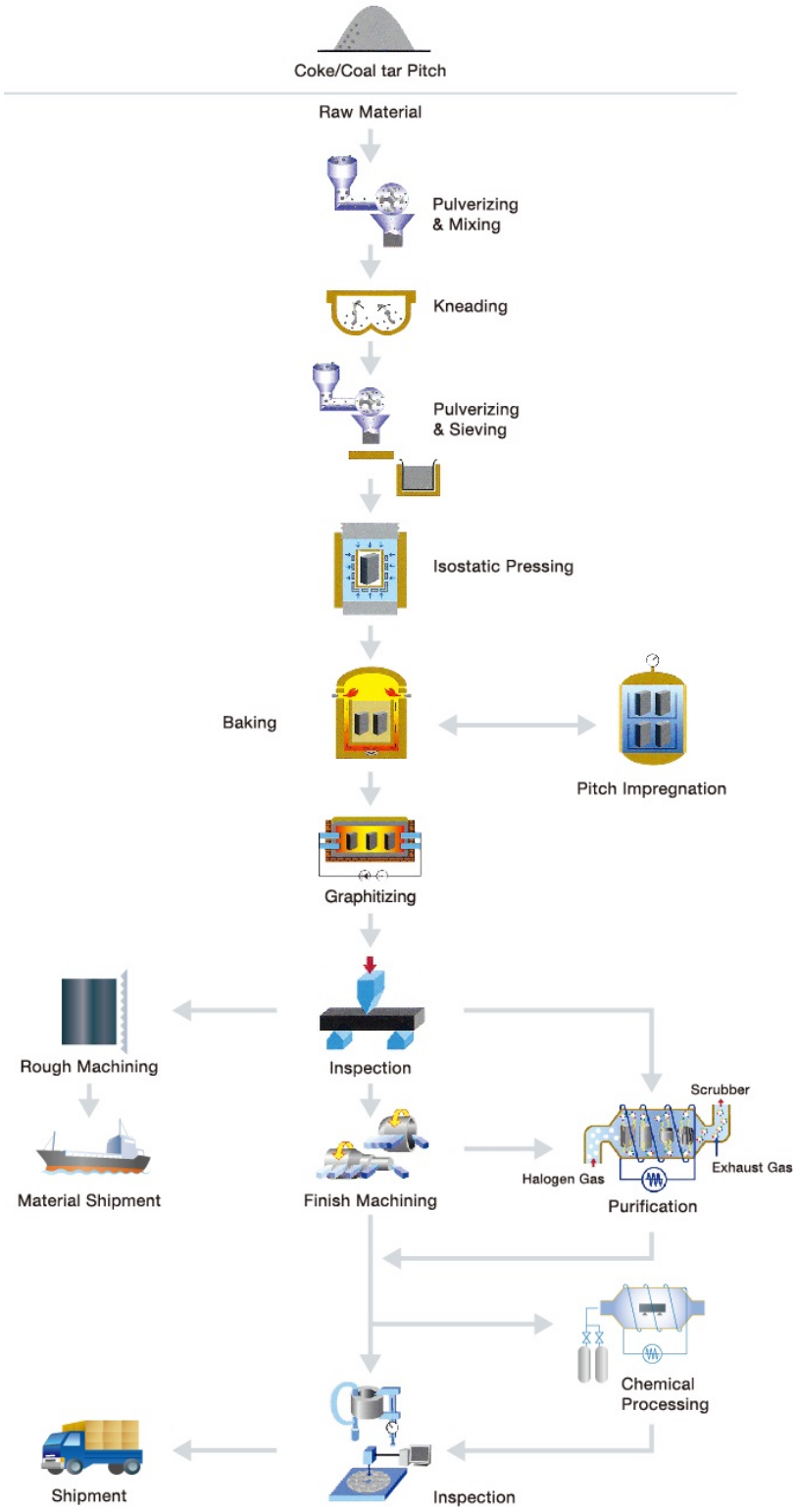

Figure 4.14. Special graphite (isotropic graphite) manufacturing process[131].

4.8 Conclusions and Implications

The GO-water continuum is now completed with a long missing dough state, which can be readily converted to thick gels by dilution or dense solids after drying. The dough state of GO is obtained without any binder and is highly processable. It can be deformed into arbitrary shapes and retains the shapes after drying. The dough can yield dense GO solids with disorderly packed sheets as a result of isotropic capillary compression during drying. Sheets in such glassy GO solids are crumpled and interlocked, leading to isotropic properties and higher hardness.

Glassy graphene solids can be made similarly after reducing GO sheets, which also exhibit isotropic properties. The graphenic glass, although made of less graphitized r-GO sheets, is even harder than commercial high-strength graphite materials due to its unique microstructure limiting sheet sliding. This proof-of-concept suggests the promise of the GO dough for fabricating high performance graphenic glass materials in the widespread applications of current bulk graphite materials.

The dough state is also a highly versatile form of GO that is ideal for manufacturing. The high mass loading and compact form factors of GO doughs make them much more economical to store and transport, and they can turn into high-quality dispersions simply by adding water. Compared to dried powders or films, they are sufficiently hydrated to avoid spontaneous exothermal self-propagating reduction reaction[58], and much safer to handle. GO doughs can also be easily converted to dense GO or r-GO foams with tunable density and porosity. Their extraordinary processability can potentially make GO and graphene as easy to use as common engineering materials to create desirable size, shape, and structures in bulk forms[138].

4.9 Experimental Details

Preparation of GO dispersions

GO was synthesized using a modified Hummers method with a two-step purification process as reported earlier[12,56,58]. Aqueous dispersions of GO at mass fractions below 2 wt. % were prepared by directly dispersing small pieces of dried GO filter cake in deionized water.

Preparation of freeze-dried GO foams

In a typical freeze-drying procedure, 10 mL of GO dispersions at a concentration of 5 mg/mL were prepared in glass vials. Such GO dispersions were then immersed in a liquid nitrogen bath to freeze for 10 minutes. After GO dispersions were frozen, the vials were then transferred to a freeze-dryer, and porous and spongy GO foams were formed after the ice in frozen GO dispersions was completely sublimated (typically in 1 - 2 days).

Preparation of GO doughs

GO doughs were obtained by partially hydrating freeze-dried GO foams using water mist from an aerosol generator. Rolling the hydrated GO foams yielded GO doughs with GO mass fractions generally between 40 - 60 wt. %. The degree of hydration can be further tuned by adjusting the amount of additional water added in the GO doughs.

From GO doughs to gels

Further hydrating the GO dough turned it into a sticky and gel-like material, which can be directly extruded via a syringe. The viscosity of the gel can be tuned at ease by adjusting the amount of water added into the dough.

Glassy GO solids

GO doughs were molded into arbitrary shapes such as a heart, a ball, and a pellet. Freeze-drying preserved their size and shape, leading to high-density foams. Air drying or vacuum drying the GO doughs resulted in dense GO solids with isotropically packed sheets that also became crumpled. Such solids are named glassy GO solids due to lack of long-range stacking order reflected in their XRD patterns.

Preparation of lamellar and glassy GO pellets

High-density lamellar GO pellets were prepared by directly compressing freeze-dried GO foams in a stainless steel die at a pressure of 200 MPa. Glassy GO pellets were prepared from GO doughs, which were first molded into pellets by gentle pressing in a Teflon die by hand, followed by drying in air. The two pellets were fractured in order to study their mechanical properties perpendicular to the top surface of the pellets.

Graphenic glass

GO doughs with mass loading over 50 wt. % were reduced using hydroiodic acid vapor[93]. GO doughs were put in a glass petri dish, and the petri dish was placed in a sealed beaker containing 1 mL of HI solution, which was then heated to around 60 °C for 2 days. The reduction process yielded r-GO solids with volume shrinkage. The r-GO solids were then washed with ethanol, after which they were loaded in a graphite die and hot pressed at 800 °C under a pressure of 50 MPa for 10 minutes. The heating rate was 5 °C/min.

Isotropic graphite

Based on a survey of disclosed isotropic graphite properties, two isotropic graphite rods with higher strengths and hardness were purchased from MERSEN USA Greenville-MI Corp. and McMaster-Carr for hardness measurement. The sample from MERSEN USA Greenville-MI Corp. was measured to have a higher hardness and was chosen as a control sample.

Characterization

SEM images were obtained by field emission scanning electron microscopy (NOVA NanoSEM 600 and Hitachi SU8300). The XRD patterns were collected with a Rigaku Dmax powder diffractometer with Cu Kα radiation (λ = 1.5418 Å) at 40 kV. Static mechanical uniaxial compressive tests were conducted with a dynamic mechanical analyzer (EltroForce 5500, BOSE). Rheological characterization was performed on a rheometer (Anton Paar, MCR 302) using a stainless steel cone-and-plate geometry at room temperature. Hardness was obtained via nanoindentation (Hysitron TI 950 Triboindenter) using a standard three-sided pyramidal Berkovich probe with contact areas of around 1-20 μm^2. Since the grains of commercial isotropic graphite are bigger than the nanoindentation tip, its hardness was measured using Vickers hardness tests on a Duramin 5 (Struers) microhardness tester equipped with a square-based pyramidal diamond indenter. An indentation load of 300 gf and a holding time of 10 s were applied with contact areas of around 6000 - 12000 μm^2. Raman spectroscopy was performed with a laser beam wavelength of 532 nm (Acton TriVista CRS System).

Chapter 5

Overall Conclusions and Outlook

Over the past decade or so, the interest in graphene oxide has resurged mainly because of the discovery of graphene. GO and its r-GO products have been extensively utilized for a wide variety of applications. For various forms of graphene-based materials, understanding the inter-layer interactions between the sheets is of great importance because it helps to better design processing strategy, control the structure of the assemblies, and thereby determine the properties of the final products. This dissertation first looks into the layer-to-layer interactions in stacked GO sheets in GO membranes and presents a puzzle: while GO membranes are often times reported as highly stable in water, they should disintegrate because individual GO sheets dissolve in water very well. Our findings provide answers to this apparent contradiction and show that pristine GO membranes indeed disintegrate in water, and that it's the metal ion contaminants unintentionally introduced during synthesis and processing of GO that render the stability of membranes in water. Apart from affecting the water stability of GO membranes, the unintentionally introduced contaminants also have influence on the mechanical properties of the membranes. GO membranes have been reported to possess superior mechanical properties, raising great attention in the community. Yet this work shows that some of the GO membranes with high stiffness might already have been cross-linked by the contaminants from the AAO filters. Therefore, this work resets the base of membrane mechanical properties. We expect that this will help researchers handle these membrane materials in a more appropriate fashion and inspire further work on designing strategies to strengthen the membranes and to stabilize them in water.

As for ion-stabilized GO membranes, because they remain stable in water with swollen inter-layer spacings, they are utilized for template-assisted synthesis of layered materials. The two-dimensional, large-area, and continuous inter-layer spacing between the GO sheets with vertical spatial confinement can help guide the formation of two-dimensional inorganic materials. In fact, a similar method has been utilized in a later report where two-dimensional oxide nanolayers including TiO_2, ZnO, Fe_2O_3, and SiO_2 were synthesized inside the gaps of GO papers[76]. It will be very interesting to study materials growth in the nanosized gaps between the GO layers which might lead to unique properties that are absent in their bulk counterparts. In addition, previous work presented in the Huang group have shown that hydrating the two-dimensional galleries between stacked GO sheets created a network of nanosized two-dimensional ion channels. Nanofluidic ion transport through GO paper was demonstrated, and the characteristic surface-charge-governed ion transport was enabled by the negatively charged GO sheets[80]. Now that our work shows ion contaminants could be unintentionally introduced on GO sheets during synthesis and processing, it is therefore worthwhile to re-visit the compositions of the GO papers because ion contamination should change the charge distribution in the papers and thereby influence their ionic transport properties.

Next, let's move our attention back to pristine GO papers. The inter-layer interactions between GO sheets in clean papers suggest that all pristine GO structures should disintegrate in water since they are made of stacked or folded GO sheets. A "cut-and-paste" approach is inspired by this implication, and water is found to heal damaged GO, reconnect GO pieces, and release the stress in pre-strained GO papers. This approach provides potential to transform existing GO structures into new geometries with extreme dimensions, which cannot be obtained by traditional

fabrication methods. The capability of making GO into unique geometries such as a Möbius strip and a cross should inspire further study. For example, how would ions transport in cross-shape nanofluid nanochannels? Would ions flowing through one direction cut off the passage for ions flowing through the other direction? Furthermore, GO membranes consisting horizontally stacked GO sheets have been extensively used for desalination, water purification, and ionic and molecular separation[30,39,47,53,55]. However, ions and molecules have to travel in the direction perpendicular to the stacked GO sheets and zigzag through the membrane. The tortuous path drastically increases the travel length and slows down the transport of ions and molecules. If the nanosheets that form the channel walls were oriented vertically, then the transport properties can be greatly improved. A possible way to make GO membranes with vertically aligned sheets is to first prepare a GO membrane that is sufficiently thick, followed by cutting a thin slice out of the thick membrane. However, it has been very difficult and time-consuming to make thick GO membranes by filtration. This obstacle can now be overcome by the pasting approach, which provides an effective way to fabricate thick GO membranes and opens up opportunities to study ionic and molecular transport in the vertical direction. Yet, another possible research direction is to investigate the effect of different glues. Water is used in this work since GO dissolves in water very well. Changing a different solvent might alter the evaporation rate and affect the reconstruction process of GO sheets, which will then influence the properties of reconnected or reshaped GO structures. This line of study can provide further information to comprehend the cut-and-paste approach.

Moving on, a GO-water continuum with continuous transitions between states of a dilute dispersion, a thick gel, a malleable dough, and a dense solid is demonstrated, as the water content is reduced. This work focuses on the investigation of the dough state since it is a new state of GO

with great processability (you can literally manipulate it like playing with play doughs). The GO dough serves as a versatile material to construct free-standing and three-dimensional GO structures with arbitrary shapes. Air drying a GO dough yields a dense GO solid with disorderly packed sheets; however, its microstructure can be tuned by designing appropriate processing methods. For example, cold rolling shear aligns the GO sheets and renders the GO dough super extensibility. Remarkably, a block of GO dough can be extended to a long lamellar strip with extension degrees as high as 10,500 %. Apart from making densely packed solids and lamellar films, porous GO foams with tunable densities and pore sizes can be prepared by altering the water content within GO doughs followed by freeze-drying. The GO dough therefore provides a great material platform to fabricate three-dimensional architectures with controllable structures and shapes.

In this work, we demonstrate that SWCNTs can be incorporated in the starting GO dispersion and the resulting product still remains a dough-state. One can immediately think of introducing other materials for functional purposes. For example, RuO_2, MnO_2, and Co_3O_4 are commonly used electrode materials for supercapacitors. Once they can be dispersed well in GO solutions as starting materials, the resulting GO/oxide doughs may serve as good precursors to form binder-free electrode materials and their density and porosity can be tuned by controlling the concentration of the corresponding composite doughs. Meanwhile, among the various forms of graphene-based architectures, graphene-based porous foams are of great interest owing to their promising potential for electrochemical energy storage applications (*e.g.*, supercapacitors and Li-ion batteries)[139-142]. However, for graphene-based foams prepared from dispersions, the resulting foams usually have low densities because of the low mass fraction of starting GO dispersions, which limits their potential for practical applications due to low volumetric performance[143,144].

Instead, using the GO dough as a starting material, we can obtain high-density yet still porous r-GO foams, which could lead to more compact and high-performance electrochemical energy storage devices. Further, the doughs prepared in this work are composed of either GO or GO/SWCNT composite, the next challenge would be to create a dough-state r-GO, which can be readily used as a flexible and conductive material. One day, perhaps there will be a "transformable battery" which can be deformed into various shapes and charge our laptops, cell phones, and even cars right away!

Lastly, a dense GO pellet with disorderly packed and heavily deformed sheets is prepared from air drying a molded GO dough. Such a pellet exhibits a much higher hardness than the GO pellet with a lamellar microstructure, and it also shows an isotropic mechanical response to indentation. Layered ordering is commonly seen in dense GO solids, and making GO solids without long-range stacking order reminds us of the vitrification process where a substance is transformed into a glass. Bulk amorphous metal (also known as "bulk metallic glass") has been reported to exhibit superior strength and hardness than the crystalline metal[145]. With the capability of making a bulk "glassy" GO and r-GO, we expect to see some very interesting properties other than those of their lamellar counterparts, and this could potentially open up a new line of research.

References

1 Novoselov, K. S., Geim, A. K., Morozov, S. V., Jiang, D., Zhang, Y., Dubonos, S. V. *et al.* Electric field effect in atomically thin carbon films. *Science* **306**, 666-669, (2004).

2 Allen, M. J., Tung, V. C. & Kaner, R. B. Honeycomb carbon: A review of graphene. *Chemical Reviews* **110**, 132-145, (2010).

3 Schwierz, F. Graphene transistors. *Nature Nanotechnology* **5**, 487-496, (2010).

4 Stankovich, S., Dikin, D. A., Dommett, G. H. B., Kohlhaas, K. M., Zimney, E. J., Stach, E. A. *et al.* Graphene-based composite materials. *Nature* **442**, 282-286, (2006).

5 Stoller, M. D., Park, S. J., Zhu, Y. W., An, J. H. & Ruoff, R. S. Graphene-based ultracapacitors. *Nano Letters* **8**, 3498-3502, (2008).

6 Xiang, Q. J., Yu, J. G. & Jaroniec, M. Graphene-based semiconductor photocatalysts. *Chemical Society Reviews* **41**, 782-796, (2012).

7 Wan, X. J., Huang, Y. & Chen, Y. S. Focusing on energy and optoelectronic applications: A journey for graphene and graphene oxide at large scale. *Accounts of Chemical Research* **45**, 598-607, (2012).

8 "The Nobel Prize in Physics 2010". *Nobelprize.org.* Nobel Media AB 2014. Web. 12 May 2018. <http://www.nobelprize.org/nobel_prizes/physics/laureates/2010/>.

9 Li, X. S., Cai, W. W., An, J. H., Kim, S., Nah, J., Yang, D. X. *et al.* Large-area synthesis of high-quality and uniform graphene films on copper foils. *Science* **324**, 1312-1314, (2009).

10 Berger, C., Song, Z. M., Li, T. B., Li, X. B., Ogbazghi, A. Y., Feng, R. *et al.* Ultrathin epitaxial graphite: 2D electron gas properties and a route toward graphene-based nanoelectronics. *Journal of Physical Chemistry B* **108**, 19912-19916, (2004).

11 Brodie, B. C. On the atomic weight of graphite. *Philosophical Transactions of the Royal Society of London* **149**, 249-259, (1859).

12 Hummers, W. S. & Offeman, R. E. Preparation of graphitic oxide. *Journal of the American Chemical Society* **80**, 1339, (1958).

13 Lerf, A., He, H. Y., Forster, M. & Klinowski, J. Structure of graphite oxide revisited. *Journal of Physical Chemistry B* **102**, 4477-4482, (1998).

14 Gao, W., Alemany, L. B., Ci, L. J. & Ajayan, P. M. New insights into the structure and reduction of graphite oxide. *Nature Chemistry* **1**, 403-408, (2009).

15 Cai, W. W., Piner, R. D., Stadermann, F. J., Park, S., Shaibat, M. A., Ishii, Y. *et al.* Synthesis and solid-state NMR structural characterization of (13)C-labeled graphite oxide. *Science* **321**, 1815-1817, (2008).

16 Li, D., Muller, M. B., Gilje, S., Kaner, R. B. & Wallace, G. G. Processable aqueous dispersions of graphene nanosheets. *Nature Nanotechnology* **3**, 101-105, (2008).

17 Stankovich, S., Piner, R. D., Chen, X. Q., Wu, N. Q., Nguyen, S. T. & Ruoff, R. S. Stable aqueous dispersions of graphitic nanoplatelets via the reduction of exfoliated graphite oxide in the presence of poly(sodium 4-styrenesulfonate). *Journal of Materials Chemistry* **16**, 155-158, (2006).

18 Becerril, H. A., Mao, J., Liu, Z., Stoltenberg, R. M., Bao, Z. & Chen, Y. Evaluation of solution-processed reduced graphene oxide films as transparent conductors. *ACS Nano* **2**, 463-470, (2008).

19 Cote, L. J., Cruz-Silva, R. & Huang, J. X. Flash reduction and patterning of graphite oxide and its polymer composite. *Journal of the American Chemical Society* **131**, 11027-11032, (2009).

20 Williams, G., Seger, B. & Kamat, P. V. TiO_2-graphene nanocomposites. UV-assisted photocatalytic reduction of graphene oxide. *ACS Nano* **2**, 1487-1491, (2008).

21 Luo, L., Wu, J., Luo, J., Huang, J. & Dravid, V. P. Dynamics of electrochemical lithiation/delithiation of graphene-encapsulated silicon nanoparticles studied by in-situ TEM. *Scientific Reports* **4**, 3863, (2014).

22 Schniepp, H. C., Li, J. L., McAllister, M. J., Sai, H., Herrera-Alonso, M., Adamson, D. H. *et al.* Functionalized single graphene sheets derived from splitting graphite oxide. *Journal of Physical Chemistry B* **110**, 8535-8539, (2006).

23 Compton, O. C. & Nguyen, S. T. Graphene oxide, highly reduced graphene oxide, and graphene: Versatile building blocks for carbon-based materials. *Small* **6**, 711-723, (2010).

24 Park, S. & Ruoff, R. S. Chemical methods for the production of graphenes. *Nature Nanotechnology* **4**, 217-224, (2009).

25 Eda, G. & Chhowalla, M. Chemically derived graphene oxide: Towards large-area thin-film electronics and optoelectronics. *Advanced Materials* **22**, 2392-2415, (2010).

26 Kim, J., Cote, L. J. & Huang, J. X. Two dimensional soft material: New faces of graphene oxide. *Accounts of Chemical Research* **45**, 1356-1364, (2012).

27 Cote, L. J., Kim, J., Tung, V. C., Luo, J. Y., Kim, F. & Huang, J. X. Graphene oxide as surfactant sheets. *Pure and Applied Chemistry* **83**, 95-110, (2011).

28 Kim, J., Cote, L. J., Kim, F., Yuan, W., Shull, K. R. & Huang, J. X. Graphene oxide sheets at interfaces. *Journal of the American Chemical Society* **132**, 8180-8186, (2010).

29 Cote, L. J., Kim, F. & Huang, J. X. Langmuir-Blodgett assembly of graphite oxide single layers. *Journal of the American Chemical Society* **131**, 1043-1049, (2009).

30 Sun, P. Z., Zhu, M., Wang, K. L., Zhong, M. L., Wei, J. Q., Wu, D. H. *et al.* Selective ion penetration of graphene oxide membranes. *ACS Nano* **7**, 428-437, (2013).

31 Chen, C. M., Yang, Q. H., Yang, Y. G., Lv, W., Wen, Y. F., Hou, P. X. *et al.* Self-assembled free-standing graphite oxide membrane. *Advanced Materials* **21**, 3007-3011, (2009).

32 Dikin, D. A., Stankovich, S., Zimney, E. J., Piner, R. D., Dommett, G. H. B., Evmenenko, G. *et al.* Preparation and characterization of graphene oxide paper. *Nature* **448**, 457-460, (2007).

33 Luo, J., Jang, H. D., Sun, T., Xiao, L., He, Z., Katsoulidis, A. P. *et al.* Compression and aggregation-resistant particles of crumpled soft sheets. *ACS Nano* **5**, 8943-8949, (2011).

34 Amadei, C. A., Stein, I. Y., Silverberg, G. J., Wardle, B. L. & Vecitis, C. D. Fabrication and morphology tuning of graphene oxide nanoscrolls. *Nanoscale* **8**, 6783-6791, (2016).

35 Xu, Z. & Gao, C. Graphene chiral liquid crystals and macroscopic assembled fibres. *Nature Communications* **2**, 571, (2011).

36 Yeh, C. N., Raidongia, K., Shao, J. J., Yang, Q. H. & Huang, J. X. On the origin of the stability of graphene oxide membranes in water. *Nature Chemistry* **7**, 166-170, (2015).

37 Liu, X. J., Pan, L. K., Zhao, Q. F., Lv, T., Zhu, G., Chen, T. Q. *et al.* UV-assisted photocatalytic synthesis of ZnO-reduced graphene oxide composites with enhanced photocatalytic activity in reduction of Cr(VI). *Chemical Engineering Journal* **183**, 238-243, (2012).

38 Hu, T., Sun, X., Sun, H. T., Yu, M. P., Lu, F. Y., Liu, C. S. *et al.* Flexible free-standing graphene-TiO_2 hybrid paper for use as lithium ion battery anode materials. *Carbon* **51**, 322-326, (2013).

39 Li, H., Song, Z., Zhang, X., Huang, Y., Li, S., Mao, Y. *et al.* Ultrathin, molecular-sieving graphene oxide membranes for selective hydrogen separation. *Science* **342**, 95-98, (2013).

40 Nair, R. R., Wu, H. A., Jayaram, P. N., Grigorieva, I. V. & Geim, A. K. Unimpeded permeation of water through helium-leak-tight graphene-based membranes. *Science* **335**, 442-444, (2012).

41 Schedin, F., Geim, A. K., Morozov, S. V., Hill, E. W., Blake, P., Katsnelson, M. I. *et al.* Detection of individual gas molecules adsorbed on graphene. *Nature Materials* **6**, 652-655, (2007).

42 Wei, Z. Q., Barlow, D. E. & Sheehan, P. E. The assembly of single-layer graphene oxide and graphene using molecular templates. *Nano Letters* **8**, 3141-3145, (2008).

43 Kim, K. S., Zhao, Y., Jang, H., Lee, S. Y., Kim, J. M., Kim, K. S. *et al.* Large-scale pattern growth of graphene films for stretchable transparent electrodes. *Nature* **457**, 706-710, (2009).

44 Li, D. & Kaner, R. B. Materials science - Graphene-based materials. *Science* **320**, 1170-1171, (2008).

45 Loh, K. P., Bao, Q. L., Eda, G. & Chhowalla, M. Graphene oxide as a chemically tunable platform for optical applications. *Nature Chemistry* **2**, 1015-1024, (2010).

46 Zhu, Y., James, D. K. & Tour, J. M. New routes to graphene, graphene oxide and their related applications. *Advanced Materials* **24**, 4924-4955, (2012).

47 Joshi, R. K., Carbone, P., Wang, F. C., Kravets, V. G., Su, Y., Grigorieva, I. V. *et al.* Precise and ultrafast molecular sieving through graphene oxide membranes. *Science* **343**, 752-754, (2014).

48 Kim, H. W., Yoon, H. W., Yoon, S. M., Yoo, B. M., Ahn, B. K., Cho, Y. H. *et al.* Selective gas transport through few-layered graphene and graphene oxide membranes. *Science* **342**, 91-95, (2013).

49 Cote, L. J., Kim, J., Zhang, Z., Sun, C. & Huang, J. X. Tunable assembly of graphene oxide surfactant sheets: Wrinkles, overlaps and impacts on thin film properties. *Soft Matter* **6**, 6096-6101, (2010).

50 Luo, J. Y., Cote, L. J., Tung, V. C., Tan, A. T. L., Goins, P. E., Wu, J. S. *et al.* Graphene oxide nanocolloids. *Journal of the American Chemical Society* **132**, 17667-17669, (2010).

51 Stankovich, S., Dikin, D. A., Compton, O. C., Dommett, G. H. B., Ruoff, R. S. & Nguyen, S. T. Systematic post-assembly modification of graphene oxide paper with primary alkylamines. *Chemistry of Materials* **22**, 4153-4157, (2010).

52 Sun, S., Wang, C., Chen, M. & Li, M. The mechanism for the stability of graphene oxide membranes in a sodium sulfate solution. *Chemical Physics Letters* **561**, 166-169, (2013).

53 Han, Y., Xu, Z. & Gao, C. Ultrathin graphene nanofiltration membrane for water purification. *Advanced Functional Materials* **23**, 3693-3700, (2013).

54 Hu, M. & Mi, B. Layer-by-layer assembly of graphene oxide membranes via electrostatic interaction. *Journal of Membrane Science* **469**, 80-87, (2014).

55 Hu, M. & Mi, B. X. Enabling graphene oxide nanosheets as water separation membranes. *Environmental Science & Technology* **47**, 3715-3723, (2013).

56 Luo, J., Kim, J. & Huang, J. Material processing of chemically modified graphene: Some challenges and solutions. *Accounts of Chemical Research* **46**, 2225-2234, (2013).

57 Hung, W. S., Tsou, C. H., De Guzman, M., An, Q. F., Liu, Y. L., Zhang, Y. M. *et al.* Cross-linking with diamine monomers to prepare composite graphene oxide-framework membranes with varying d-spacing. *Chemistry of Materials* **26**, 2983-2990, (2014).

58 Kim, F., Luo, J., Cruz-Silva, R., Cote, L. J., Sohn, K. & Huang, J. Self-propagating domino-like reactions in oxidized graphite. *Advanced Functional Materials* **20**, 2867-2873, (2010).

59 Park, S., Lee, K.-S., Bozoklu, G., Cai, W., Nguyen, S. T. & Ruoff, R. S. Graphene oxide papers modified by divalent ions - Enhancing mechanical properties via chemical cross-linking. *ACS Nano* **2**, 572-578, (2008).

60 Housecroft, C. E. & Sharpe, A. G. *Inorganic Chemistry* 2nd edn (Pearson Prentice Hall, 2005).

61 Rayner-Canham, G. & Overton, T. *Descriptive Inorganic Chemistry* 5th edn (W.H. Freeman, 2010).

62 Rubin, A. J. *Aqueous-Environmental Chemistry of Metals* (Ann Arbor Science Publishers, 1974).

63 Cano, M., Khan, U., Sainsbury, T., O'Neill, A., Wang, Z. M., McGovern, I. T. *et al.* Improving the mechanical properties of graphene oxide based materials by covalent attachment of polymer chains. *Carbon* **52**, 363-371, (2013).

64 Wang, X. L., Bai, H. & Shi, G. Q. Size fractionation of graphene oxide sheets by pH-assisted selective sedimentation. *Journal of the American Chemical Society* **133**, 6338-6342, (2011).

65 Gao, Y., Liu, L. Q., Zu, S. Z., Peng, K., Zhou, D., Han, B. H. *et al.* The effect of inter layer adhesion on the mechanical behaviors of macroscopic graphene oxide papers. *ACS Nano* **5**, 2134-2141, (2011).

66 Lin, X. Y., Shen, X., Zheng, Q. B., Yousefi, N., Ye, L., Mai, Y. W. *et al.* Fabrication of highly-aligned, conductive, and strong graphene papers using ultra large graphene oxide sheets. *ACS Nano* **6**, 10708-10719, (2012).

67 Satti, A., Larpent, P. & Gun'ko, Y. Improvement of mechanical properties of graphene oxide/poly(allylamine) composites by chemical crosslinking. *Carbon* **48**, 3376-3381, (2010).

68 Shao, J. J., Wu, S. D., Zhang, S. B., Lv, W., Su, F. Y. & Yang, Q. H. Graphene oxide hydrogel at solid/liquid interface. *Chemical Communications* **47**, 5771-5773, (2011).

69 Hamley, I. W. *Introduction to Soft Matter: Polymers, Colloids, Amphiphiles and Liquid Crystals* 2nd edn (Wiley, 2007).

70 Zhu, Y. W., Murali, S., Cai, W. W., Li, X. S., Suk, J. W., Potts, J. R. *et al.* Graphene and graphene oxide: Synthesis, properties, and applications. *Advanced Materials* **22**, 3906-3924, (2010).

71 Lopez-Sanchez, O., Lembke, D., Kayci, M., Radenovic, A. & Kis, A. Ultrasensitive photodetectors based on monolayer MoS_2. *Nature Nanotechnology* **8**, 497, (2013).

72 Hernandez, Y., Nicolosi, V., Lotya, M., Blighe, F. M., Sun, Z., De, S. *et al.* High-yield production of graphene by liquid-phase exfoliation of graphite. *Nature Nanotechnology* **3**, 563, (2008).

73 Coleman, J. N., Lotya, M., O'Neill, A., Bergin, S. D., King, P. J., Khan, U. *et al.* Two-dimensional nanosheets produced by liquid exfoliation of layered materials. *Science* **331**, 568-571, (2011).

74 Song, L., Ci, L., Lu, H., Sorokin, P. B., Jin, C., Ni, J. *et al.* Large scale growth and characterization of atomic hexagonal boron nitride layers. *Nano Letters* **10**, 3209-3215, (2010).

75 Ramakrishna Matte, H., Gomathi, A., Manna, A. K., Late, D. J., Datta, R., Pati, S. K. *et al.* MoS_2 and WS_2 analogues of graphene. *Angewandte Chemie International Edition* **49**, 4059-4062, (2010).

76 Saito, Y., Luo, X., Zhao, C. S., Pan, W., Chen, C. M., Gong, J. H. *et al.* Filling the gaps between graphene oxide: A general strategy toward nanolayered oxides. *Advanced Functional Materials* **25**, 5683-5690, (2015).

77 Li, N., Liu, G., Zhen, C., Li, F., Zhang, L. & Cheng, H.-M. Battery performance and photocatalytic activity of mesoporous anatase TiO_2 nanospheres/graphene composites by template-free self-assembly. *Advanced Functional Materials* **21**, 1717-1722, (2011).

78 Goncalves, G., Marques, P. A. A. P., Granadeiro, C. M., Nogueira, H. I. S., Singh, M. K. & Gracio, J. Surface modification of graphene nanosheets with gold nanoparticles: The role of oxygen moieties at graphene surface on gold nucleation and growth. *Chemistry of Materials* **21**, 4796-4802, (2009).

79 Xu, C., Chen, Z. & Fu, X. Graphene oxide-mediated formation of freestanding, thickness controllable metal oxide films. *Journal of Materials Chemistry* **21**, 12889-12893, (2011).

80 Raidongia, K. & Huang, J. Nanofluidic ion transport through reconstructed layered materials. *Journal of the American Chemical Society* **134**, 16528-16531, (2012).

81 Luo, C., Yeh, C. N., Baltazar, J. M. L., Tsai, C. L. & Huang, J. X. A cut-and-paste approach to 3D graphene-oxide-based architectures. *Advanced Materials* **30**, 6, (2018).

82 Rogers, J. A., Someya, T. & Huang, Y. G. Materials and mechanics for stretchable electronics. *Science* **327**, 1603-1607, (2010).

83 Zhang, Y. H., Zhang, F., Yan, Z., Ma, Q., Li, X. L., Huang, Y. G. *et al.* Printing, folding and assembly methods for forming 3D mesostructures in advanced materials. *Nature Reviews Materials* **2**, 16, (2017).

84 Dou, X., Koltonow, A. R., He, X. L., Jang, H. D., Wang, Q., Chung, Y. W. *et al.* Self-dispersed crumpled graphene balls in oil for friction and wear reduction. *Proceedings of the National Academy of Sciences of the United States of America* **113**, 1528-1533, (2016).

85 Silverberg, J. L., Evans, A. A., McLeod, L., Hayward, R. C., Hull, T., Santangelo, C. D. *et al.* Using origami design principles to fold reprogrammable mechanical metamaterials. *Science* **345**, 647-650, (2014).

86 Mu, J. K., Hou, C. Y., Wang, H. Z., Li, Y. G., Zhang, Q. H. & Zhu, M. F. Origami-inspired active graphene-based paper for programmable instant self-folding walking devices. *Science Advances* **1**, 8, (2015).

87 Shyu, T. C., Damasceno, P. F., Dodd, P. M., Lamoureux, A., Xu, L., Shlian, M. *et al.* A kirigami approach to engineering elasticity in nanocomposites through patterned defects. *Nature Materials* **14**, 785-789, (2015).

88 Blees, M. K., Barnard, A. W., Rose, P. A., Roberts, S. P., McGill, K. L., Huang, P. Y. *et al.* Graphene kirigami. *Nature* **524**, 204-207, (2015).

89 Xu, S., Yan, Z., Jang, K. I., Huang, W., Fu, H. R., Kim, J. *et al.* Assembly of micro/nanomaterials into complex, three-dimensional architectures by compressive buckling. *Science* **347**, 154-159, (2015).

90 Koltonow, A. R. & Huang, J. X. Ionic transport - Two-dimensional nanofluidics. *Science* **351**, 1395-1396, (2016).

91 Dreyer, D. R., Park, S., Bielawski, C. W. & Ruoff, R. S. The chemistry of graphene oxide. *Chemical Society Reviews* **39**, 228-240, (2010).

92 Bai, H., Li, C. & Shi, G. Q. Functional composite materials based on chemically converted graphene. *Advanced Materials* **23**, 1089-1115, (2011).

93 Pei, S. F., Zhao, J. P., Du, J. H., Ren, W. C. & Cheng, H. M. Direct reduction of graphene oxide films into highly conductive and flexible graphene films by hydrohalic acids. *Carbon* **48**, 4466-4474, (2010).

94 Cheng, H. H., Huang, Y. X., Cheng, Q. L., Shi, G. Q., Jiang, L. & Qu, L. T. Self-healing graphene oxide based functional architectures triggered by moisture. *Advanced Functional Materials* **27**, 8, (2017).

95 Timoshenko, S. *Strength of Materials* 3rd edn (Krieger Publishing Co., 1983).

96 Zhang, P. P., Li, J., Lv, L. X., Zhao, Y. & Qu, L. T. Vertically aligned graphene sheets membrane for highly efficient solar thermal generation of clean water. *ACS Nano* **11**, 5087-5093, (2017).

97 Yoon, Y., Lee, K., Kwon, S., Seo, S., Yoo, H., Kim, S. *et al.* Vertical alignments of graphene sheets spatially and densely piled for fast ion diffusion in compact supercapacitors. *ACS Nano* **8**, 4580-4590, (2014).

98 Fyles, T. M. Synthetic ion channels in bilayer membranes. *Chemical Society Reviews* **36**, 335-347, (2007).

99 Cheng, H. H., Liu, J., Zhao, Y., Hu, C. G., Zhang, Z. P., Chen, N. *et al.* Graphene fibers with predetermined deformation as moisture-triggered actuators and robots. *Angewandte Chemie-International Edition* **52**, 10482-10486, (2013).

100 Park, S., An, J., Suk, J. W. & Ruoff, R. S. Graphene-based actuators. *Small* **6**, 210-212, (2010).

101 Yeh, C. N., Huang, H. Y., Lim, A. T. O. & Huang, J. X. Binder-free graphene oxide doughs. - *submitted*, (2018).

102 Qiu, L., Liu, J. Z., Chang, S. L., Wu, Y. & Li, D. Biomimetic superelastic graphene-based cellular monoliths. *Nature Communications* **3**, 1241, (2012).

103 Tung, V. C., Allen, M. J., Yang, Y. & Kaner, R. B. High-throughput solution processing of large-scale graphene. *Nature Nanotechnology* **4**, 25, (2009).

104 Akbari, A., Sheath, P., Martin, S. T., Shinde, D. B., Shaibani, M., Banerjee, P. C. *et al.* Large-area graphene-based nanofiltration membranes by shear alignment of discotic nematic liquid crystals of graphene oxide. *Nature Communications* **7**, 12, (2016).

105 Tesfai, W., Singh, P., Shatilla, Y., Iqbal, M. Z. & Abdala, A. A. Rheology and microstructure of dilute graphene oxide suspension. *Journal of Nanoparticle Research* **15**, 1989, (2013).

106 Naficy, S., Jalili, R., Aboutalebi, S. H., Gorkin, R. A., Konstantinov, K., Innis, P. C. *et al.* Graphene oxide dispersions: Tuning rheology to enable fabrication. *Materials Horizons* **1**, 326-331, (2014).

107 Valles, C., Young, R. J., Lomax, D. J. & Kinloch, I. A. The rheological behaviour of concentrated dispersions of graphene oxide. *Journal of Materials Science* **49**, 6311-6320, (2014).

108 Bai, H., Li, C., Wang, X. L. & Shi, G. Q. A pH-sensitive graphene oxide composite hydrogel. *Chemical Communications* **46**, 2376-2378, (2010).

109 Xu, Y. X., Wu, Q. O., Sun, Y. Q., Bai, H. & Shi, G. Q. Three-dimensional self-assembly of graphene oxide and DNA into multifunctional hydrogels. *ACS Nano* **4**, 7358-7362, (2010).

110 Bai, H., Li, C., Wang, X. L. & Shi, G. Q. On the gelation of graphene oxide. *Journal of Physical Chemistry C* **115**, 5545-5551, (2011).

111 Chiou, K., Byun, S., Kim, J. & Huang, J. Additive-free carbon nanotube dispersions, pastes, gels, and doughs in cresols. *Proceedings of the National Academy of Sciences of the United States of America* **115**, 5703-5708, (2018).

112 Oh, J. Y., Kim, S., Baik, H. K. & Jeong, U. Conducting polymer dough for deformable electronics. *Advanced Materials* **28**, 4455-4461, (2016).

113 Li, Y. R., Chen, J., Huang, L., Li, C. & Shi, G. Q. "Pottery" of porous graphene materials. *Advanced Electronic Materials* **1**, 7, (2015).

114 Shuyuan, L., Yujia, Z., Xuanliang, Z., Toshiki, S., Xinming, L., Wenhai, L. *et al.* (in press). Synthetic multifunctional graphene composites with reshaping and self-healing features via a facile biomineralization-inspired process. *Advanced Materials*, doi:10.1002/adma.201803004.

115 Jiang, Y., Shao, H. B., Li, C. X., Xu, T., Zhao, Y., Shi, G. Q. *et al.* Versatile graphene oxide putty-like material. *Advanced Materials* **28**, 10287-10292, (2016).

116 Li, Y., Chen, J., Huang, L., Li, C., Hong, J. D. & Shi, G. Highly compressible macroporous graphene monoliths via an improved hydrothermal process. *Advanced Materials* **26**, 4789-4793, (2014).

117 Sun, H., Xu, Z. & Gao, C. Multifunctional, ultra-flyweight, synergistically assembled carbon aerogels. *Advanced Materials* **25**, 2554-2560, (2013).

118 Xu, Y., Sheng, K., Li, C. & Shi, G. Self-assembled graphene hydrogel via a one-step hydrothermal process. *ACS Nano* **4**, 4324-4330, (2010).

119 Krueger, M., Berg, S., Stone, D. A., Strelcov, E., Dikin, D. A., Kim, J. *et al.* Drop-casted self-assembling graphene oxide membranes for scanning electron microscopy on wet and dense gaseous samples. *ACS Nano* **5**, 10047-10054, (2011).

120 Lu, L., Sui, M. & Lu, K. Superplastic extensibility of nanocrystalline copper at room temperature. *Science* **287**, 1463-1466, (2000).

121 Kumar, P., Maiti, U. N., Lee, K. E. & Kim, S. O. Rheological properties of graphene oxide liquid crystal. *Carbon* **80**, 453-461, (2014).

122 Søndergaard, R. R., Hösel, M. & Krebs, F. C. Roll-to-roll fabrication of large area functional organic materials. *Journal of Polymer Science Part B: Polymer Physics* **51**, 16-34, (2013).

123 Joshi, R., Alwarappan, S., Yoshimura, M., Sahajwalla, V. & Nishina, Y. Graphene oxide: The new membrane material. *Applied Materials Today* **1**, 1-12, (2015).

124 Movva, M. & Kommineni, R. Extraction of cellulose from pistachio shell and physical and mechanical characterisation of cellulose-based nanocomposites. *Materials Research Express* **4**, 045014, (2017).

125 Gibson, L. J. & Ashby, M. F. *Cellular Solids: Structure and Properties* (Cambridge University Press, 1999).

126 Worsley, M. A., Kucheyev, S. O., Satcher Jr, J. H., Hamza, A. V. & Baumann, T. F. Mechanically robust and electrically conductive carbon nanotube foams. *Applied Physics Letters* **94**, 073115, (2009).

127 Worsley, M. A., Kucheyev, S. O., Mason, H. E., Merrill, M. D., Mayer, B. P., Lewicki, J. *et al.* Mechanically robust 3D graphene macroassembly with high surface area. *Chemical Communications* **48**, 8428-8430, (2012).

128 Tang, Z., Shen, S., Zhuang, J. & Wang, X. Noble-metal-promoted three-dimensional macroassembly of single-layered graphene oxide. *Angewandte Chemie International Edition* **122**, 4707-4711, (2010).

129 Miller, M. & Liaw, P. *Bulk Metallic Glasses: An Overview* (Springer Science & Business Media, 2007).

130 Oku, T. & Eto, M. Correlation between the strength and Vickers hardness of some nuclear graphite. *Carbon* **12**, 477-479, (1974).

131 "Manufacturing Process". *Toyo Tanso Co.* 25 May 2018. <http://www.toyotanso.com/Products/Special_graphite/manufacturing-process.html>.

132 Somiya, S. *Handbook of Advanced Ceramics: Materials, Applications, Processing, and Properties* 2nd edn (Academic Press, 2013).

133 Nautiyal, P., Embrey, L., Boesl, B. & Agarwal, A. Multi-scale mechanics and electrical transport in a free-standing 3D architecture of graphene and carbon nanotubes fabricated by pressure assisted welding. *Carbon* **122**, 298-306, (2017).

134 Nieto, A., Lahiri, D. & Agarwal, A. Synthesis and properties of bulk graphene nanoplatelets consolidated by spark plasma sintering. *Carbon* **50**, 4068-4077, (2012).

135 Bi, H., Yin, K., Xie, X., Zhou, Y., Wan, N., Xu, F. *et al.* Low temperature casting of graphene with high compressive strength. *Advanced Materials* **24**, 5124-5129, (2012).

136 Worsley, M. A., Charnvanichborikarn, S., Montalvo, E., Shin, S. J., Tylski, E. D., Lewicki, J. P. *et al.* Toward macroscale, isotropic carbons with graphene-sheet-like electrical and mechanical properties. *Advanced Functional Materials* **24**, 4259-4264, (2014).

137 Tao, Y., Xie, X., Lv, W., Tang, D.-M., Kong, D., Huang, Z. *et al.* Towards ultrahigh volumetric capacitance: Graphene derived highly dense but porous carbons for supercapacitors. *Scientific Reports* **3**, 2975, (2013).

138 Luo, J., Gao, J., Wang, A. & Huang, J. Bulk nanostructured materials based on two-dimensional building blocks: A roadmap. *ACS Nano* **9**, 9432-9436, (2015).

139 Liu, C., Younesi, R., Tai, C.-W., Valvo, M., Edström, K., Gustafsson, T. *et al.* 3-D binder-free graphene foam as a cathode for high capacity Li-O_2 batteries. *Journal of Materials Chemistry A* **4**, 9767-9773, (2016).

140 Shao, Y., El-Kady, M. F., Lin, C. W., Zhu, G., Marsh, K. L., Hwang, J. Y. *et al.* 3D freeze-casting of cellular graphene films for ultrahigh-power-density supercapacitors. *Advanced Materials* **28**, 6719-6726, (2016).

141 Yu, M., Huang, Y., Li, C., Zeng, Y., Wang, W., Li, Y. *et al.* Building three-dimensional graphene frameworks for energy storage and catalysis. *Advanced Functional Materials* **25**, 324-330, (2015).

142 Xu, Y., Lin, Z., Huang, X., Wang, Y., Huang, Y. & Duan, X. Functionalized graphene hydrogel-based high-performance supercapacitors. *Advanced Materials* **25**, 5779-5784, (2013).

143 Simon, P. & Gogotsi, Y. Capacitive energy storage in nanostructured carbon-electrolyte systems. *Accounts of Chemical Research* **46**, 1094-1103, (2012).

144 Gogotsi, Y. & Simon, P. True performance metrics in electrochemical energy storage. *Science* **334**, 917-918, (2011).

145 Trexler, M. M. & Thadhani, N. N. Mechanical properties of bulk metallic glasses. *Progress in Materials Science* **55**, 759-839, (2010).